AD_____

Award Number: DAMD17-00-1-0500

TITLE: Novel Histone Deacetylase Inhibitors

PRINCIPAL INVESTIGATOR: Jeannine Strobl, Ph.D.

CONTRACTING ORGANIZATION: West Virginia University Research Corporation
Morgantown, West Virginia 26506-6845

REPORT DATE: July 2004

TYPE OF REPORT: Final

PREPARED FOR: U.S. Army Medical Research and Materiel Command
Fort Detrick, Maryland 21702-5012

DISTRIBUTION STATEMENT: Approved for Public Release;
Distribution Unlimited

REPORT DOCUMENTATION PAGE

Form Approved
OMB No. 074-0188

1. AGENCY USE ONLY (Leave blank)	2. REPORT DATE	3. REPORT TYPE AND DATES COVERED
	July 2004	Final (15 Jun 2000 - 14 Jun 2004)

4. TITLE AND SUBTITLE
Novel Histone Deacetylase Inhibitors

5. FUNDING NUMBERS
DAMD17-00-1-0500

6. AUTHOR(S)
Jeannine S. Strobl, Ph.D.

7. PERFORMING ORGANIZATION NAME(S) AND ADDRESS(ES)
West Virginia University Research Corporation
Morgantown, West Virginia 26506-6845

E-Mail: Jseibert2004@cox.net

8. PERFORMING ORGANIZATION REPORT NUMBER

9. SPONSORING / MONITORING AGENCY NAME(S) AND ADDRESS(ES)
U.S. Army Medical Research and Materiel Command
Fort Detrick, Maryland 21702-5012

10. SPONSORING / MONITORING AGENCY REPORT NUMBER

11. SUPPLEMENTARY NOTES
Original contains color plates: All DTIC reproductions will be in black and white.

12a. DISTRIBUTION / AVAILABILITY STATEMENT
Approved for Public Release; Distribution Unlimited

12b. DISTRIBUTION CODE

13. ABSTRACT (Maximum 200 Words)

Advanced breast cancer is not curable by existing treatment regimens. The purpose of this project is to discover new drugs to treat breast cancer that act to restore the differentiated and non-growing state of breast tumor cells by inhibition of histone deacetylase. We screened a series of antitumor antimalarial drugs as well as structural analogs of antimalarials. Our work identified 5 novel quinolines that were more potent and efficacious than the antitumor antimalarial drugs in arresting the growth of human breast tumor cells in culture. These are NSC3852,NSC69603,NSC86371,NSC10010, and NSC305819. Of these 5 compounds, only NSC3852 was a direct inhibitor of histone deacetylase activity, an established mechanism for induction of differentiation in breast tumor cells. Further experimentation showed a second mechanism of action of NSC3852 that contributed importantly to inhibition of tumor cell growth inhibition. NSC3852 is a redox active compound that generates superoxide radicals in tumor cells and causes DNA strand breakage. The mechanism of action of the other 4 compounds involves accumulation of pRb in its hypophosphorylated state and a down-regulation of E2F1 protein levels associated with blockade of cell growth in G1 phase of the cell cycle.

14. SUBJECT TERMS
Histone deacetylase, differentiation therapy, quinolines

15. NUMBER OF PAGES
54

16. PRICE CODE

17. SECURITY CLASSIFICATION OF REPORT	18. SECURITY CLASSIFICATION OF THIS PAGE	19. SECURITY CLASSIFICATION OF ABSTRACT	20. LIMITATION OF ABSTRACT
Unclassified	Unclassified	Unclassified	Unlimited

Table of Contents

INTRODUCTION

Histone deacetylases (HDAC) are a family of enzymes that modify chromatin structure, transcription factor acetylation status, and regulate gene expression. Interest in HDAC as a target for anti-cancer drug development is based upon the antiproliferative and differentiating activity of HDAC inhibitors in tissue culture cell lines and their anti-tumor properties in transplanted tumors in animals. We are engaged in a drug screening process to identify antimalarial drugs, and drugs with analogous quinoline ring chemical structures, that promote the differentiation of human breast cancer cell lines, MCF-7 and MDA-MB-231. While we have identified only two new compounds that cause direct inhibition of HDAC enzyme, we have identified many quinoline ring compounds that cause growth arrest, differentiation and apoptosis in human breast cancer cells. The significance of this work is that it provides the basis for the development of novel breast cancer differentiation agents.

BODY

Tasks 1-3 – Complete

Task 4 – Histone deacetylase (HDAC) in vitro inhibition assays, apoptosis assays, growth inhibition assays, and cell differentiation assays- Complete.
Histone hyperacetylation assays with antimalarials – Complete.
Histone hyperacetylation assays with the NSC (National Service Center of the National Institutes of Health, Bethesda, MD) differentiation agents – Complete.
Data are included in the Appendix. Please refer to the Table below for the citations of interest.

TASK 4 SUMMARY TABLE 1.

Assay	Manuscript	Figure/Table
HDAC	Martirosyan, et al. Differentiation-inducing quinolines as experimental breast cancer agents in the MCF-7 human breast cancer model. Biochemical Pharmacology, in press, 2004	Table 1
	Zhou et al. JBC, 275:35256 (2000)	Figures 1 and 2
Apoptosis/Growth Inhibition	Martirosyan, et al.,*ibid*	Table 1, Figures 4, 6, 7
	Zhou et al (2000) J. Biol. Chem. 275: 35256	Figure 6
DNA damage	Martirosyan, et al, *ibid*	Figure 5
Cell Differentiation Lipid Droplet accumulation assays and Ki67 Expression	Martirosyan, et al., *ibid*	Table 1
	Zhou et al. , *ibid*	Figures 7 and 8

Histone Hyperacetylation (antimalarials)	*Zhou et al., ibid*	Figures 1 and 9
Histone Hyperacetylation (NSC compounds)	Complete	Unpublished data in Appendix

Task 5 – New objective: establish HDAC as a target for ubiquitination - Complete. Ubiquitinated HDAC proteins were demonstrated using Western blots. Total HDAC1 was immunoprecipitated from whole cell MCF-7 extracts and electrophoresed through SDS-polyacrylamide gels. After transfer and immobilization of the protein on membranes, ubiquitinated HDAC was detected with polyclonal antibodies directed against ubiquitin. MCF-7 human breast cancer cells treated with chloroquine or quinidine displayed increased levels of polyubiquitinated HDAC 1. Cells exposed to NSC 3852 (n=1) or NSC 10010 (n=1) exhibited a slight decrease in the level of polyubiquitinated HDAC1 compared with controls. This is Figure 1B (Appendix). We also showed rapid loss of HDAC1 protein from MCF-7 cells treated with either chloroquine or quinidine, but little or no loss of HDAC1 in response to NSC 3852 (Figure 1A ,Appendix).

Task 6- Complete. The MTS screen for inhibition of cell growth using the MTS (a tetrazolium enzyme substrate) assay for mitochondrial dehydrogenase activity of living cells and for induction of apoptosis using the nucleosome ELISA was completed in MCF-7, MDA-MB-231, and MCF10A cell lines. Please refer to the Task 4 Summary Table above for the location of the published data.

The MCF-10A cell line is an immortalized, non-tumorigenic human mammary epithelial line. The purpose of comparing toxicity of the active breast tumor differentiation agents in the three cell lines was to assess the degree of selective toxicity against the tumor cells compared with the immortalized cells. These in vitro assessments will require validation in whole animal studies. In Table 2 found below, the results of MTS cell survival assays performed after a 48 h exposure to each compound at 10 concentrations (n=2 for all compounds except as noted) are found in Table 2. The reference compounds in Table 2 are chloroquine (NSC14050, n=3)) and hydroxychloroquine (NSC4375, n=3). Both reference compounds are safe for human administration. Both reference compounds showed relatively greater toxicity in the transformed cell lines, MCF-7 and MDA-231 than the immortalized MCF-10A line in this assay as determined by calculating the ratios of the IC50 in tumor/immortalized cell lines (indicated in the columns marked relative toxicity). For example, the NSC14050 was approximately 11 times more toxic to MCF-7 cells than MCF10A cells by this measure. Not all of the breast tumor differentiation quinoline NSC compounds showed this level of relative toxicity. However, NSC305819, NSC86371, and NSC3852 show somewhat more toxicity in the tumor lines than the MCF10A line using the MTS IC50 ratio method to compare toxicities.

The toxicity of the breast tumor differentiation compounds in the immortalized MCF10A cell line was also evaluated on the basis of their ability to induce apoptosis as measured using the nucleosome release ELISA (unpublished). A nucleosome release value = 1.0 represents the low level observed in control cells. Any number greater than 1.0 is an indicative of apoptotic potential. The reference compound in the nucleosome release

assay is etoposide which yields a value of 2.7 in 48 hours. The nucleosome release assay data for the differentiation inducing quinolines in the MCF10A cells and MCF-7 cells are compared below in Table 3. Chloroquine is the most active apoptosis inducer in the tumor cell line and shows little toxicity to the immortalized cells. NSC3852 and NSC86371 showed modest apoptotic activity that was relatively selective for the tumor cells compared with the immortalized cells at the 72 h time point shown. In addition (not shown), both NSC3852 and NSC86371 showed even greater degree of apoptosis after 48 h. We conclude that NSC14050 (chloroquine) , NSC 3852 and NSC86371 are promising antitumor agents based upon the relativelyl selective induction of apoptosis in the tumor cell line compared to the immortalized cell line. In addition, we conclude that MCF10A cells are especially sensitive to apoptosis in response to NSC69603, a compound that failed to induce apoptosis in MCF-7 cells. This interesting observation requires further investigation because it highlights an important difference in tumor vs. immortalized breast cells.

RELATIVE TOXICITY ASSAY. Table 2.

	MCF-7		MDA-231		MCF-10A	RELATIVE TOXICITY	
NSC #	MTS IC50 (μM)	SRB GI50 (μM)	MTS IC50 (μM)	SRB GI50 (μM)	MTS IC50 (μM)	MCF-7	MDA-231
14050	33±1.5	19	11±1.8	16	365±5.9	11.1	33.2
4375	57±1.3	Nd	28±1.4	nd	218±3.1	3.8	7.8
69603	14	0.9	0.9	0.6	0.7	0.05	0.78
305819	7	13	3.9	9.4	34.2	4.9	8.8
124637	13	14	34.4	17	nd	nd	nd
86371	6	nd	1.1	nd	153	25.5	139
86373	13	nd	12.9	nd	12.3	0.95	0.95
85700	7	7	nd	33.2	12.7	1.8	nd
3852	10	2	2	6.4	9.5	0.95	4.8
10010	4	5.4	1	1.3	3.2	0.8	3.2

NUCLEOSOME RELEASE ASSAY. Table 3.

Cell line	3852	10010	69603	86371	305819	Chloroquine
MCF-7	2.0	0.8	1.0	3.5	3.0	7.0
MCF-10A	1.5	0	5.5	2.0	1.5	0.8

Task 7 – Dropped

Task 8 – Four manuscripts appeared in print or were accepted for publication as a result of the work supported by this grant. A fifth full-length research publication is nearly ready for submission to J. Pharmacol. Exp. Therapeutics. A sixth research publication is under preparation. Thirteen abstracts based upon the work outlined in this grant were published. Two additional abstracts will be submitted during the Fall, 2004 to present the final experiments supported by this grant. A specific listing of all the publications can be found in the Reportable Outcomes section of this Report.

Approximately 2 entire months were devoted to the development of a SYBYL CoMFA (conformational molecular field analysis) based model for the prediction of novel breast tumor differentiation agents. The minimum recommended statistical parameters for the establishment of a CoMFA model are: 1) 5 compounds, 2) a compound response range of at least 2 orders of magnitude, and 3) an r^2 value >0.8. In our analyses, we analyzed our entire data set, as well as subsets of the compounds, using at least 5 compounds per condition. We used the Ki67 differentiation index as the end-point because this was the only parameter we measured that had a response range of 2 orders of magnitude as well as the MTS IC50 values as an end-point. A summary of the approaches used is presented in the CoMFA Summary Table below. The structures of all the compounds in our data base are presented in Figures 1 and 2 in Martirosyan et al, Biochemical Pharmacology, in press. None of the CoMFA approaches used yielded regression coefficients (r^2) that showed a statistically valid model of compound structure for predicting differentiation activity (Ki67 index) or growth inhibition (IC50). Our conclusion is that a CoMFA based model cannot be developed from the existing set of compounds.

CoMFA SUMMARY TABLE 4.

Compound Set Used in the Analysis	**Templates Used for the Chemical Alignment**	**R^2** Ki67	IC50
All compounds with a substituted position 4 pyrimidine ring	a) Quinoline ring b) Benzene ring c) Pyrimidine ring	a)-0.4 b)-0.9 c)-0.4	-0.2 -0.6 -0.2
All compounds with position 2 and 4 substituted pyrimidine ring	a) benzene ring b) quinoline ring	a)-0.4 b)-0.4	-0.2 -0.6
9 Compounds with Highest Ki67 Index	a) quinoline ring b) pyrimidine ring c) benzene ring	a)-0.3 b)-0.3 c)-0.2	-0.1 -0.1 -0.5
Compounds with a single quinidine ring	Quinoline ring	-0.2	-0.4
All compounds		-0.3	+0.1

KEY RESEARCH ACCOMPLISHMENTS

1. We demonstrated that HDAC1 protein in MCF-7 human breast tumor cells is a target for ubiquitination. The antimalarials chloroquine and quinidine stimulate levels of HDAC1 ubiquitination and lead to increased degradation of HDAC1. This is a potential mechanism for the breast tumor cell differentiation activity of chloroquine and quinidine. The finding that HDAC1 protein is regulated by ubiquitination was a novel finding. Our data demonstrate that HDAC1 ubiquitination is amenable to pharmacologic manipulation opening a new avenue for development of novel differentiation agents to treat breast cancer.
2. Chloroquine exhibits low toxicity to normal cells and has significant apoptotic activity in breast tumor cells indicative of cancer chemopreventative activity.
3. A screen conducted using structural analogs of quinidine and chloroquine in the NCI compound library identified four differentiation-inducing quinolines that have potential for further development as oral breast cancer differentiation agents: NSC3852, NSC86371, NSC305819 and NSC69603.
4. In depth analysis of the mechanism of actions of these differentiation-inducing quinolines indicated that neither HDAC1 down-regulation nor histone H4 hyperacetylation were markers for these differentiation agents. Down-regulation of the transcription factor E2F1 was a more reliable marker of the active differentiation agents of this class. This is a novel finding suggesting that a screen conducted for down-regulation of E2F1 protein might identify additional breast tumor differentiation agents.
5. NSC3852 is a promising new breast tumor differention agent that caused DNA damage and cell death in breast tumor cells to a greater degree than normal, immortalized breast cells. The cell death and DNA damage responses to this compound are dependent upon superoxide generation.NSC3852 is also modest direct histone deacetylase inhibitor.
6. NSC86371 is also a novel histone deacetylase inhibitor and this mechanism may contribute to its differentiation and growth arrest properties.NSC86371 also exhibits relatively selective pro-apoptotic activity in the tumor cells compared with the normal cells.

REPORTABLE OUTCOMES

Manuscripts published (4)

1. Zhou Q., Melkoumian, Z.K., Lucktong, A., Moniwa, M., Davie, J.R. and Strobl, J.S. (2000) Rapid induction of histone hyperacetylation and cellular differentiation in human breast tumor cell lines following degradation of histone deacetylase I . J. Biol. Chem. 275: 35256-35263.
2. Zhou Q, McCracken MA, Strobl JS (2002) Control of mammary tumor cell growth in vitro by novel cell differentiation and apoptosis agents. Breast Cancer Research and Treatment 75: 107-117.

3. Melkoumian ZK, Martirosyan AR, Strobl JS (2002)Myc protein is differentially sensitive to quinidine in tumor versus immortalized human breast epithelial cells. International Journal of Cancer 102: 60-69.

4. Martirosyan AR, Rahim-Bata R, Freeman AB, Clarke CD, Howard RI and Strobl JS (2004) Differentiation-inducing quinolines as experimental breast cancer agents in the MCF-7 human breast cancer model. Biochemical Pharmacology, in press.

Abstracts (13)

1. Melkoumian ZK and Strobl JS (1999) Suppression of c-myc mRNA levels and G0/G1 cell cycle arrest of MCF-7 and MCF-ras human breast cancer cells in response to quinidine. Proc. American Assoc. Cancer Res.,Abst.#188.
2. Zhou Q, Melkoumian ZK and Strobl JS (1999) Quinidine activates p21/WAF1/CIP1 expression and phosphorylation of pRb prior to onset of apoptosis in MCF-7 human breast cancer cells. Proc. American Assoc. Cancer Res.,Abst.#1503.
3. Zhou Q and Strobl JS (1999) Quinidine-induced hyperacetylation of histone H4 in MCF-7 human breast cancer cells. Amer. Soc. Cell Biol., Abst.#2569.
4. Melkoumian ZK and Strobl JS (1999) Quinidine suppresses c-myc promoter activity and induces differentiation of MCF-7 human breast cancer cells. Amer. Soc. Cell Biol. ,Abst. #2483.
5. Johnson DN, Melkoumian ZK, Lucktong A and Strobl JS (1999) Differentiation of human breast tumor cell lines by quinolines.Molecular Targets and Cancer Therapeutics,AACR-NCI-EORTC, Abst. #437.
6. Zhou Q, Moniwa M, Davie JR and Strobl JS (2000) Quinidine inhibits histone deacetylase I activity in MCF-7 human breast cancer cells,Proc. Amer. Assoc. Cancer Res. , Abst.#369.
7. Zhou Q and Strobl JS (2000) Role of heat shock proteins in the apoptotic response to an ion channel blocker, quinidine, OC15/ASBMB-ASPET, Abst. #LB131.
8. Melkoumian ZK, McCracken MA and Strobl JS (2001) Suppression of c-Myc protein and induction of cellular differentiation in human breast cancer cells but not in normal human breast epithelial cells by quinidine.Amer. Soc. Cell Biol. Abst. #70.
9. Martirosyan A, Zhou Q, Bata RR, McCracken MA, Freeman AB, Morato-Lara C, and Strobl JS (2001) New pharmacologic agents promote cell differentiation in human breast tumor cells. Amer. Soc. Cell Biol. Abst.#762.
10. Strobl JS, Zhou Q, Martirosyan AR (2002) Novel breast tumor differentiation agents. Era of Hope DOD Breast Cancer Research Program Meeting, Abst# 31-21. Poster presentation and Oral Symposium Presentation.
11. Martirosyan AR, Freeman AB, Strobl JS (2003) NSC3852, a new histone deacetylase inhibitor with breast tumor cell differentiation activity. Proc.Amer. Assoc. Cancer Res., Abst #R797.

12. Bata RR, Zhou Q and Strobl JS (2003) Combination drug therapy with antitumor antimalarials augment the differentiation response to breast cancer cells, Proc.Amer. Assoc. Cancer Res.,Abst.#3725.
13. Strobl JS, Martirosyan AR, Rahim-Bata R, Freeman A, Clarke C (2004) Experimental breast cancer differentiation agents NSC3852, NSC69603, NSC10010, and NSC305819. 1st ISC International Conference on Cancer Therapeutics, Molecular Targets, Pharmacology and Clinical Applications, Abst.#23.

Presentations (2)

1. Oral Presentation to the Era of Hope 2002 Meeting for the DOD Breast Cancer Research Program.
2. "Novel Differentiation Therapies for Breast Cancer" Basic Biomedical Science Department, Virgina College of Osteopathic Medicine, Blacksburg, VA, November, 2002.

Funding Record (5)

1. Strobl, JS (PI) Susan G. Komen Foundation BCTR0201140 "Breast Tumor Differentiation by Novel Agents Targeting Histone Deacetylase Ubiquitination and Heat Shock Proteins" Status: Superior rating, Alternate Grant Designation, Not-Funded.
2. Rahim, RR (PI) DAMD17-02-1-0622, Predoctoral Training Grant, "Augmentation of the Differentiation Response to Antitumor Antimalarials", 2002-2005 ($66,000).
3. Strobl, JS (PI) Susan G. Komen Foundation DISS0201686 "New Drug Candidates Target Rb/E2F/Myc Pathway" Status: Not-Funded.
4. Strobl, JS (PI) US Army BCRP-Concept Award "Breast Tumor Differentiation by HIF-1alpha Interference" Status: Not-Funded.
5. Strobl, JS (PI) WVU School of Medicine Internal Grant #1000161W "Breast Tumor Differentiation by Novel Agents Targeting Histone Deacetylase Ubiquitination and Heat Shock Protein Pathways" Status: Funded ($10,000).
6. Strobl, JS (PI) US Army BCRP-Idea Award BC030501 "Restoration of Retinoblastoma Protein Function in Breast Cancer" Status: Not Funded.

Training Opportunities Supported (8)

1. Zaroui Melkoumian completed the Ph.D. Degree in Pharmacology and Toxicology in 2001. She is conducting breast cancer research in the Cancer Laboratory of Cornell University.
2. Qun Zhou, M.D. completed the Ph.D in Pharmacology and Toxicology and received his degree in 2002. He completed postdoctoral training in cancer research at the Mary Babb Randolph Cancer Center of West Virginia University and will now pursue breast cancer research at Johns Hopkins University.
3. Meredith McCracken completed the Ph.D. degree in Genetics and Developmental Biology in 2002. Dr. McCracken (now Dr. Meredith Morgan)

is pursuing postdoctoral research at the University of Michigan in Ann Arbor, Department of Radiation Oncology.

4. Anna Martirosyan, M.D. will receive her Ph.D in Pharmacology and Toxicology, August, 2004; this grant provided stipend and supplies for her research. She will pursue postdoctoral training in Toronto, Canada.
5. Rayhana Rahim-Bata is studying for the Ph.D. degree in Pharmacology and Toxicology; this grant provided supplies for her research.
6. Charles Clarke, undergraduate Biology student (WVU) summer research experience and training in cancer cell biology and drug development; this grant provided supplies for his research. Mr. Clarke is currently pursuing the M.D. degree at Ohio State University School of Medicine.
7. Andrew Freeman, undergraduate Biology student at West Virginia Weslyan University received research experience and training in cancer cell biology for 2 summers. Mr. Freeman is currently enrolled in the M.D. program in the West Virginia University School of Medicine.
8. Ms. Rachel Howard, undergraduate Biology student at Washington and Jefferson College in Washington, PA received research training in cancer biology through this grant.

Personnel Receiving salary support from this award

1. Jeannine S. Strobl
2. Anna R. Martirosyan

CONCLUSIONS

HDAC1 continues to be viewed as important new target for new cancer drug discovery. Other investigators have shown that direct inhibition of HDAC1 enzyme activity produces tumor cell differentiation, and some agents of this type are being introduced into clinical trials. By stimulating ubiquitination and proteasomal degradation of HDAC1 protein in MCF-7 cells, our experiments show that the antimalarials chloroquine and quinidine modulate the biological activity of this important new cancer drug target in breast tumor cells. A new mode of action for breast tumor differentiation, regulation of HDAC1 protein levels, has been identified by our research.

We identified several other new quinoline breast tumor differentiation agents by screening the NCI compound library. Our results indicate that each appears to act through different mechanisms in MCF-7 cells. NSC 3852 is a direct inhibitor of HDAC enzymatic activity that does not stimulate HDAC1 ubiquitination. NSC382 has a novel activity to cause DNA damage and apoptosis via the generation of superoxide radicals in an NADPH-dependent mechanism. *In silico* (computer simulated-analysis) of the absorption-distribution properties of NSC 3852 indicates that this compound has promise for further drug development. It is a low molecular weight compound (M.W. 174) with less than 5 hydrogen bond acceptors and only one hydrogen bond donor. It has two potential routes of absorption via paracellular (between cells) and passive diffusion, and is highly unlikely to be a substrate for the multi-drug resistance pump. Future work will focus on the further development of NSC 3852 as a therapeutic agent alone and in

combination with chloroquine for breast cancer treatment. This agent will serve as a prototype for additional drug development on the basis of its relative selectivity for tumor vs. immortalized breast cells, its novel mechanisms of action and its favorable drug absorption profile.
NSC 10010 actively promotes breast tumor differentiation agent, but does not stimulate HDAC1 ubiquitination or inhibit HDAC enzyme activity. This highly toxic agent is predicted to act as a DNA intercalating agent and supports literature reports that DNA intercalating agents sometimes promote cell differentiation.

NSC86371 is another promising quinoline breast tumor differentiation drug prototype. This compound is an HDAC activity inhibitor and induced apoptosis in the breast tumor cell lines more readily than in the immortalized breast cells.

NSC305819 is quinoline differentiation agent we identified in our screens that was structurally the most similar to chloroquine; as did chloroquine, NSC305819 displayed favorable drug absorption properties. However, in cell growth and apoptosis assays, NSC305819 was less active than the reference compound chloroquine and therefore development of this agent is not a high priority.

NSC69603 is a quinoline differentiation agent that remarkably reduced levels of the transcription factor E2F1. This compound is of interest for its ability to relatively selectively induce apoptosis in the immortalized cells relative to the tumor cells. This observation should be investigated further because it might identify a critical biochemical difference distinguishing the immortalized and the tumor cells that subsequently could be used to design selective tumor differentiation agents.

In summary, the identification of novel breast tumor differentiation agents with different modes of action opens the possibility for new drug development and new combinations of drugs to achieve even more effective control of tumor growth through the induction of cell differentiation. This was the goal of this research grant and we think that we have several promising leads for the development breast tumor differentiation agents. The CoMFA approach of the current compound data base failed to provide a predictive model for the refinement of quinolines as breast tumor differentiation agents. The structural diversity of compounds within this data base was such that compounds capable of stimulating differentiation through multiple mechanisms were included, thus explaining the failure to define a single critical pharmacophore.

REFERENCES

none

APPENDICES

Figure 1. (A) HDAC1 ubiquitination in MCF-7 cells; (B) HDAC1 protein levels in MCF-7 cells.

Figure 2. Histone H4 Acetylation in MCF-7 cells treated with NSC3852

Manuscript 1. Zhou, et al. (2000) Journal of Biological Chemistry 275: 35256-35263.

Manuscript 2 Zhou, et al. (2002) Breast Cancer Research and Treatment 75: 107-117.

Manuscript 3. Melkoumian, et al. (2002) International Journal of Cancer 102: 60-69.

Manuscript 4. Martirosyan, et al. (2004) Biochemical Pharmacology, in press.

Figure 1

A

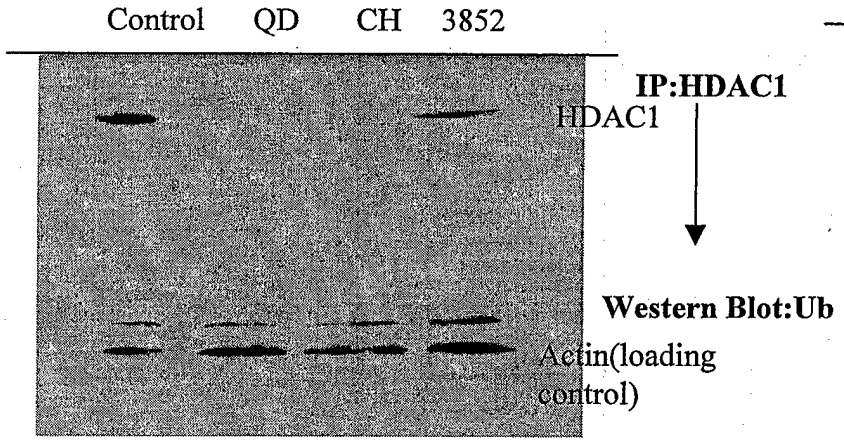

Effect of Antimalarials on the expression of HDAC1 protein in MCF-7 Cells. MCF-7 cells were untreated (control) or treated with antimalarials for 1 h. Total protein extracts(60ug) from each treatment indicated were subjected to 7.5% SDS-PAGE and blotted with anti-HDAC1.

B

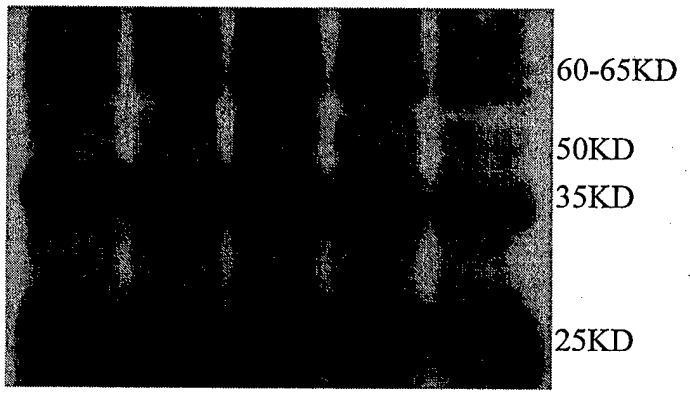

Effect of Antimalarials on HDAC1-Ub in MCF-7 Cells. Cells were untreated (control) or treated with antimalarials for 1 h. Cell lysates (200ug) were immunoprecipitated with anti-HDAC1, subjected to SDS-PAGE, and blotted with anti-Ub. QD = 90 uM Quinidine, CL = 33 uM Chloroquine.

Figure 2. Histone H4

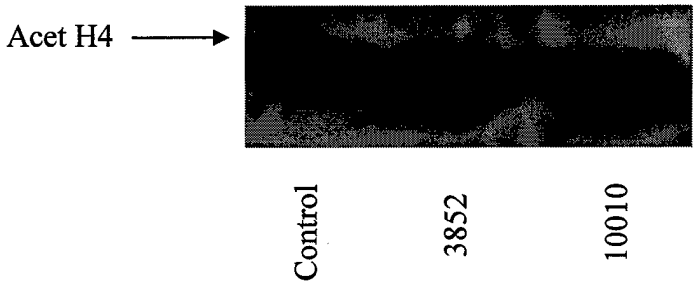

Total histones were extracted from MCF-7 cells
Treated with NSC3852 or NSC10010 for 24 hours.
Acetylated Histone H4 was measured by Western blotting
Using antiserum specific to the acetylated form of H4. Data show
A modest increase in histone H4 acetylation in response to drug treatment

THE JOURNAL OF BIOLOGICAL CHEMISTRY
Vol. 275, No. 45, Issue of November 10, pp. 35256–35263, 2000
Printed in U.S.A.

Rapid Induction of Histone Hyperacetylation and Cellular Differentiation in Human Breast Tumor Cell Lines following Degradation of Histone Deacetylase-1*

Received for publication, April 12, 2000, and in revised form, August 2, 2000
Published, JBC Papers in Press, August 10, 2000, DOI 10.1074/jbc.M003106200

Qun Zhou‡, Zaroui K. Melkoumian‡, Ann Lucktong‡, Mariko Moniwa§, James R. Davie§, and Jeannine S. Strobl‡¶

From the ‡Department of Pharmacology & Toxicology, Robert C. Byrd Health Sciences Center, West Virginia University, Morgantown, West Virginia 26506 and §Manitoba Institute of Cell Biology, University of Manitoba, Winnipeg R3E 0V9, Canada

Quinidine inhibits proliferation and promotes cellular differentiation in human breast tumor epithelial cells. Previously we showed quinidine arrested MCF-7 cells in G_1 phase of the cell cycle and led to a G_1 to G_0 transition followed by apoptotic cell death. The present experiments demonstrated that MCF-7, MCF-7*ras*, T47D, MDA-MB-231, and MDA-MB-435 cells transiently differentiate before undergoing apoptosis in response to quinidine. The cells accumulated lipid droplets, and the cytokeratin 18 cytoskeleton was reorganized. Hyperacetylated histone H4 appeared within 2 h of the addition of quinidine to the medium, and levels were maximal by 24 h. Quinidine-treated MCF-7 cells showed elevated $p21^{WAF1}$, hypophosphorylation and suppression of retinoblastoma protein, and down-regulation of cyclin D1, similar to the cell cycle response observed with cells induced to differentiate by histone deacetylase inhibitors, trichostatin A, and trapoxin. Quinidine did not show evidence for direct inhibition of histone deacetylase enzymatic activity *in vitro*. HDAC1 was undetectable in MCF-7 cells 30 min after addition of quinidine to the growth medium. The proteasome inhibitors MG-132 and lactacystin completely protected HDAC1 from the action of quinidine. We conclude that quinidine is a breast tumor cell differentiating agent that causes the loss of HDAC1 via a proteasomal sensitive mechanism.

Histone deacetylase (HDAC)[1] proteins comprise a family of related proteins that act in conjunction with histone acetyltransferase proteins to modulate chromatin structure and transcriptional activity via changes in the acetylation status of histones. Histones H3 and H4 are the principal histone targets of HDAC enzymatic activity, and these histones undergo acetylation at lysine residues at multiple sites within the histone tails extending from the histone octamer of the nucleosome core. The association of HDAC proteins with mSin3, N-CoR, or SMRT and other transcriptional repressors has led to the hypothesis that HDAC proteins function as transcriptional corepressors (reviewed in Ref. 1). The spectrum of genes that show alterations in gene transcription rates in response to decreased HDAC activity is quite restricted (2). Yet, small molecule inhibitors of the enzyme histone deacetylase (HDAC) such as trichostatin A (TSA), superoylanilide hydroxamic acid (SAHA), trapoxin, and phenyl butyrate cause major alterations in cellular activity including the induction of cellular differentiation and apoptosis (3–5). Trichostatin A, SAHA, and trapoxin stimulate histone acetylation by acting as direct inhibitors of HDAC enzyme activity (6). Trichostatin A, SAHA, and trapoxin possess lysine-like side chains and act as chemical analogs of lysine substrates. Molecular models based upon the x-ray crystal structure of an HDAC-like protein indicate that trichostatin A and SAHA can bind within the active site of the HDAC enzyme and interact with a zinc metal ion within the catalytic pocket that is critical for enzymatic activity (7). Trapoxin is an irreversible HDAC enzyme inhibitor (8).

Much remains to be learned about the biochemical events subsequent to HDAC inhibition that lead to cell cycle arrest, cellular differentiation, and apoptosis. However, a spectrum of biological responses characteristic of HDAC inhibitors has emerged, including cell cycle arrest in G_1, elevated $p21^{WAF1}$ expression, hypophosphorylation of retinoblastoma protein (pRb), hyperacetylation of histones, particularly H3 and H4, and apoptosis. Histone hyperacetylation is directly linked to the activation of p21 transcription and is p53-independent (5). This observation provides an important link between HDAC inhibition and cell cycle arrest because $p21^{WAF1}$ plays a critical role in causing G_1 cell cycle arrest via inhibition of the G_1 cyclin-dependent kinase family (9). Overexpression of $p21^{WAF1}$ has also been associated with apoptosis, but the mechanism of $p21^{WAF1}$ induction of apoptosis requires further investigation (10).

Cancer therapy that targets the activity of genes or gene products controlling cell cycle progression, differentiation, and apoptosis is a promising new strategy. Because HDAC inhibitors regulate the cell cycle and cause both cellular differentiation and apoptosis, they comprise an interesting group of compounds with potential for development into a new category of clinically significant anti-tumor agents. Single, key protein targets for "gene-regulatory chemotherapy" are difficult to identify due to the existence of parallel, functionally overlap-

* This work was supported by West Virginia University School of Medicine, the Spurlock Cancer Research Fund, the Susan G. Komen Breast Cancer Foundation, Grants DAMD 17-99-1-9447 and DAMD 17-00-1-0500, and the Medical Research Council of Canada Grant MT-9186. The costs of publication of this article were defrayed in part by the payment of page charges. This article must therefore be hereby marked "*advertisement*" in accordance with 18 U.S.C. Section 1734 solely to indicate this fact.

¶ To whom correspondence should be addressed: Dept. of Pharmacology and Toxicology, Robert C. Byrd Health Sciences Center, West Virginia University, Morgantown, WV 26506-9223. Tel.: 304-293-7151; E-mail: jstrobl@hsc.wvu.edu.

[1] The abbreviations used are: HDAC, histone deacetylase; DMEM, Dulbecco's modified Eagle's medium; FBS, fetal bovine serum; MG-132, carbobenzoxy-L-leucyl-L-leucyl-L-leucinal; PBS, phosphate-buffered saline; pRb, retinoblastoma protein; SAHA, superoylanilide hydroxamic acid; TSA, trichostatin A; HRP, horseradish peroxidase; HMEC, human mammary epithelial cells; ER, estrogen receptor; MTS, 3-(4,5-dimethylthiazol-2-yl)-5-(3-carboxymethoxyphenyl)-2-(4-sulfophenyl)-2*H*-tetrazolium; CDK, cyclin-dependent kinase.

ping signaling cascades. For this reason, use of cancer therapies that target multiple intracellular signaling pathways, such as observed with the HDAC inhibitors, is an intriguing approach that addresses the problem of redundancy in growth signaling pathways. In this regard, the HDAC inhibitor phenyl butyrate was recently shown to have clinical anti-tumor activity (11).

Quinidine is a natural product therapeutic agent originally used as an anti-malarial and as an anti-arrhythmic agent. Previous studies with human breast tumor cell lines demonstrated that quinidine (90 μM) is an anti-proliferative agent as well. Quinidine arrested cells in early G_1 phase and induced apoptosis by 72–96 h in MCF-7 cells (12), but the biochemical basis for the anti-proliferative effect of quinidine was not well understood. To clarify the molecular mechanisms of the anti-proliferative activity of quinidine, we investigated the effects of quinidine on histone acetylation and cell cycle regulatory proteins. In this report, we show that quinidine causes hyperacetylation of histone H4, down-regulation of HDAC1 protein levels, and cellular differentiation in a panel of human breast tumor cell lines. We conclude that quinidine is a novel differentiating agent that stimulates histone hyperacetylation as a result of HDAC1 protein degradation.

MATERIALS AND METHODS

Cell Culture—Permanent cell lines derived from patients with breast carcinomas were used in these studies. MCF-7 cells, passage numbers 40–55, MCF-7*ras* (13), T47D, MDA-MB-231, and MDA-MD-435 cells were maintained in Dulbecco's modified Eagle's medium (DMEM) (Bio-Whittaker, Walkersville, MD) supplemented with 10% heat-inactivated fetal bovine serum (FBS) (HyClone Laboratories, Inc., Logan, Utah), 2 mM glutamine, and 40 μg/ml gentamicin. Experiments were performed in this medium supplemented with 5% FBS. The cells were maintained at 37 °C in a humidified atmosphere of 93% air, 7% CO_2. After 6 days, cells became about 70–80% confluent and were passaged at a 1:5 ratio (MCF-7) or at a 1:10 ratio (all others). Normal human mammary epithelial cells (HMEC) were obtained from Clonetics, San Diego, CA, and were grown according to directions of the suppliers. Cells were grown from frozen stocks and used for 1–3 passages. Quinidine, TSA, and all-*trans*-retinoic acid were purchased from Sigma. The cell-permeant proteasome inhibitors, MG-132 and lactacystin, were purchased from Calbiochem.

Growth Inhibition Assays—Growth inhibition by cell numbers was assayed by plating cells in 35-mm^2 dishes ($1–1.5 \times 10^5$) containing DMEM, 5% FBS plus quinidine (90 μM). Viable cells were counted using a hemocytometer, and trypan blue (0.02%) exclusion was used as an indicator of viability. Cell growth was also monitored in a 96-well plate format using the One Solution Cell Proliferation Assay (Promega, Madison, WI), which is based upon metabolic bioreduction of a tetrazolium compound (Owen's reagent) to a colored formazan product that absorbs light at 490 nm. The plating density for the 96-well dishes (cells/well) was varied depending upon the relative growth rates of the cell lines as follows: HMEC (2000), MCF-7 (1000), MDA-MB-231 (500), T47D (1500), and MCF-7*ras* (500). The One Cell Proliferation Assay Reagent was added to each well and incubated for 2 h at 37 °C. Absorbance (490 nm) was read using a Molecular Devices PC340 (Sunnyvale, CA).

Microscopic Imaging—Cells were plated (1×10^5) on sterile coverslips in 35-mm^2 dishes and grown for 96 h in DMEM, 5% FBS supplemented with either 10 μM all-*trans*-retinoic acid (in 0.01% ethanol) or 90 μM quinidine (in H_20). Control cells were grown in medium containing a final concentration of 0.01% ethanol. The presence of ethanol had no effect upon lipid droplet accumulation compared with cells grown in DMEM, 5% FBS. Cells were fixed in 3.7% formaldehyde/PBS, rinsed in PBS (PBS: 140 mM NaCl, 2 mM KCl, 80 mM $Na_2HPO_4 \cdot 7H_2O$, 1.5 mM KH_2PO_4, pH 7.0), then treated briefly with 0.4% Triton X-100 in PBS. After rinsing three times in PBS, the cells on coverslips were incubated for 30 min at 37 °C with a primary antibody to cytokeratin 18 (1:1 dilution, provided by Dr. Guillaume van Eys, Maastricht University), rinsed, and incubated (30 min/37 °C) with Texas Red conjugated secondary antibody (goat anti-mouse IgG, Sigma). Alternatively, cells were incubated with fluorescein-phalloidin (1:200 dilution of a-5 μg/0.1 ml solution, Sigma) in the dark for 40 min at room temperature, rinsed, and incubated for 5 min (room temperature) with the fluorescent lipid stain, Nile Red (1:10,000 dilution of a 1 mg/ml acetone solution, Sigma) (14–15). All coverslips were rinsed in PBS and mounted with Fluoromount-G containing 2.5% *N*-propyl galate. Images were obtained using a Zeiss Axiovert 100 M confocal microscope (× 63 objective).

Immunoblotting—Cells were harvested from confluent T-75 flasks and subcultured (1×10^6) in 60-mm^2 dishes. On subcultivation, this confluent population of cells (85% in G_1) synchronously proceeded through the cell cycle. To prepare whole cell lysates, the cells were harvested at the times indicated by scraping into ice-cold buffer (50 mM Tris-HCl, 0.25 M NaCl, 0.1% (v/v) Triton X-100, 1 mM EDTA, 50 mM NaF, and 0.1 mM Na_3VO_4, pH 7.4). Protease inhibitors (protease inhibitor mixture, Roche Molecular Biochemicals) were added immediately. Cell lysates were centrifuged in an Eppendorf microcentrifuge (14,000 rpm, 5 min) at 4 °C, and the supernatants were used in immunoblotting experiments.

Histones were prepared from cells grown at a density of 1×10^7/T-162 flask. To harvest the cells, the flasks were placed on ice, and the growth medium was removed. Following a quick rinse with ice-cold PBS, cells were scraped into 1 ml of ice-cold lysis buffer (10 mM Tris-HCl, 50 mM sodium bisulfite, 1% Triton X-100 (v/v), 10 mM $MgCl_2$, 8.6% sucrose, pH 6.5) and nuclei released by Dounce homogenization. The nuclei were collected by centrifugation (3,000 rpm, 10 min, SS-34 rotor) and washed three times with the lysis buffer. Histones were extracted from the crude nuclear pellets using the procedure of Nakajima *et al.* (16). The pellets were resuspended in 0.1 ml of ice-cold sterile water using a vortex and concentrated H_2SO_4 to 0.4 N was added. The preparation was incubated at 4 °C for 1 h and then centrifuged (17,000 rpm, 10 min, Sorvall SS-34 rotor). The supernatant containing the extracted histones was mixed with 10 ml of acetone, and the precipitate was obtained after an overnight incubation at −20 °C, collected, and air-dried. The acid-soluble histone fraction was dissolved in 50 μl of H_2O and stored at −70 °C.

The protein concentration of the whole cell lysate supernatants or histone preparations was determined using the BCA protein assay (Pierce) and bovine serum albumin as a standard. Equal amounts of protein were loaded onto SDS-polyacrylamide gels. Molecular weights of the immunoreactive proteins were estimated based upon the relative migration with colored molecular weight protein markers (Amersham Pharmacia Biotech). Proteins were transferred to polyvinylidene difluoride membranes (NOVEX, San Diego, CA) and blocked at 4 °C using 5% nonfat milk blocking buffer (1 M glycine, 1% albumin (chicken egg), 5% non-fat dry milk, and 5% FBS) overnight. The membranes were incubated with primary antibodies for 3 h at room temperature. The antibody sources were as follows: mouse monoclonal anti-p27 (F-8, SC-1641), rabbit polyclonal anti-CDK4 (C-22), goat polyclonal anti-HDAC1 (N-19, SC-6299), all from Santa Cruz Biotechnology (Santa Cruz, CA); mouse monoclonal anti-pRb (14001A) from PharMingen (San Diego, CA); mouse monoclonal anti-cyclin D1 (NCL-cyclin D1, 113105) from Novocastra (Burlingame, CA); mouse monoclonal anti-p16 (Ap-1), p21 (WAF1,Ap-1), p53 (Ap-6) from Calbiochem; and anti-acetylated histone H4 antibody (rabbit polyclonal, Upstate Biotechnology Inc.). The primary antibodies were diluted at 1:500 in Western washing solution (0.1% non-fat dry milk, 0.1% albumin (chicken egg), 1% FBS, 0.2% (v/v) Tween 20, in PBS, pH 7.3). The antigen-antibody complexes were incubated for 1 h at room temperature with horseradish peroxidase (HRP)-conjugated secondary antibodies (goat IgG-HRP (SC-2020), rabbit IgG-HRP (SC-2004), or mouse IgG-HRP (SC-2005) from Santa Cruz Biotechnology) at a final dilution of 1:3000 in Western washing solution. After washing three times with Tris-buffered saline (10 mM Tris-HCl, pH 7.5, 0.5 M NaCl, and 0.05% (v/v) Tween 20), antibody binding was visualized using enhanced chemiluminescence (SuperSignal West Pico, Pierce) and autoradiography.

In Vitro HDAC Activity Assay—Quinidine HCl was added to a chicken erythrocyte cellular extract, which contained HDAC activity, at concentrations of 90 μM (18). HDAC assays were performed as described in Hendzel *et al.* (17). Briefly, the cellular extract was incubated with 500 μg of acid-soluble histones isolated from [^{3}H]acetate-labeled chicken erythrocytes for 60 min at 37 °C. Reactions were terminated by addition of acetic acid/HCl to a final concentration of 0.12/0.72 N. Released [^{3}H]acetate was extracted using ethyl acetate and quantified by scintillation counting. Samples were assayed three times, and the non-enzymatic release of label was subtracted to obtain the reported values.

RESULTS

Hyperacetylation of Histone H4—Antibodies that recognize acetylated forms of histone H4 have been used as a probe for agents that cause histone hyperacetylation (19). In Western blot experiments, we compared the ability of quinidine to cause

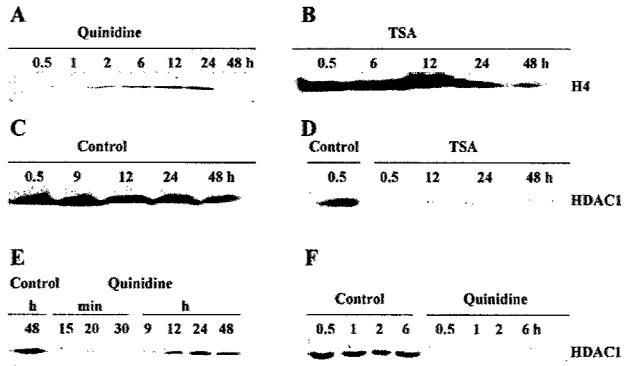

FIG. 1. **Histone hyperacetylation in MCF-7 cells.** *A,* histones were extracted from cells grown in the presence of 90 μM quinidine for 0.5, 1, 2, 6, 12, 24, or 48 h; histones (20 μg/lane) were electrophoresed in 15% polyacrylamide gels containing 1% SDS and assayed for the presence of acetylated H4 by immunoblotting. *B,* histones were extracted from cells grown in the presence of 300 nM TSA for 0.5, 6, 12, 24, or 48 h; 20 μg of histone/lane were electrophoresed and analyzed for acetylated histone H4 by immunoblotting. *C* and *D,* HDAC1 protein in whole cell lysates was prepared from control MCF-7 cells at 0.5, 9, 12, 24, or 48 h (*C*) or cells treated with 300 nM TSA 0.5, 12, 24, or 48 h (*D*); 50 μg of protein/lane were electrophoresed in 12% polyacrylamide gels containing 1% SDS and assayed for HDAC1 protein by immunoblotting. *E* and *F,* HDAC1 protein in whole cell extracts from cells grown in the presence of 90 μM quinidine for 15, 20, and 30 min or 9, 12, 24, or 48 h (*E*) or 0.5, 1, 2, or 6 h (*F*); extracts were electrophoresed (50 μg protein/lane) and assayed for HDAC1 protein by immunoblotting.

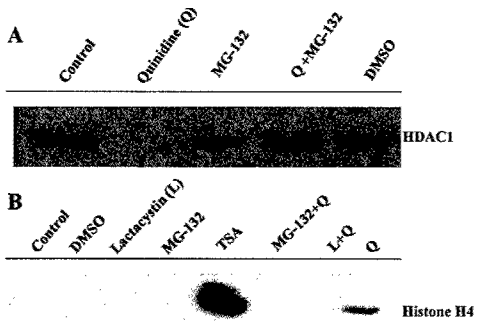

FIG. 2. **Protection of HDAC1 protein by proteasome inhibitors.** *A,* MCF-7 cells were released from confluency and subcultured in normal growth medium supplemented with 30 μM MG-132 in 0.1% Me_2SO (*DMSO*), 90 μM quinidine plus 0.1% Me_2SO or 0.1% Me_2SO alone as indicated. Cells were harvested after 30 min, and Western blot analysis of HDAC1 protein was performed as detailed in methods. *B,* MCF-7 cells were cultured as described above or with lactacystin (3 μM in 0.1% Me_2SO) except were harvested after 24 h and analyzed for the presence of immunoreactive acetylated histone H4.

hyperacetylation of H4 in MCF-7 cells with that of TSA, an established HDAC inhibitor, known to inhibit proliferation in MCF-7 cells (20). H4 acetylation in response to TSA was rapid (within 0.5 h) (Fig. 1*B*) and reached a maximum around 12 h. Some level of H4 acetylation persisted in the TSA-treated cells for 48 h. In cells treated with quinidine (Fig. 1*A*), detectable H4 acetylation was slightly delayed and could be seen at 2 h but not 1 h of treatment. H4 acetylation was maximal between 12 and 24 h but then sharply fell to an undetectable level at 48 h. Hyperacetylation of H4 was a transient response to both agents. Acetylated H4 is present in MCF-7 cells but under the conditions of Western blotting and immunochemical staining was not detected in control cells (data not shown).

HDAC1 is expressed in MCF-7 cells, and this enzyme contributes to the control of histone deacetylation rates (18). Quinidine caused the rapid disappearance of HDAC1 from MCF-7 cells. HDAC1 protein levels in quinidine-treated cells were reduced after 15–20 min compared with control cells, and HDAC1 protein was undetectable between 30 min and 6 h (Fig. 1, *E* and *F*). Partial restoration of HDAC1 protein occurred beginning at 9 h of treatment, but even after 48 h, HDAC1 levels in quinidine-treated cells were still less than control cells. Levels of HDAC1 protein in control MCF-7 cells were relatively constant during this time (Fig. 1*C*). TSA-treated MCF-7 cells also showed reduced levels of HDAC1 protein as early as 30 min after drug addition, and the reduced HDAC1 protein level was maintained through 48 h (Fig. 1*D*). The data indicate that loss of HDAC1 protein might contribute to the H4 acetylation response to both TSA and quinidine. However, HDAC1 protein levels were never reduced by TSA below the level of detection as was observed with quinidine. In light of the more extensive H4 acetylation response to TSA than quinidine, we conclude that the direct inhibition of HDAC1 catalytic activity by TSA remains an important component of the H4 acetylation response *in vivo*. In addition, the time course of the HDAC1 response to quinidine and TSA differ. In response to quinidine, there is initially a more marked decrease in HDAC1 protein levels but a more rapid recovery. TSA treatment caused a sustained reduction in HDAC1 protein levels through 48 h.

To determine if the rapid loss of HDAC protein in the presence of quinidine were mediated through the 26 S proteasome pathway, MCF-7 cells were treated simultaneously for 30 min with quinidine and MG-132 (30 μM), an inhibitor of the 26 S proteasome. Cells treated with 90 μM quinidine showed a complete loss of HDAC1 protein, which was prevented when MG-132 and quinidine were added simultaneously (Fig. 2*A*). Treatment with the solvent, Me_2SO, or MG-132 in solvent (0.1%) caused a modest reduction in the level of HDAC1 protein. These reductions in HDAC1 did not elicit a detectable stimulation of H4 acetylation, and we suggest that other HDAC enzymes present in MCF-7 cells, insensitive to Me_2SO, could compensate for the lost HDAC1 in the maintenance of deacetylated histone H4. This action of quinidine on HDAC1 protein was not reflected in a general decrease in cellular protein content (12), nor were all cell cycle regulatory proteins downregulated in MCF-7 cells in the presence of quinidine (*e.g.* $p21^{WAF1}$ and p53 protein, Fig. 3). Additional studies are required to define the spectrum of proteins affected by quinidine in a proteasome-sensitive manner. Quinidine (90 or 250 μM) did not inhibit the activity of the isolated chicken erythrocyte HDAC1 enzyme *in vitro* (data not shown) suggesting that quinidine caused histone hyperacetylation by eliciting a rapid and transient loss of HDAC1 protein without a direct inhibition of the HDAC enzyme. The suppression of HDAC protein levels in MCF-7 cells was accompanied by a decrease in HDAC enzyme activity in the cell extracts. Histone acetylation and depressed HDAC1 protein levels persisted for approximately 48 h in the presence of quinidine. When MCF-7 cells were exposed to quinidine for 24 h in the presence of either MG-132 or lactacystin, there was no detectable H4 acetylation (Fig. 2*B*). These results support the idea that quinidine-induced loss of HDAC1 protein is involved in the H4 acetylation response via a proteasomal sensitive pathway.

G_1 Phase Cell Cycle Regulatory Profile in MCF-7 Cells—G_1 cell cycle arrest is characteristic of HDAC inhibitors, and reports of alterations in several cell cycle proteins in cells exposed to HDAC inhibitors, particularly the elevation of the $p21^{WAF1}$ protein, are numerous (21–23). It was of interest to determine whether $p21^{WAF1}$ and other key cell cycle regulatory proteins such as the retinoblastoma protein (pRb) and the G_1 phase cyclin-dependent kinase activator, cyclin D1, were targets of quinidine action in MCF-7 cells. Western blotting analysis showed that by 12 h the levels of $p21^{WAF1}$ were increased in response to quinidine treatment approximately 11-fold, and this elevated level of protein expression persisted through 48 h.

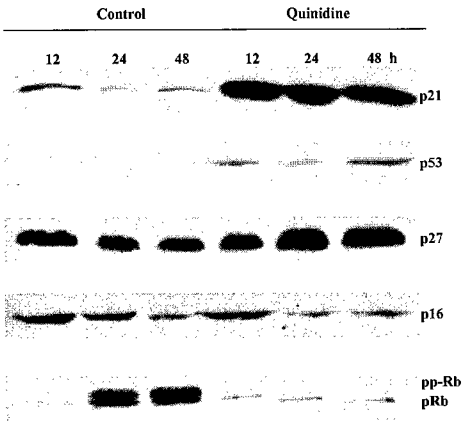

FIG. 3. **G_1 cell cycle proteins in MCF-7 cells.** Cells released from confluency were plated into control medium or medium containing 90 μM quinidine. Whole cell lysates were prepared 12, 24, or 48 h after plating and assayed by immunoblotting for the cyclin-dependent kinase inhibitors, $p21^{WAF1}$ (n = 3), p27 (n = 1), p16 (n = 3), and p53 (n = 3) after electrophoresis of 50 μg of protein/lane through 12% SDS-polyacrylamide gels. pRb protein was immunoprecipitated from 500 μg of whole cell lysate protein using an antibody that recognizes phosphorylated and non-phosphorylated pRb (56). This entire immunoprecipitate was electrophoresed in a 7.5% SDS-polyacrylamide gel and immunoblotted using this same antibody. Results shown are typical of two independent analyses.

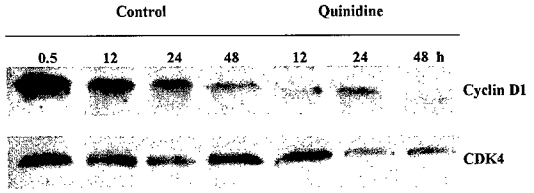

FIG. 4. **Cyclin D-CDK4 in MCF-7 cells.** Confluent MCF-7 cells were subcultured in control medium or medium containing 90 μM quinidine. Whole cell lysates were prepared 0.5, 12, 24, and 48 h after subculture. Equal protein aliquots (50 μg/lane) were electrophoresed in 12% SDS-polyacrylamide gels and assayed for cyclin D1 and CDK protein levels by immunoblotting. Results shown are representative of three independent experiments.

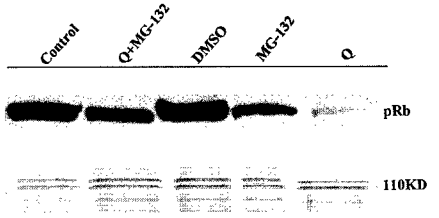

FIG. 5. **Proteasome inhibitor modulates retinoblastoma protein levels.** Confluent MCF-7 cells were subcultured in the presence of 90 μM quinidine, 30 μM MG-132, or quinidine + MG-132 for 24 h, then harvested, and whole cell extracts (100 μg/lane) were analyzed for pRb. A Coomassie Blue-stained protein is shown as the loading control.

A small, less than 2-fold increase in p27 levels was observed in cells exposed to quinidine for 24–48 h, whereas levels of p16 were unchanged (Fig. 3). Quinidine treatment decreased cyclin D1 and CDK4 protein levels after 12 h of treatment (Fig. 4), indicating that the cyclin-dependent kinase inhibitor, $p21^{WAF}$, as well as an important G_1 phase target of $p21^{WAF1}$, the cyclin D1-CDK4 complex, are early targets of quinidine in MCF-7 cells. This profile of activity is consistent with the observed cell cycle arrest of quinidine-treated MCF-7 cells in mid-G_1 phase (12).

In MCF-7 cell extracts probed using anti-pRb antibodies, two separate but closely migrating bands were distinguishable. The upper band contained more highly phosphorylated pRb, and the lower band contained unphosphorylated or hypophosphorylated pRb. Control cells showed a faint pRb signal at 12 h, typical of cells in early G_1 phase, and increased expression of both phosphorylated and unphosphorylated pRb at 24 and 48 h. Quinidine-treated MCF-7 cells had no detectable hyperphosphorylated pRb at any time point examined, and total levels of pRb protein failed to increase with progression through G_1 phase as seen in the control, proliferating cells (Fig. 3). The decrease in pRb phosphorylation level was predictable based on the increase in $p21^{WAF1}$ and decreased levels of both cyclin D1 and CDK4 (Fig. 4). In addition, Nakanishi *et al.* (24) showed that $p21^{WAF1}$ can bind pRb protein and block its phosphorylation. However, the actions of quinidine upon $p21^{WAF1}$ and cyclin D-CDK4 activity do not explain why the levels of total pRb protein were so low. Reductions in the cellular content of phosphorylated pRb protein in MCF-7 cells by quinidine is an important additional level of cell cycle control that effectively attenuates progression of cells out of G_1 phase and has been reported in other tumor cell lines in response to HDAC inhibition (22). In Fig. 5 we show data suggesting that the 26 S proteasome pathway regulates the total pRb content. MCF-7 cells incubated for 24 h in MG-132 or MG-132 plus quinidine had more total pRb than cells incubated with quinidine alone. Thus, quinidine promoted the loss of both HDAC1 and pRb, and inhibition of the 26 S proteasome pathway restored the levels of both of these proteins to that seen in the untreated cells. We have no direct evidence that quinidine promotes the proteasomal degradation of either protein. We hypothesize that quinidine may direct degradation of HDAC1 by the proteasome or, alternatively, quinidine might stimulate the proteasomal degradation of other regulatory factor(s) that act to maintain HDAC1 and pRb protein levels.

MCF-7 cells express wild-type p53 protein. Normal p53 is a short lived protein that is maintained at low levels, but in response to cell stress or DNA damage, p53 is stabilized and accumulates in the nucleus where it functions as a transcription factor inducing $p21^{WAF}$, G_1 cell cycle arrest, and apoptosis (25). Wild-type p53 down-regulates pRb levels in MCF-7 cells (26). Although Saito *et al.* (22) showed that p53 is not required for pRb down-regulation by HDAC inhibitors in all cell lines, quinidine-treated MCF-7 cells have elevated p53 levels (5–7-fold) (Fig. 3). Thus, p53 could contribute to the maintenance of the G_1 cell cycle arrest in MCF-7 by sustaining $p21^{WAF1}$ protein levels and suppressing pRb protein levels.

Growth Arrest and Cellular Differentiation in Human Breast Tumor Cell Lines—In contrast to MCF-7 cells, human breast tumor cell lines T47D, MDA-MB-231, and MDA-MB-435 express p53 proteins with distinct point mutations (27). To test for a requirement of p53, this panel of human breast tumor cell lines was exposed to quinidine, and the effects of quinidine on cell growth were compared (Fig. 6). The data shown are viable cell numbers/well, bioreductive metabolism/well, or both. In all four cell lines growth was suppressed in a concentration-dependent fashion between 10 and 90 μM quinidine, and maximal growth inhibition was observed at ~90 μM quinidine (data not shown). These data showed that growth suppression by quinidine is a p53-independent response. It is interesting that quinidine was not overtly cytotoxic in HMEC, a line of normal human mammary cells (28).

Evidence that quinidine elicited cellular differentiation in MCF-7 human breast tumor cells in conjunction with the inhibition of cell growth was obtained using maximally effective concentrations of quinidine or retinoic acid (data not shown). Antibodies directed against cytokeratin 18 (29) were used to probe the organization of the cytoskeleton (Fig. 7). In these studies, all-*trans*-retinoic acid (10 μM) was used to compare the differentiation response (30). Control MCF-7 cells showed expression of cytoplasmic cytokeratin 18 in a disorganized fash-

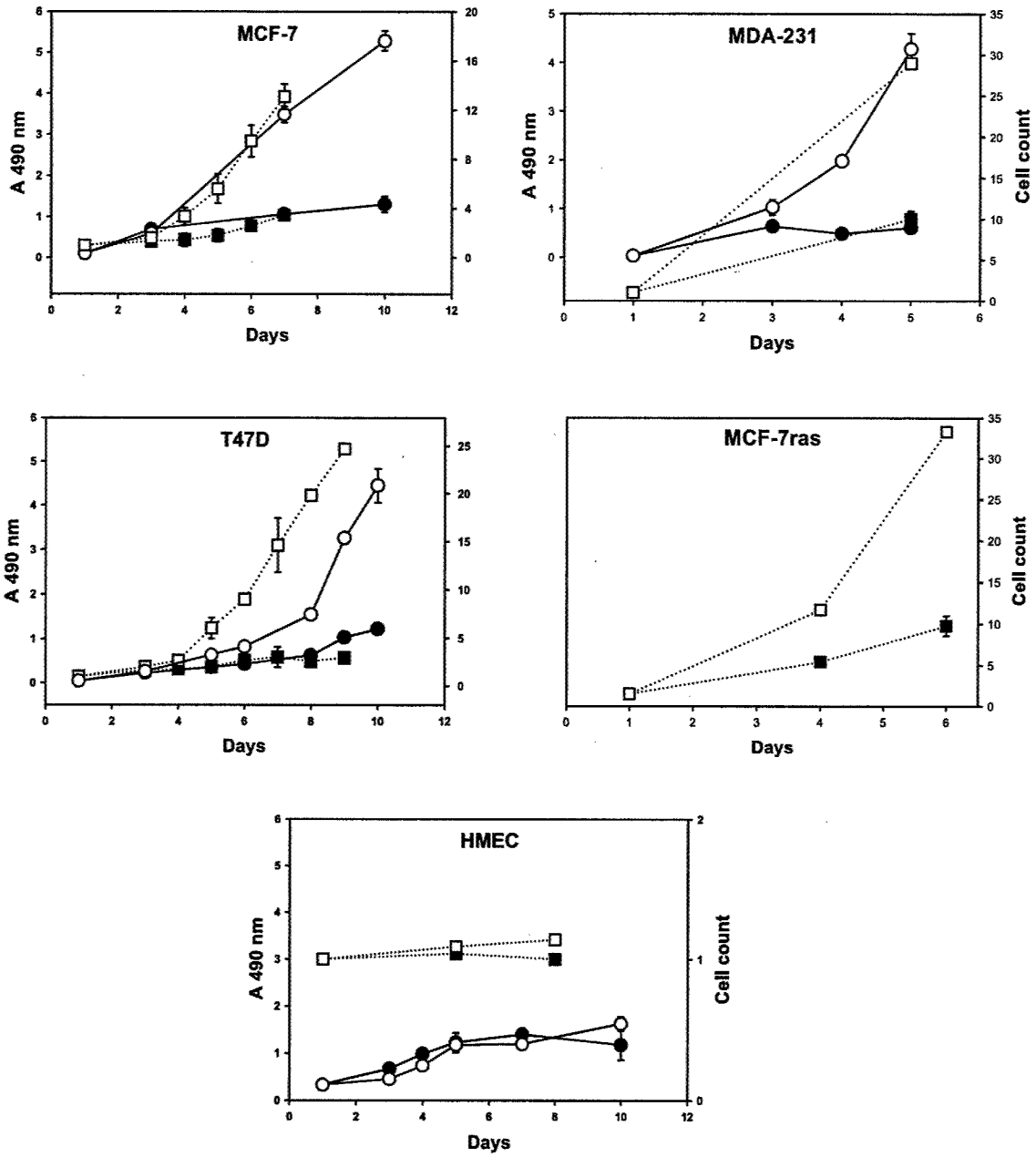

FIG. 6. **Growth of human breast cell lines in quinidine.** MCF-7, MDA-MB-231, T47D, MCF-7*ras* tumor cells, and normal HMEC were replica-plated in 96-well plates in control medium (*open symbols*) or medium containing 90 μM quinidine (*solid symbols*). Cell growth as monitored using the MTS assay is shown with solid lines. Results shown are the average of quadruplicates in one experiment. Quinidine had no effect on MTS metabolism in the MCF-7*ras* cell line (data not shown). Viable cell counts/dish of replica-plated MCF-7, MDA-MB-231, T47D, and MCF-7*ras* tumor cells and normal HMEC cells in 35-mm^2 dishes in control medium (*open symbols*) and medium containing 90 μM quinidine (*solid symbols*) is indicated by *dashed lines*. The cell number (growth curve data) represent the mean and S.E. of three independent experiments for the MCF-7, T47D, and MDA-231 cell lines performed in duplicate dishes (MCF-7 and T47D) or single dishes (MDA-231) for each experiment. MCF-7*ras* data are the mean (± range) of two experiments performed in duplicate dishes. HMEC data are from one experiment performed in single dishes.

ion. Cells that were treated for 96 h with retinoic acid showed an increase in the intensity of the cytokeratin 18 staining and relocalization of cytokeratin 18 throughout the nucleus as well as the cytoplasm. In contrast, cytokeratin 18 staining occurred in a highly organized pattern in MCF-7 cells treated with quinidine for 96 h and the cells adopted a shape and nuclear localization more typical of columnar epithelium.

Lipid droplets are found in the cytoplasm of normal mammary epithelium (31), and cytoplasmic lipid droplet accumulation occurs in a variety of differentiating cell systems. Induction of differentiation in human breast cancer cell lines by oncostatin M (32), the HER-2/neu kinase inhibitor, emodin (33), overexpression of c-e,rbB-2 (34), the vitamin D analog, 1-α-hydroxyvitamin D5 (35), the HDAC inhibitor, sodium butyrate (36), and retinoic acid (36) is accompanied by the accumulation of cytoplasmic lipid droplets. We utilized a fluorescent stain, Nile Red to monitor lipid droplet formation in mammary tumor cells in response to quinidine. The cells were counterstained with fluorescein-phalloidin that binds actin filaments to assay for changes in the actin cytoskeleton (Fig. 8). The distribution of actin in four human breast tumor cell lines, MCF-7, T-47D, MDA-MB-231, and MDA-MB-435 is seen clearly in the control cells. Three of these lines show strong nuclear staining of actin characteristic of transformed cells, whereas the fourth, MDA-MB-435, shows more cytoplasmic actin. In all cases except MDA-MB-435, the presence of quinidine did not significantly alter the actin cytoskeleton. Lipid droplet accumulation was weak or absent in the control cell

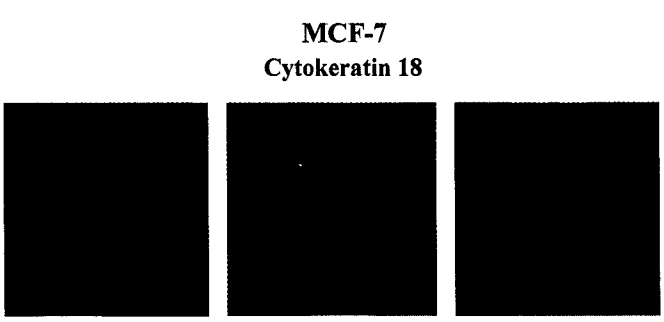

FIG. 7. **Cytokeratin 18 in MCF-7 cells.** Cells were replica-plated (2×10^5) on sterile coverslips in 35-mm^2 dishes in medium containing 0.01% ethanol (control), 10 μM retinoic acid, or 90 μM quinidine and grown for 96 h. Cytokeratin 18 detection using a Texas Red-tagged secondary antibody is shown using confocal microscopy. Data shown are typical fields representative of two independent experiments.

lines and increased by retinoic acid and quinidine. Lipid droplet accumulation was more marked in all four cell lines treated with quinidine than with retinoic acid. These data demonstrate that induction of a more differentiated phenotype is a general response of human mammary tumor cells to quinidine.

Hyperacetylation of Histone H4 in Mammary Tumor Cell Lines by Quinidine—To determine whether differentiation and histone acetylation were linked, we investigated the histone H4 acetylation status of quinidine-treated T47D, MDA-MB-231, and MCF-7$_{ras}$ cells. MCF-7, MCF-7*ras*, T47D, and MDA-MB-231 cells were incubated for 24 h in the presence or absence of quinidine, and then histones were extracted for immunoblotting. Fig. 9 shows that histone H4 was hyperacetylated in all cell lines treated with quinidine. Control cells contained no hyperacetylated histone H4.

DISCUSSION

Quinidine-induced histone H4 hyperacetylation in MCF-7 human breast carcinoma cells can be attributed to the rapid elimination of HDAC1 protein, a response that was blocked by MG-132 and lactacystin, two inhibitors of proteasome-mediated proteolysis. HDAC1 protein was undetectable within 30 min after the addition of quinidine to the medium of MCF-7 cells, and hyperacetylated histone H4 appeared between 1 and 2 h. Levels of HDAC1 protein were completely suppressed between 0.5 and 6 h, and during this time H4 acetylation levels increased. H4 acetylation was maintained at 12 and 24 h, despite the partial restoration of HDAC1 protein at these same time points. These data indicate that quinidine-induced reductions in HDAC1 protein levels are unlikely to explain fully the regulation of H4 acetylation state in MCF-7 cells by quinidine. Additional HDAC enzymes or effects upon histone acetylation rates could possibly play a role as well.

An earlier study showed that over this initial 48-h period, 80% of the MCF-7 cell population had shifted into G_0, a quiescent state marked by the absence of Ki67 antigen immunoreactivity (12). Cellular differentiation manifested as the accumulation of lipid droplets, and a reorganization of the cytokeratin 18 cytoskeleton was evident after this initial 48-h period. Quinidine exhibited all the responses typical of known HDAC inhibitory drugs, with the exception that quinidine had no direct inhibitory effect upon HDAC1 enzymatic activity. We conclude from the current studies that quinidine is a novel differentiating agent that causes histone hyperacetylation, in part, by physical elimination of HDAC1 protein rather than the inhibition of HDAC enzymatic activity.

Histone H4 hyperacetylation and induction of cellular differentiation by quinidine were seen in a panel of human breast tumor cell lines that were selected for study on the basis of their diversity of genetic backgrounds. The differentiation response to quinidine was independent of the estrogen receptor (ER) status. Cell lines representative of ER-positive and ER-negative human breast carcinoma cells were induced to differentiate in the presence of quinidine. The ER status of the estrogen receptor positive cell lines is MCF-7 (ER-α and ER-β), T47D (ER-α and ER-β), and MDA-MB-231 (ER-β). MDA-MB-435 cells expressed very low levels of ER-β and no ER-α (37, 38). MCF-7 and T47D cells display an epithelial morphology and show similarities with mammary ductal and luminal epithelial cells, respectively (30, 39). MDA-MB-231 cells exhibit an elongated cellular morphology that is also typical of MDA-MB-435 cells. Our results demonstrate that quinidine is a differentiation agent in both types of mammary tumor cells.

HDAC inhibitors reverse the transformed phenotype of NIH3T3*ras* cells, and this property has been used successfully as a screening assay for the identification of new HDAC inhibitors (40, 41). Quinidine elicited a more differentiated phenotype in MCF-7*ras* cells, an MCF-7 cell derivative produced by stable transformation with v-Ha-*ras,* thus demonstrating that quinidine, like other HDAC inhibitors, can reverse an Ha-*ras*-induced phenotype.

Quinidine induced differentiation independently of wild-type p53. The ability of quinidine to cause differentiation of p53 mutant cell lines is consistent for a role of histone hyperacetylation in the response. HDAC inhibitors typically induce a p53-independent activation of p21^{WAF1} gene expression (5, 22). Growing MCF-7 and T47D cells express p21^{WAF1} protein in moderate to low levels (42), and quinidine raised p21^{WAF1} protein levels in MCF-7 cells approximately 11-fold within 12 h. Although p21^{WAF1} was reported to be low to undetectable in MDA-MB-231, p21^{WAF1} was detected in Western analyses of both MDA-MB-231 and T47D cells in a p53-independent fashion in response to serum deprivation, adriamycin, etoposide (42, 43), and quinidine (data not shown). These data support the idea that the p21^{WAF1} gene is present but inactive in growing MDA-MB-231 cells. Since histone hyperacetylation of the p21^{WAF1} gene occurs in response to HDAC inhibitors, it might be involved in the pathway of p53-independent activation of p21^{WAF1} gene expression (5).

The processes of cellular differentiation and cell cycle progression are interdependent. G_1 arrest is a necessary but insufficient condition for differentiation in numerous cell types including leukemic cells, keratinocytes, colonic epithelium, and muscle cells. In all of these cells, induction of p21^{WAF1} protein and G_1 cell cycle arrest occurred prior to differentiation (44–50) and was generally independent of p53. We hypothesize that the differentiated state can be viewed as a cellular response to G_1 arrest, requiring a change in gene expression profile and suppression of cell death pathways. The response of MCF-7 breast tumor cells to quinidine is consistent with this model.

To begin to understand how quinidine might elicit G_1 arrest of MCF-7 cells, we have focused on the action of quinidine as a potassium channel blocking agent. Quinidine enters cells and inhibits cardiac potassium channels by binding to the intracellular face of the ion pore (51). Although the location of the quinidine-binding site on the ATP-sensitive potassium channel is unknown, quinidine is freely permeable across membranes and inhibits the ATP-sensitive potassium channels whether it is applied to the external or internal surface of a lipid membrane bilayer (52).

In the presence of quinidine, MCF-7 cells accumulate at a position 12 h into G_1 phase (12). This position, defined by cell cycle arrest and release experiments, precedes the lovastatin arrest point by 5–6 h and is clearly distinct from the restriction

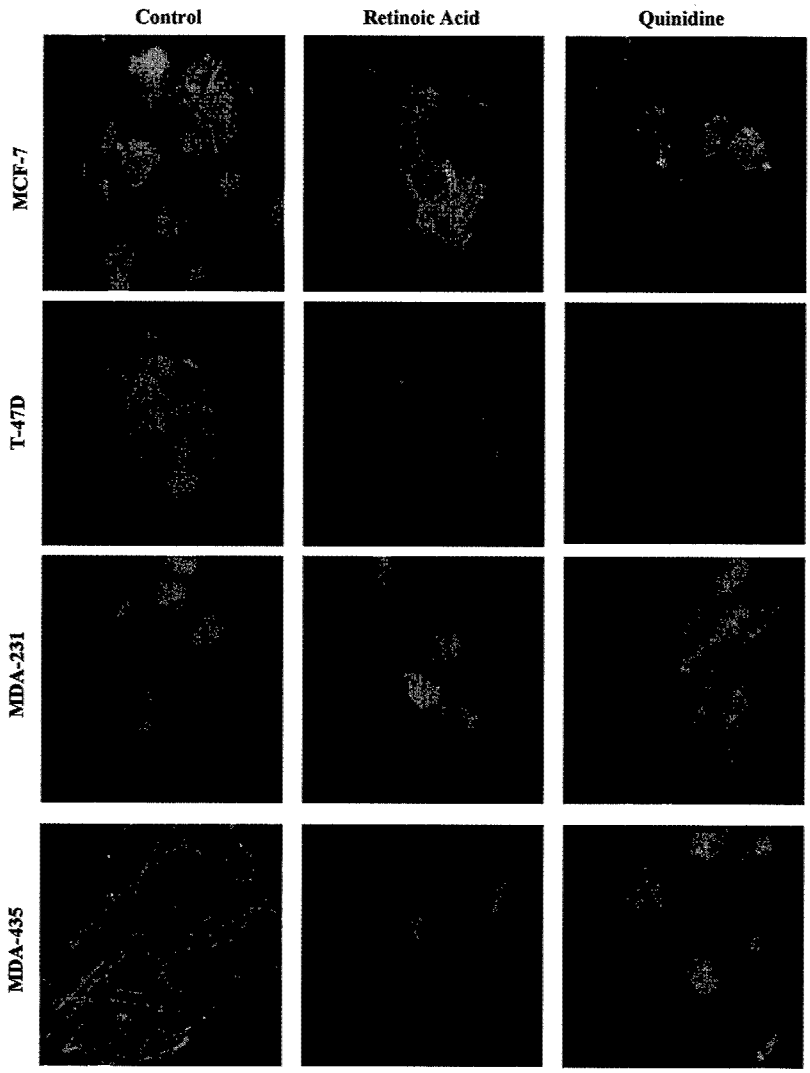

FIG. 8. **Lipid accumulation as an index of cellular differentiation in human breast tumor cell lines.** MCF-7, T47D, MDA-MB-231, and MDA-MB-435 cells were replica-plated ($0.8–3 \times 10^5$) on sterile coverslips in 35-mm^2 dishes in medium containing 0.01% ethanol (control), 10 μM retinoic acid (0.01% ethanol), or 90 μM quinidine (in water). Cells were fixed, permeabilized, and then incubated sequentially with fluorescein-phalloidin to identify actin filaments and Nile Red to identify lipid droplets after 96 h. Images were obtained by confocal microscopy. The results are typical of three experiments conducted in each cell line.

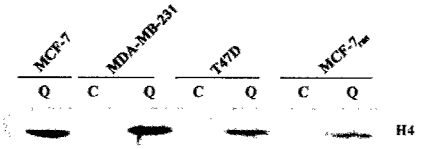

FIG. 9. **Histone H4 hyperacetylation in human breast tumor cell lines.** MCF-7, MCF-7*ras*, T47D, MDA-MB-231, tumor cells were replica-plated (1×10^7/T-162 flask) in control medium (*C*) or medium containing 90 μM quinidine (*Q*). Histones were extracted from the cells after 24 h, and 20 μg/lane of histone proteins were electrophoresed in 15% SDS-polyacrylamide gels. Immunoblotting was performed to detect acetylated histone H4.

point described by Pardee (53) near the G_1/S transition. The present work showed that quinidine treatment caused elevated levels of p53 and p21^{WAF1} protein by 12 h (Fig. 3), the point within G_1 where MCF-7 cells arrest in response to quinidine (12). When p53 and p21^{WAF1} proteins were assayed before 12 h, p53 was undetectable, and p21^{WAF} was first detected after 8 h of quinidine treatment (data not shown), suggesting a p53-independent induction of p21^{WAF1} occurred prior to arrest in G_1. CDK4 and cyclin D1 protein levels were also reduced, as was CDK4 activity as demonstrated by the abundance of hypophosphorylated pRb protein. Based upon our observations in MCF-7 cells, we conclude that p21^{WAF1} protein levels become elevated prior to the G_1 arrest in response to quinidine and could initiate the G_1 arrest. Hypophosphorylated pRb protein is prominent in quinidine-treated MCF-7 cells, and this could act to sustain the G_1 state by preventing the transition into S phase. The G_1 arrest induced by quinidine in MCF-7 cells was correlated with the blockade of ATP-sensitive potassium channels in MCF-7 cells (12, 54, 55). Direct evidence for the involvement of potassium ions in the G_1 arrest was provided using valinomycin, a potassium-selective ionophore to stimulate a G_1-S phase transition in the presence of quinidine (12).

In summary, quinidine, a drug that is used therapeutically in the treatment of malarial infections and cardiac arrhythmia, was shown to be useful as an inducer of cellular differentiation in human breast tumor epithelial cells. Quinidine caused histone H4 hyperacetylation and cellular differentiation in human breast tumor cells following the rapid loss of HDAC1 involving a proteasome-dependent pathway. Additional experiments are needed to determine how the action of quinidine upon ATP-sensitive potassium channels initiates the molecular events underlying the differentiation response.

REFERENCES

1. Davie, J. R., and Chadee, D. N. (1998) *J. Cell. Biochem.* **30,** (suppl.) 203–213
2. Van Lint, C., Emiliani, S., and Verdin, E. (1996) *Gene Expr.* **5,** 245–253
3. Medina, V., Edmonds, B., Young, G. P., James, R., Appleton, S., and Zalewski, P. D. (1997) *Cancer Res.* **57,** 3697–3707
4. Richon, V. M., Emiliani, S., Verdin, E., Webb, Y., Breslow, R., Rifkind, R. A., and Marks, P. A. (1998) *Proc. Natl. Acad. Sci. U. S. A.* **95,** 3003–3007
5. Sambucetti, L. C., Fischer, D. D., Zabludoff, S., Kwon, P. O., Chamberlin, H., Trogani, N., Xu, H., and Cohen, D. (1999) *J. Biol. Chem.* **274,** 34940–34947
6. Yoshida, M., and Horinouchi, S. (1999) *Ann. N. Y. Acad. Sci.* **886,** 23–36
7. Finnin, M. S., Donigian, J. R., Cohen, A., Richon, V. M., Rifkind, R. A., Marks, P. A., Breslow, R., and Pavletich, N. P. (1999) *Nature* **401,** 188–193
8. Kijima, M., Yoshida, M., Sugita, K., Horinouchi, S., and Beppu, T. (1993) *J. Biol. Chem.* **268,** 22429–22435

9. Xiong, Y., Zhang, H., and Beach, D. (1993) *Genes Dev.* **7,** 1572–1583
10. Sheikh, M. S., Rochefort, H., and Garcia, M. (1995) *Oncogene* **11,** 1899–1905
11. Warrell, R. P., Jr., He, L.-Z., Richon, V., Calleja, E., and Pandolfi, P. P. (1998) *J. Natl. Cancer Inst.* **90,** 1621–1625
12. Wang, S., Melkoumian, Z. K., Woodfork, K. A., Cather, C., Davidson, A. G., Wonderlin, W. F., and Strobl, J. S. (1998) *J. Cell. Physiol.* **176,** 456–464
13. Kasid, A., Lippman, M. E., Papageorge, A. G., Lowy, D. R., and Gelmann, E. P. (1985) *Science* **228,** 725–728
14. Greenspan, P., Mayer, E. P., and Fowler, S. D. (1985) *J. Cell Biol.* **100,** 965–973
15. Toscani, A., Soprano, D. R., and Soprano, K. J. (1990) *J. Biol. Chem.* **265,** 5722–5730
16. Nakajima, H., Kim, Y. B., Torano, H., Yoshida, M., and Horinouchi, S. (1998) *Exp. Cell Res.* **241,** 126–133
17. Hendzel, M. J., Delcuve, G. P., and Davie, J. R. (1991) *J. Biol. Chem.* **266,** 21936–21942
18. Sun, J.-M., Chen, H. Y., Moniwa, M., Samuel, S., and Davie, J. R. (1999) *Biochemistry* **38,** 5939–5947
19. Saunders, N., Dicker, A., Popa, C., Jones, S., and Dahler, A. (1999) *Cancer Res.* **59,** 399–404
20. Schmidt, K., Gust, R., and Jung, M. (1999) *Arch. Pharm. (Weinheim)* **332,** 353–357
21. Kim, Y. B., Lee, K. H., Sugita, K., Yoshida, M., and Horinouchi, S. (1999) *Oncogene* **18,** 2461–2470
22. Saito, A., Yamashita, T., Mariko, Y., Nosaka, Y., Tsuchiya, K., Ando, T., Suzuki, T., Tsuruo, T., and Nakanishi, O. (1999) *Proc. Natl. Acad. Sci. U. S. A.* **96,** 4592–4597
23. Sowa, Y., Orita, T., Minamikawa-Hiranabe, S., Mizuno, T., Nomura, H., and Sakai, T. (1999) *Cancer Res.* **59,** 4266–4270
24. Nakanishi, M., Kanedo, Y., Matsushime, H., and Ikeda, K. (1999) *Biochem. Biophys. Res. Commun.* **263,** 35–40
25. Levine, A. J. (1997) *Cell* **88,** 323–331
26. Ameyar, M., Shatrov, V., Bouquet, C., Capoulade C., Cai, Z., Stancou, R., Badie, C., Haddada H., and Chouaib, S. (1999) *Oncogene* **18,** 5464–5472
27. Nieves-Neira, W., and Pommier, Y. (1999) *Int. J. Cancer* **82,** 396–404
28. Stampfer, M. R., and Yaswen, P. (1993) *Cancer Surv.* **18,** 7–34
29. Stingl, J., Eaves, C. J., Kuusk, U., and Emerman, J. T. (1998) *Differentiation* **63,** 201–213
30. Jing, Y., Zhang, J., Waxman, S., and Mira-y-Lopez, R. (1996) *Differentiation* **60,** 109–117
31. Halm, H. A., Ip, M. M., Darcy, K., Black, J. D., Shea, W. K., Forczek, S., Yoshimura, M., and Oka, T. (1990) *In Vitro Cell Dev. Biol.* **26,** 803–814
32. Douglas, A. M., Grant, S. L., Goss, G. A., Clouston, D. R., Sutherland, R. L., and Begley, C. G. (1998) *Int. J. Cancer* **75,** 64–73
33. Zhang, L., Chang, C. J., Bacus, S. S., and Hung, M. C. (1995) *Cancer Res.* **55,** 3890–3896
34. Giani, C., Casalini, P., Pupa, S. M., De Vecchi, R., Ardini, E., Colnaghi, M. I., Giordano, A., and Menard, S. (1998) *Oncogene* **17,** 425–432
35. Mehta, R. R., Bratescu, L., Graves, J. M., Green, A., and Mehta, R. G. (2000) *Int. J. Oncol.* **16,** 65–73
36. Bacus, S. S., Kiguchi, K., Chin, D., King, C. R., and Huberman, E. (1990) *Mol. Carcinogen.* **3,** 350–362
37. Fuqua, S. A., Schiff, R., Parra, I., Friedrichs, W. E., Su, J. L., McKee, D. D., Slentz-Kesler, K., Moore, L. B., Willson, T. M., and Moore, J. T. (1999) *Cancer Res.* **59,** 5425–5428
38. Vladusic, E. A., Hornby, A. E., Guerra-Vladusic, F. K., Lakins, J., and Lupu, R. (2000) *Oncol. Rep.* **7,** 157–167
39. Soule, H. D., Vazquez, J., Long, A., and Albert, S. (1973) *J. Natl. Cancer Inst.* **51,** 1409–1416
40. Futamura, M., Monden, Y., Okabe, T., Fujita-Yoshigaki, J., Yokoyama, S., and Nishimura, S. (1995) *Oncogene* **10,** 1119–1123
41. Itazaki, H., Nagashima, K., Sugita, K., Yoshida, H., Kawamura, Y., Yasuda, Y., Matsumoto, K., Ishii, K., Uotani, N., Nakai, H., Terui, A., Yoshimatsu, S., Ikenishi, Y., and Nakagawa, Y. (1990) *J. Antibiot. (Tokyo)* **43,** 1524–1532
42. Sweeney, K. J., Swarbrick, A., Sutherland, R. L., and Musgrove, E. A. (1998) *Oncogene* **16,** 2865–2878
43. Sheikh, M. S., Li, X.-S., Chen, J.-C., Shao, Z.-M., Ordonez, J. V., and Fontana, J. A. (1994) *Oncogene* **9,** 3407–3415
44. Chang, B. D., Wuan, Y., Broude, E. V., Zhu, H., Schott, B., Fang, J., and Roninson, I. B. (1999) *Oncogene* **18,** 4808–4018
45. DiCunto, F., Topley, G., Calautti, E., Hsiao, J., Ong, L., Seth, P. K., and Dotto, G. P. (1998) *Science* **280,** 1069–1072
46. Evers, B. M., Ko, T. C., Li, J., and Thompson, E. A. (1996) *Am. J. Physiol.* **271,** G722–G727
47. Freemerman, A. J., Vrana, J. A., Tombes, R. M., Jiang, H., Chellappan, S. P., Fisher, P. B., and Grant, S. (1997) *Leukemia (Baltimore)* **11,** 504–513
48. Missero, C., Di Cunto, F., Kiyokawa, H., Kof, F. A., and Dotto, G. P. (1996) *Genes Dev.* **10,** 3065–3075
49. Matsumura, I., Ishikawa, J., Nakajima, K., Oritani, K., Tomiyama, Y., Miyagawa, J.-I., Kato, T., Miyazaki, H., Matsuzawa, Y., and Kanakura, Y. (1997) *Mol. Cell. Biol.* **17,** 2933–2943
50. Parker, S. B., Eichele, G., Zhang, P., Rawls, A., Sands, A. T., Bradley, A., Olson, E. N., Harper, J. W., and Elledge, S. T. (1995) *Science* **267,** 1024–1027
51. Yeola, S. W., Rich, T, C., Uebele, V. N., Tamkun, M. M., and Snyders, D. J. (1996) *Circ. Res.* **78,** 1105–1114
52. Iliev, I. G., and Marino, A. A. (1993) *Cell. & Mol Biol. Res.* **39,** 601–611
53. Pardee, A. B. (1974) *Proc. Natl. Acad. Sci. U. S. A.* **71,** 1286–1290
54. Woodfork, K. A., Wonderlin, W. F., Peterson, V. A., and Strobl, J. S. (1995) *J. Cell. Physiol.* **162,** 163–171
55. Klimatcheva, E., and Wonderlin, W. F. (1999) *J. Membr. Biol.* **171,** 35–46
56. Liu, X., Zou, H., Widlak, P., Garrard, W., and Wang, X. (1999) *J. Biol. Chem.* **274,** 13836–13840

Int. J. Cancer: **102,** 60–69 (2002)

Publication of the International Union Against Cancer

MYC PROTEIN IS DIFFERENTIALLY SENSITIVE TO QUINIDINE IN TUMOR *VERSUS* IMMORTALIZED BREAST EPITHELIAL CELL LINES

Zaroui K. MELKOUMIAN, Anna R. MARTIROSYAN, and Jeannine S. STROBL*

Department of Biochemistry and Molecular Pharmacology, West Virginia University, Morgantown, WV, USA

Quinidine regulates growth and differentiation in human breast tumor cells, but the immortalized mammary epithelial MCF-10A cell line is insensitive to quinidine. We found that a morphologically similar differentiation response was evoked by quinidine and c-*myc* antisense oligonucleotides in MCF-7 cells and this prompted us to investigate the actions of quinidine on c-*myc* gene expression. Myc protein levels were suppressed in human breast tumor cell lines, but not in MCF-10A cells, an observation that supports the hypothesis that suppression of c-*myc* gene expression is involved in the preferential growth and differentiation response of breast tumor cells to quinidine. Quinidine reduced c-*myc* mRNA levels in MCF-7 cells. Acute induction of c-*myc* mRNA by estradiol, as well as the c-*myc* response to sub-cultivation in fresh serum and H-*ras* driven elevations in c-*myc* mRNA were depressed by 50–60% in the presence of quinidine. Quinidine decreased c-*myc* promoter activity in MCF-7 cells in a transient reporter gene assay and a 168 bp region of human c-*myc* promoter (−100 to +68 with respect to the P1 promoter) was sufficient to confer responsiveness to quinidine. Quinidine is a potential lead compound for developing pharmacological agents to regulate Myc. In addition, the study of quinidine-regulated events is a promising approach to unravel differentiation control pathways that become disrupted in breast cancer.

Key words: *breast cancer; c-myc; differentiation; E2F; MCF-10A; MCF-7; Rb; quinidine*

Our study investigates the actions of quinidine on Myc expression in breast epithelial cells. Quinidine, a natural alkaloid, was first used therapeutically as an anti-malarial and only later, its effectiveness in the suppression of cardiac arrhythmia was discovered. The response of cardiac muscle to quinidine is caused by the blockade of sodium and potassium ion channels however, the basis for quinidine action on the malarial parasite is unknown.[1] The anti-proliferative activity of quinidine in human breast cancer cells *in vitro* was first established in our laboratory. MCF-7, MCF-7*ras*, MDA-MB-231, MDA-MB-435 and T47D human breast cancer cell lines were growth arrested and exhibited a differentiation response to quinidine.[2] A number of approaches have been taken to elucidate the mechanism of action of quinidine in human breast epithelium.[2–4] Disruption of potassium ion permeability as a result of blockade of the plasma membrane ATP-sensitive potassium channels (K_{ATP}) is hypothesized to control cell cycle progression in MCF-7 cells by preventing cell transit from G1 into S-phase.[4,5] Within 12–24 hr, the profile of G1 regulatory proteins in MCF-7 cells was typical of a G1-arrested condition. The protein, p21/WAF1, an inhibitor of cyclin-dependent kinases 4 and 6 was increased. Total retinoblastoma protein, Rb was suppressed and the hypophosphorylated Rb form was prominent. After several days in quinidine, cells exhibited evidence of cellular differentiation. The current studies address the changes in c-*myc* gene expression that accompany the anti-proliferative actions of quinidine in human breast epithelial cells. Downregulation of c-*myc* occurred in MCF-7 tumor cells but not in the immortalized breast epithelial cell line, MCF-10A. We used quinidine as a chemical probe to explore the pathways involved in the differential regulation of Myc in these 2 cell lines.

C-myc is a protooncogene whose gene product has a regulatory role in cell cycle progression, cell differentiation and apoptosis.[6,7] Aberrant expression of *c-myc* is very common in breast cancers,[8] suggesting its importance in the genesis or progression of breast cancer. It has been demonstrated that *c-myc* expression is critical for the growth of both ER-positive and ER-negative breast cancer cells *in vitro* as well as for tumor growth *in vivo*.[9] *C-myc* mRNA induction occurs within 20 min after addition of estradiol to quiescent MCF-7 human breast cancer cells.[10] In the complex with its dimerization partner, Max, Myc then act as a transcription factor to activate/suppress the expression of its target genes involved in the regulation of cell cycle progression and proliferation. Some of the *c-myc* target genes include *cdc25A*, *p15Ink4b*, *p19ARF*, *gadd 45*, *odc*, *cad*, *p53*, *cyclin D1* and *E2F*.[11,12] Reversible control of mammary epithelial cell proliferation is possible by the turn-on and turn-off of Myc protein production using a tetracycline-inducible Myc expression system.[13] Studies in different cell lines have shown that downregulation of *c-myc* by antisense oligonucleotides or expression of dominant negative *c-myc* gene accompanies terminal differentiation and permanent withdrawal from the cell cycle.[14–18] Collectively, these studies suggest that Myc is an appropriate pharmacologic target for breast cancer intervention.

MATERIAL AND METHODS

Tissue culture

MCF-7 cells passage 40–50, MCF-7*ras*,[19] MDA-MB-231 and MDA-MB-435 cells were maintained in DMEM (BioWhittaker, Walkersville, MD) supplemented with 10% heat-inactivated FBS (HyClone, Logan, UT), 2 mM glutamine and 40 μg/ml gentamicin. MDA-MB-468 (ATCC) cells were grown in 50:50 DMEM/F-12 medium (Invitrogen, Carlsbad, CA). Phenol-red free (PRF) DMEM was obtained from BioWhittaker (Walkersville, MD). Most experiments were carried out in DMEM supplemented with 5% FBS. To study the effects of quinidine on estradiol induction of c-*myc*, cells were subcultivated into PRF-DMEM containing 2% charcoal-stripped FBS and subjected to several exchanges of the media to strip cells of endogenous estrogens.[20,21] Normal human mammary epithelial cells, HMEC, (Clonetics, San Diego, CA) and MCF-10A (ATCC) were grown in MEGM according to the directions from suppliers. HMEC were grown from frozen stocks and

Abbreviations: ER, estrogen receptor; HBSS, Hank's Balanced Salt Solution; HMEC, human mammary epithelial cells; K_{ATP}, ATP-sensitive potassium channel; MAPK, mitogen activated protein kinase; MEGM, mammary epithelium growth medium; PRF, phenol red-free; Q, quinidine; Rb, retinoblastoma protein; TBS, Tris-buffered saline; TGFβ1, transforming growth factor beta-1.

Grant sponsor: US Department of Defense Breast Cancer Research Program; Grant number: DAMD 17-99-1-9447, DAMD 17-00-1-500.

*Correspondence to: Department of Biochemistry and Molecular Pharmacology, West Virginia University, Morgantown, WV 26506-9142. Fax: +304-293-6854. E-mail: jstrobl@hsc.wvu.edu

Received 10 January 2002; Revised 3 June 2002; Accepted 13 July 2002

DOI 10.1002/ijc.10648

Published online 29 August 2002 in Wiley InterScience (www.interscience.wiley.com).

used for 1–3 passages only. The cells were maintained at 37°C in a humidified atmosphere of 94% air, 6% CO_2. Cells were passaged every 5–6 days (about 70–80% confluent) at ratios of 1:5 (MCF-7, MDA-MB-468) or 1:10 (MCF-7*ras*, MDA-MB-231, MDA-MB-435 and MCF-10A). All cell counts were carried out using a hemocytometer and 0.02% Trypan blue to assess cell viability.

Chemicals

Quinidine-HCl (Q) was purchased from Sigma Chemical Co. (St. Louis, MO). Concentrated stock solutions (10 mM) were prepared fresh for use by dissolving in sterile water. Estradiol-17β (Steraloids, Wilton, NH) was dissolved in 95% ethanol at a concentration of 2 mM and diluted $1:10^6$ in the medium to a final concentration of 2 nM. Transforming growth factor-beta (TGFβ1, T) (R&D Systems, Minneapolis, MN) stock solution (2.5 μg/ml) was prepared in 4 mM HCl, 1 mg/ml BSA and stored at −20°C.

Plasmids

The human *c-myc* probe used for Northern blots was a 9 kb *EcoR*1-*Hind* III genomic fragment spanning exons I and II and intron I isolated from the plasmid pHSR-1 obtained from the American Type Culture Collection.[22] The reporter plasmids containing different regions of the human *c-myc* promoter (Del-1, Del-2, Del-4, Frag-E) linked to the firefly luciferase gene were kindly provided by Dr. Bert Vogelstein (Johns Hopkins University).[23] The promoterless luciferase plasmid was constructed by deleting the *c-myc* promoter region from the Del-4 plasmid using *Pvu* II restriction enzyme. The human *cyclin D1*-luciferase plasmid (1745CD1-Luc) was kindly provided by Dr. Richard Pestell (The Albert Einstein College of Medicine, Bronx, NY).[24] The E2F-TA-Luc plasmid and control plasmid, TA-Luc, were purchased from Clontech Laboratories, Inc. (Palo Alto, CA).

Oligonucleotide transfections

C-Myc antisense (5′-AACGTTGAGGGGCAT-3′) and sense oligonucleotides (5′-ATGCCCCTCAACGTT-3′) were purchased from Sigma-Genosys (Woodlands, TX) and diluted in sterile water to yield concentrated stock solutions of 175 μM. The stock solutions were stored at −20°C for 2 months. Cells were plated at the density of 2.2×10^5/35 mm^2 dish on glass cover slips in DMEM/5% FBS. Cells were allowed to attach to the cover slips and then the medium was exchanged to DMEM/2% FBS ± 9 μM *c-myc* antisense oligonucleotides or 9 μM of *c-myc* sense oligonucleotides as the negative control.

Antibodies

Myc (9E10, sc-40), β-catenin (E-5, sc-7963), Sp1 (PEP2), Sp3 (D-20) and E2F-1 (KH 95), antibodies (Santa Cruz Biotechnology, Santa Cruz, CA) were used at a dilution as recommended by the supplier. Another E2F-1 antibody (KH 20 + KH 95) directed against 2 regions of the Rb binding pocket was purchased from Upstate Biotechnology (Lake Placid, NY). Rb (clone G3-245) antibody that recognizes phosphorylated and non-phosphorylated forms was purchased from Pharmingen (San Diego, CA) and a phospho Rb-specific antibody ($Ser_{807/811}$) was purchased from Cell Signaling Technology (Beverly, MA). Peroxidase-conjugated secondary antibodies were used and signals were visualized using Super Signal (Pierce, Rockford, IL) or LumiGlo (Cell Signaling Technology).

Oil-red O assay

Cells were plated in 35 mm^2 tissue culture dishes on sterile glass cover slips in DMEM/5% FBS ± quinidine. After treatment, the cells were fixed (10% formaldehyde and 0.2% calcium acetate in PBS) for 3 min and stained with fresh Oil-Red O working solution (Oil-Red O stock solution [0.5% Oil-Red O in 98% isopropanol] diluted in distilled water in a 3:2 ratio) for 10 min. Cells were rinsed in water and counterstained with Mayer's hematoxylin to visualize the cell nuclei. The images were obtained using an Ortholux microscope (Ernst Leitz Wetzlar, Germany) (40× objective) and the data quantified using Image-Pro Plus software (Media Cybernetics, Silver Spring, MD).

Cell cycle analysis

Cell cycle analysis was carried out after propidium iodide staining[25] using a FACScan (Becton Dickinson, San Jose, CA) and CellFIT software.

Western blots

Cells were rinsed with 1× PBS (phosphate buffered saline: 137 mM NaCl, 2.7 mM KCl, 4.3 mM $Na_2HPO_4 \times 7H_2O$, 1.4 mM KH_2PO_4, pH 7.3) and harvested by scraping in boiling lysis buffer (1% SDS, 10 mM Tris, pH 7.4). After boiling for 5 min, the cell extract was the supernatant obtained after centrifugation in an Eppendorf microfuge (14,000*g*, 5 min, 4°C). Twenty microliter aliquots were removed for determination of protein concentrations (BCA assay, Pierce Company). To the remaining extracts, 1 mM DTT and protease inhibitors were added to the final concentrations indicated: PMSF (phenylmethylsulfonyl fluoride, 0.1 mM), aprotinin (1 μg/ml) and leupeptin (1 μg/ml). Cell extract proteins were diluted in sample buffer and denatured by heating at 100°C for 3 min immediately before loading onto 10% polyacrylamide gels. Proteins were separated and transferred to PVDF (polyvinylidene difluoride) membranes (Invitrogen, Bethesda, MD). Autoradiographic signals were quantified by densitometry (Personal Densitometer SI, Molecular Dynamics, Sunnyvale, CA) and Image QuaNT software, version 4.1. Myc signals were normalized to the 97 kDa β-catenin protein signals.

Northern blots

Total cellular RNA was purified by the method of Chomczynski and Sacchi.[26] Fifteen μg of RNA for each sample were separated on 1.2% agarose-1.9 % formaldehyde gels in MOPS running buffer (20 mM MOPS, 5 mM sodium acetate, 0.5 mM EDTA, pH 8.0) and transferred to 0.2 μm nitrocellulose paper (Schleicher and Schuell, Keene, NH) by capillary action. Pre-hybridization (15–20 hr) and hybridization reactions (40–42 hr) were carried out in the micro-hybridization oven (Bellco Glass Inc., Vineland, NJ) at 42°C for 15–20 hr. Hybridization solution included $1.5–2 \times 10^6$ cpm/ml of denatured *c-myc* DNA fragment labeled with [αP^{32}]dCTP by random priming (Rediprime DNA labeling kit, Amersham Corp., Arlington Heights, IL). The blots were washed in 2× SSC (standard saline citrate)-0.1% SDS twice for 20 min each at 37°C. A high stringency wash of the *c-myc* probe was carried out for 15 min at 42°C in 0.1× SSC-0.1% SDS buffer. The hybridization signals were quantified using PSI-PC (Molecular Dynamics) and ImageQuant software, version 4.1. Hybridization signals were normalized to levels of 18S or 28S RNA in the ethidium bromide stained gels.

Reporter gene assay

Confluent MCF-7 cells were re-seeded at a density of 8×10^5/60 mm^2 dish in 5 ml DMEM/5% FBS. After 20–24 hr, when cells were 40–50% confluent, the cell monolayers were rinsed with 1× HBSS buffer (5.4 mM KCl, 108 mM NaCl, 0.34 mM $Na_2HPO_4 \times 7H_2O$, 4.2 mM $NaHCO_3$, 0.44 mM KH_2PO_4, pH 7.2) and 5 ml of DMEM/2% FBS were added. One hour later, transfection mixes containing 5 μg of plasmid DNA in DOTAP transfection reagent (Roche Molecular Biochemicals) were added to the cells. Transfections were terminated 6–7 hr later by exchanging the medium with fresh medium ± quinidine. Cells were harvested 24 hr later by scraping into ice-cold lysis buffer (25 mM Tris-phosphate, pH 7.8, 1% Triton X-100, 2 mM EDTA, 10% glycerol). Supernatants from the cell lysates were obtained by centrifugation in an Eppendorf microfuge (14,000*g*, 5 min, 4°C). Aliquots (20 μl) were removed for protein determinations using the BCA assay. To measure luciferase activity, 50 μl of cell extracts were added to 250 μl of ice-cold luciferase sample buffer (25 mM glycylglycyl, pH 7.8, 15 mM $MgSO_4$) in polypropylene tubes. The samples were warmed to 25°C. Luciferase activity was measured using an Auto Luminat (LB 953, EG and G-Bertholdt) equipped with a dual

injection system for the addition of ATP and luciferin. The relative luciferase units obtained from 50 μl of cell extracts were normalized to 200 μg of cellular proteins. Light generation from purified luciferase (Sigma) was used as the standard in each experiment to ensure that all determinations were carried out under linear assay conditions.

Statistics

SigmaPlot software (SPSS Inc., Chicago, IL), version 5.0 and JMP software (SAS Institute, Inc., Cary, NC) were used for statistical analysis. One-way ANOVA followed by the Dunnett's test for comparison of multiple groups with control or the Tukey-Kramer test for comparison between the different groups was used. A significance level of 0.05 was used.

RESULTS

*Cellular differentiation of MCF-7 cells in response to C-*myc *antisense oligonucleotides and quinidine*

Lipid droplets are found in the cytoplasm of normal mammary epithelium and induction of differentiation in human breast cancer cell lines by retinoic acid,[27,28] vitamin D analog, 1-α-hydroxy-vitamin D5[29] and oncostatin M [30] is marked by the accumulation of cytoplasmic lipid droplets. Quinidine (90 μM) promoted the appearance of a more differentiated phenotype in MCF-7 cells characterized by an enlarged cytoplasm, rearrangement of the cytokeratin 18 cytoskeleton and the accumulation of cytoplasmic lipid droplets.[2] Figure 1 summarizes a series of experiments in which differentiation in human mammary cells *in vitro* in response to either quinidine (90 μM) or c-*myc* antisense or sense oligonucleotides was evaluated by Oil Red O staining of cytoplasmic lipid droplets. Only normal human mammary epithelial cells (HMEC) showed cytoplasmic lipid droplets in control, untreated cultures. HMEC exposed to quinidine (90 μM) for 72 hr showed no increase in lipid droplet accumulation and no signs of cytotoxicity. The latter observation was consistent with an earlier report that indicated quinidine did not inhibit HMEC proliferation.[2] HMEC, however, barely proliferate. In a 10-day growth experiment, the HMEC doubled over a period of ~120 hr and then remained at a stable cell number for another 5 days (in the presence or absence of 90 μM quinidine). MCF-10A cells are immortalized human mammary epithelial cells that do not form tumors in animals.[31] MCF-10A cells, however, proliferate more rapidly in culture (doubling time 37 hr) than the early passage MCF-7 cells used in these experiments (doubling time 57 hr). MCF-10A cells provide 1 test for discriminating whether quinidine acts upon all cells with a rapid proliferation rate, or whether quinidine differentially affects tumorigenic mammary epithelial cells. Control MCF-10A cells did not accumulate cytoplasmic lipid droplets and neither quinidine treatment or c-*myc* antisense oligonucleotides elicited this response (data not shown). In contrast, lipid droplet accumulation

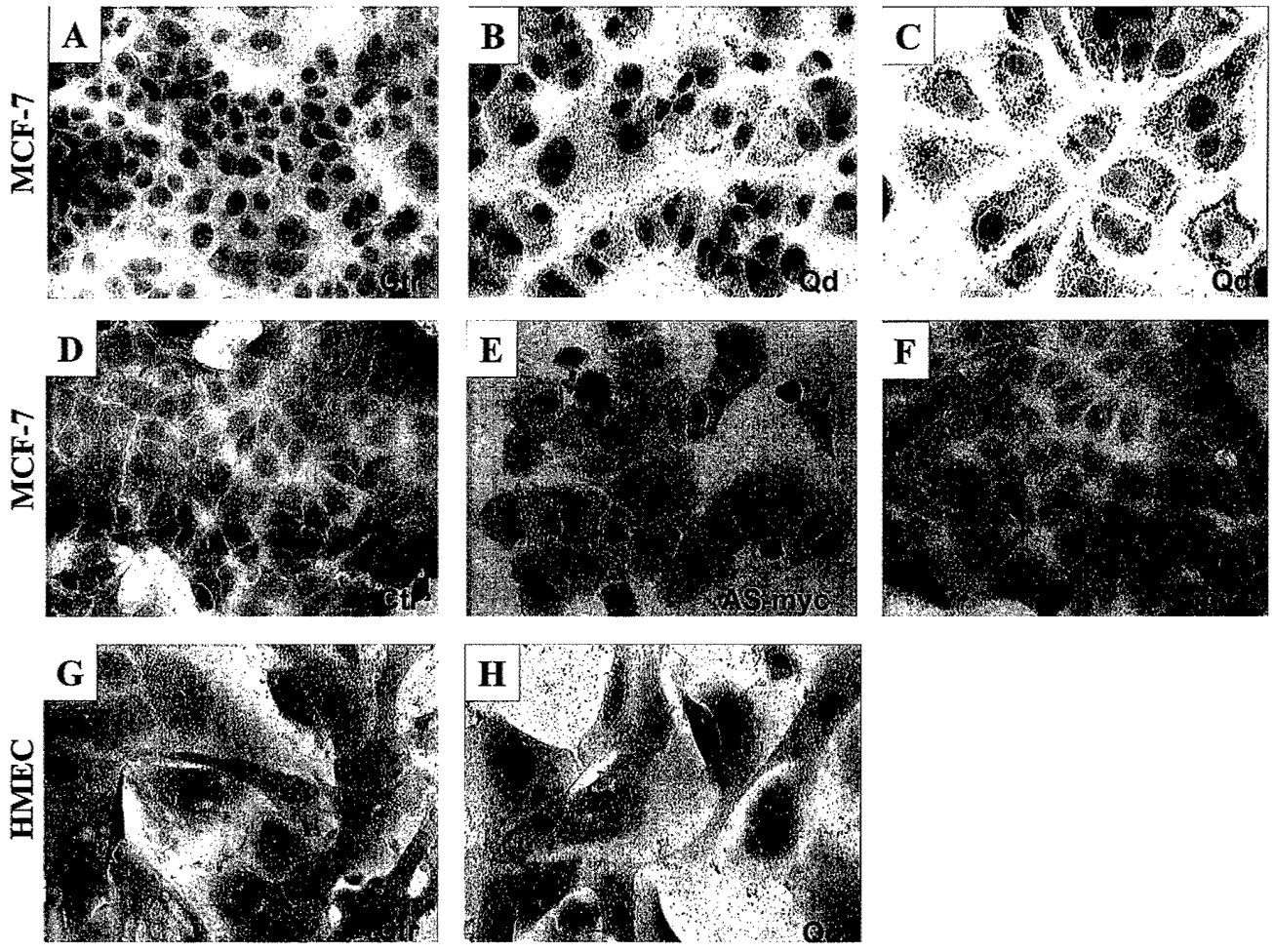

FIGURE 1 – Cellular differentiation of MCF-7 cells in response to c-myc antisense oligonucleotides and quinidine. Oil Red O staining of MCF-7 cells treated with nothing (*a,d*), 90 uM quinidine for 72 (*b*) or 120 (*c*) hr, *c-myc* antisense (*e*) or sense (*f*) oligonucleotides for 96 hr. Oil Red O staining of normal human mammary epithelial cells, HMEC, control (*g*) or treated with 90 uM quinidine (*h*) for 72 hr. Cells were counterstained with hematoxylin to visualize the cell nuclei (blue color).

and cytoplasmic enlargement was evident in MCF-7 cells treated with 90 μM quinidine for 72 hr and with c-*myc* antisense for 96 hr. Control (untreated) MCF-7 cells and MCF-7 cells exposed to c-*myc* sense oligonucleotides for 96 hr did not accumulate lipid droplets. We conclude that quinidine and c-*myc* antisense oligonucleotides promote a more differentiated phenotype in MCF-7 cells. Quinidine promoted lipid droplet accumulation in MDA-MB-231, MDA-MB-435, MCF-7*ras* and T47D cells[2] suggesting that this differentiation response is common among human mammary tumor cell lines.

Quinidine suppresses myc induction and cell growth in human breast cancer cells in vitro, *but not that of non-tumorigenic mammary epithelial cells*

Transient induction of *c-myc* mRNA and protein occurs 20–30 min after mitogenic stimulation of quiescent MCF-7 human breast cancer cells.[10] We tested whether quinidine affected Myc protein induction after release of MCF-7 cells from confluency into medium containing fresh serum. MCF-7 cells were grown in tissue culture flasks until 90–95% confluent to obtain cell populations that were 85% G0/G1 phase.[4] These confluent cells were then subcultivated into the medium containing fresh serum (5%) plus 90 μM quinidine or H_2O (vehicle). Myc protein levels were measured at the times indicated (Fig. 2). A maximal 15-fold induction of Myc protein occurred 90 min after sub-cultivation. The response is transient and Myc protein levels returned to baseline by 3 hr. Quinidine suppressed the rise in Myc protein, with a maximal 60% inhibition observed at 60 min.

Myc is a target for ubiquitination and degradation through the proteasome pathway.[32] The proteasome inhibitor, MG-132 did not preserve Myc protein levels in quinidine-treated cells (data not shown) suggesting that quinidine does not inhibit Myc levels by stimulating Myc degradation.

Quinidine also suppressed Myc expression that was stimulated in response to sub-cultivation in other breast tumor cell lines (Fig. 3, hatched bars): MCF-7*ras* (by 82%), MDA-MB-231 (by 66%), MDA-MB-435 (by 59%). The degree of suppression of Myc protein levels by quinidine correlated well with the extent of inhibition of proliferation in each of these cell lines (Fig. 3, solid bars). MCF-10A is a rapidly proliferating but non-tumorigenic mammary epithelial cell line that expresses high Myc protein levels. In contrast to the tumor cell lines, quinidine had no effect on Myc protein expression or proliferation of MCF-10A cells (Fig. 3). These results demonstrate the ability of quinidine to selectively inhibit growth and Myc protein in tumorigenic breast cells but not in an immortalized, non-tumorigenic breast epithelial line.

Suppression of myc protein and growth arrest by quinidine is not mediated through TGF-β1 response pathways

Transforming growth factor β-1 (TGF-β1) regulates epithelial cell growth, differentiation, adhesion, movement and death, but most mammary tumor cell lines are resistant to the growth inhibitory effects of TGF-β1, due to defects or deficiencies in TGF-β1 receptors or the TGF-β1 signaling pathway. C-*myc* is an important target of TGF-β1.[33,34] In MCF-10A cells, TGF-β1 stimulates the formation of an inhibitory complex on the c-*myc* promoter and rapid downregulation of *c-myc* mRNA, but this response is lost from MCF-10A cells after transformation with c-Ha-*ras* and c-*erb*B2 oncogenes.[35] TGF-β1 resistant MDA-MB-468 breast tumor cells lack Smad4, a transcription factor and an essential TGFβ1 signaling molecule.[35] In MDA-MB-231 cells, resistance to TGFβ is not fully understood, however, ectopic expression of TGF-β type III receptor suppressed tumorigenicity of MDA-MB-231 cells.[36] In contrast, MCF-7 cells have a partial response to TGFβ

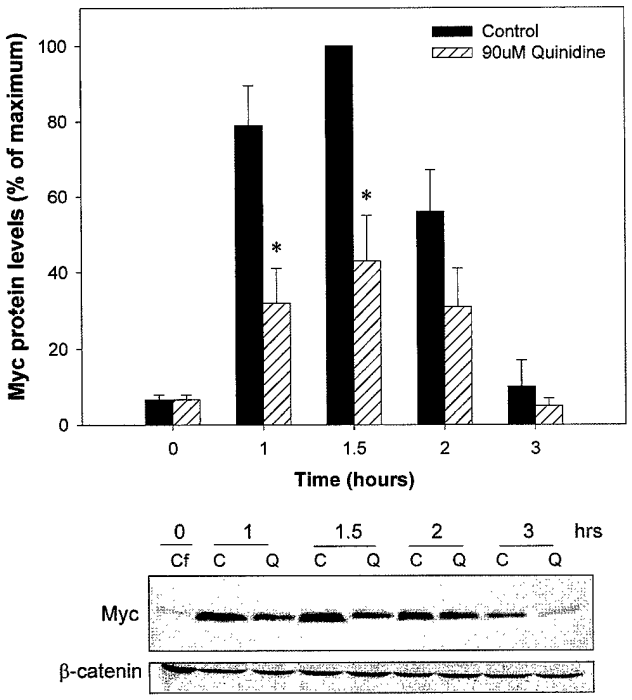

FIGURE 2 – Quinidine suppresses Myc protein induction in MCF-7 cells. Confluent (Cf) MCF-7 cells were subcultivated at 0 time in DMEM/5% FBS (solid bars) or in DMEM/5% FBS containing 90 μM quinidine (hatched bars). Cells were harvested for Western blot analysis at the times indicated. Myc protein signals were quantified by densitometry and normalized to the β-catenin signals. Data shown in the bar graph are the mean Myc protein signals ± SD of $n = 3$ experiments expressed as a percent of maximal stimulation (at 1.5 hr). The gel scans below the bar graph are a single representative experiment carried out with 80 μg of cell extract protein/lane. *Significantly different from control ($p < 0.05$).

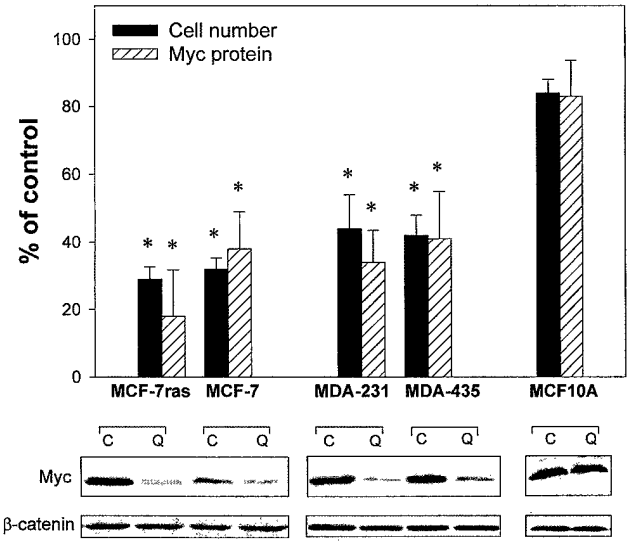

FIGURE 3 – Quinidine suppresses Myc induction and cell growth in human breast cancer cells *in vitro*, but not that of non-tumorigenic mammary epithelial cells. For the cell count assay (solid bars) confluent cells were subcultivated at the density of 1×10^5/35 mm^2 dish in DMEM/5% FBS ± 90 μM quinidine or MEGM (for MCF-10A) ± 90 μM quinidine and counted 96 hr later using a hemocytometer. For the Western blot assay (hatched bars) total cellular proteins from control or 90 μM quinidine treated cells were extracted 1 (MCF-7*ras*, MCF-7, MCF10A) or 2 (MDA-MB-231, MDA-MB-435) hr after sub-cultivation of confluent cells into DMEM/5% FBS. Myc protein signals were quantified by densitometry and normalized to the β-catenin signals. Data are the mean ± SD of $n = 3$ experiments. *Significantly different from control values ($p < 0.05$).

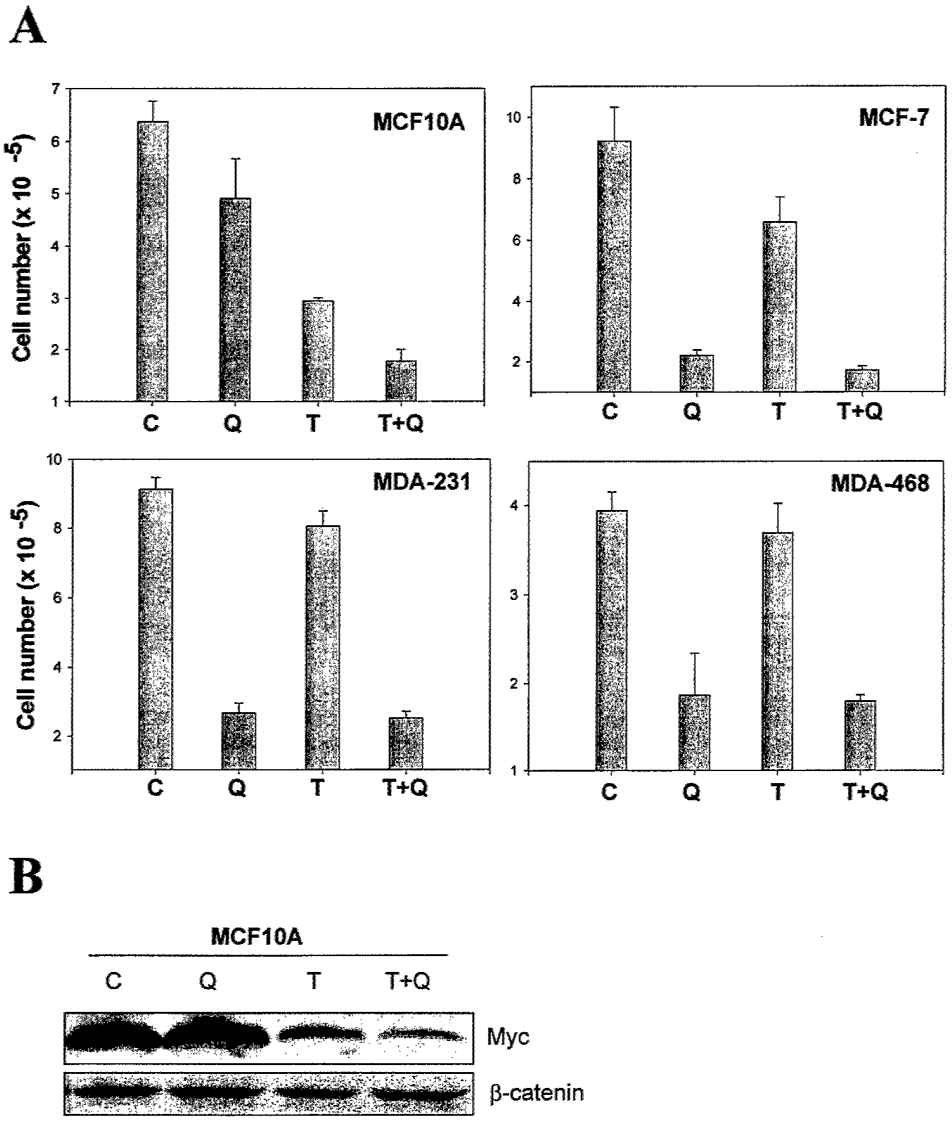

FIGURE 4 – Suppression of Myc protein and growth arrest by quinidine is not mediated by TGFβ1 response pathway. (*a*) Confluent cells were subcultivated in DMEM/5% FBS at the density of 1×10^5 (MDA-MB-231, MDA-MB-468, MCF-10A) or 2×10^5 (MCF-7) per 35 mm^2 tissue culture dish in the presence of: C-vehicle (4 mM HCl, 1 mg/ml BSA −0.5 μl/ml of medium), Q-90 μM quinidine, T-5 ng/ml TGFβ1, T+Q-90 μM quinidine + 5 ng/ml TGFβ1. Cells were harvested 72 or 96 (for MCF-7) hours later and counted using a hemocytometer. The bar graphs show cell numbers as mean ± SE of $n = 2$ experiments (MCF-7, MDA-MB-231, MDA-1B-468).The MCF-10A data are the mean ± SD of triplicates in a single experiment. (*b*) Confluent MCF-10A cells were subcultivated in MEGM containing C, Q, T or T+Q as described in (*a*). Total cellular proteins were extracted 24 hr later and analyzed for Myc and β-catenin by Western blot.

growth inhibition and ectopic TGFβRIII restores autocrine TGF-β1 activity in MCF-7 cells.[37] Despite these distinct defects in TGFβ1 signaling, quinidine inhibited proliferation in all breast tumor cell lines tested, implying that quinidine acts independently of TGF-β1 pathways (Fig. 4*a*). Furthermore, quinidine had no effect on the growth of MCF-10A cells (Fig. 3) in which the TGF-β1 pathway is intact. This result is important because it argues against the possibilities that quinidine acts either to restore a TGF-β1 response network, or to compensate for TGF-β1 defects. In Figure 4, the effects of quinidine and TGF-β1 on proliferation and Myc protein levels in a single experiment is summarized. We found (Fig. 4*a*) in this experiment that after 72 hr in quinidine MCF-10A cell numbers decreased slightly (24%), TGF-β1 alone caused a 54% reduction in cell numbers and that the combination quinidine plus TGFβ1 appeared to have an additive effect, reducing overall cell numbers by 71%. Similar reductions in the level of Myc protein in MCF-10A cells by quinidine (17%), TGF-β1 (54%) and the combination (Q+T, 71%) were observed (Fig. 4*b*). The data support the hypothesis that quinidine and TGF-β1 act through independent mechanisms to reduce c-*myc* expression and cell proliferation.

Quinidine suppresses acute induction of C-myc *MRNA and S-phase progression by estradiol*

Acute induction of *c-myc* mRNA transcription in MCF-7 cells exposed to estradiol is critical to progression through G1 phase of the cell cycle and the proliferative response to estradiol.[10,38] At 1 hr, quinidine suppressed estradiol-induced *c-myc* mRNA levels in MCF-7 cells in a concentration dependent fashion. Maximum inhibition (60%) of c-*myc* mRNA was achieved with 90 μM quinidine (Fig. 5*a*). These results are in good agreement with 60% suppression of Myc protein at 1 hr by 90 uM quinidine after cell sub-cultivation into fresh serum (Fig. 2). We conclude that inducible *myc* gene expression is suppressed but not completely inhibited by quinidine. Despite incomplete suppression of Myc, the actions of 90 μM quinidine were sufficient to inhibit estradiol stimulated MCF-7 cell cycle progression into S-phase (Fig. 5*b*). Confluent cells (80–85% G0/G1) were subcultivated into PRF-DMEM + 2% stripped FBS; 30 hr after plating, only 11% of the control cells progressed into the S-phase. Estradiol (2 nM) stimulated 34% of the cells to enter into S-phase by 30 hr and this response was nearly completely blocked in the presence of quinidine (14% S-phase cells).

Quinidine suppresses basal and H-ras-*driven* C-myc *MRNA and protein expression*

In MCF-7 cells, Myc is transiently induced during the G0-G1 phase transition and then remains at a constant low level throughout the cell cycle.[7] To ascertain whether quinidine affected basal *c-myc* expression, MCF-7 cells were incubated for 24 hr with 30 or 90 μM quinidine. A 24-hr treatment with 30 μM quinidine re-

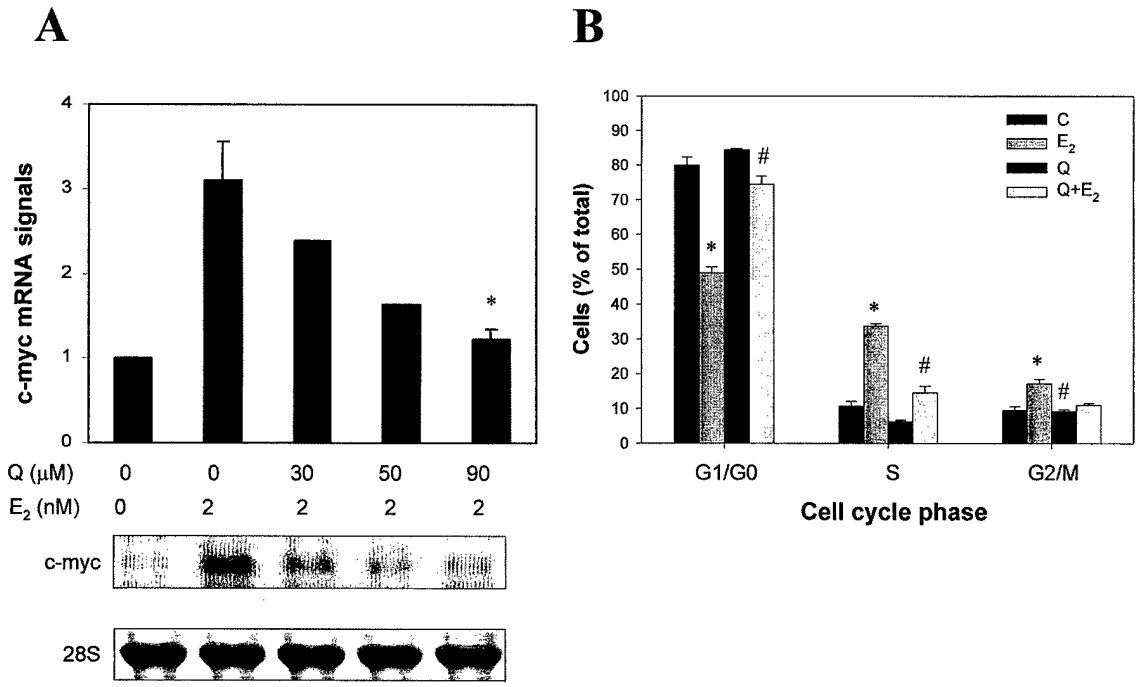

FIGURE 5 – Quinidine suppresses acute induction of c-myc mRNA and S-phase progression by estradiol. (*a*) Confluent MCF-7 cells were subcultivated in PRF-DMEM/2% stripped serum, and estrogen-depleted for 40 hr. Induction of c-myc mRNA by 2 nM estradiol ± indicated concentrations of quinidine was measured after 1 hr by isolating total cellular RNA and Northern blotting. C-*myc* mRNA signals were normalized to the 28S ribosomal signal in the ethidium bromide stained gel. Data shown on the bar graph are the mean ± SD of $n = 3$, except for 30 and 50 μM quinidine that are from a single experiment. Values for E_2 and $Q+E_2$ treated groups are reported relative to control group (control = 1). (*b*) MCF-7 cells were treated with C-0.01% ethanol (vehicle), Q-90 μM quinidine, E_2-2 nM estradiol, $Q+E_2$-90 μM quinidine + 2 nM E_2. Cell cycle phase distribution was analyzed by flow cytometry 30 hr later. Data are the mean ± SD of $n = 4$ experiments. *Significantly different from control cells ($p < 0.05$). #Significantly different from E_2 cells ($p < 0.05$).

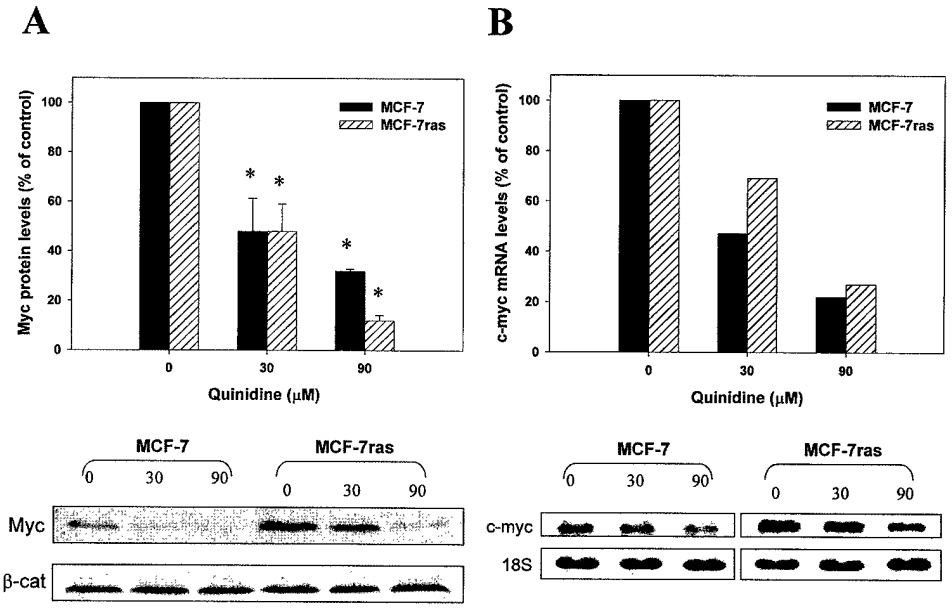

FIGURE 6 – Quinidine suppresses basal and H-*ras*-driven *c-myc* mRNA and protein expression. Confluent MCF-7 (solid bars) and MCF-7*ras* (hatched bars) cells were subcultivated into DMEM/5% FBS ± indicated concentrations of quinidine. Cells were harvested 24 hr later and Myc protein (*a*) or mRNA (*b*) levels were analyzed by Western or Northern blots, respectively. Myc protein and mRNA signals were normalized to the β-catenin and 18S ribosomal RNA signals, respectively. Data shown on the bar graphs are the mean ± SD of $n = 4$ (MCF-7) and $n = 3$ (MCF-7*ras*) experiments for (*a*) or $n = 1$ for (*b*). *Significantly different from control values ($p < 0.05$).

duced Myc protein (Fig. 6*a*) and mRNA (Fig. 6*b*) levels by approximately 50% and 90 μM quinidine had a more pronounced effect upon basal Myc protein and mRNA levels. MCF-7 cells stably transfected with H-*ras* (MCF-7*ras*) have an activated *ras* signaling pathway and express higher levels of Myc protein and mRNA than wild-type MCF-7 cells. Quinidine reduced Myc protein and mRNA expression in MCF-7*ras* cells to that seen in wild-type MCF-7 cells exposed to quinidine, suggesting that quinidine interferes with H-*ras* activated pathways that stimulate Myc. Collectively, our data demonstrate quinidine inhibits basal c-*myc* expression, estradiol-inducible c-*myc* expression, c-*myc* expression stimulated by sub-cultivation and H-*ras*-driven c-*myc* expression in MCF-7 human breast tumor cells.

*Quinidine inhibits C-*myc *promoter activity*

The ability of quinidine to inhibit c-*myc* promoter activity was tested using myc-luciferase reporter plasmids transiently transfected into MCF-7 cells. Cells were incubated in the presence of quinidine for 24 hr after transfection and luciferase activity was measured in the cell extracts. Luciferase activity in mock-transfected cells was <0.1% of the activity in control cells transfected with Del-1 (Fig. 7*a*). Quinidine treatment caused a concentration-dependent decrease in the activity of the Del-1 *c-myc* promoter. Ninety μM quinidine decreased *c-myc* promoter activity by 60%, similar to the observed levels of inhibition of Myc protein and mRNA.

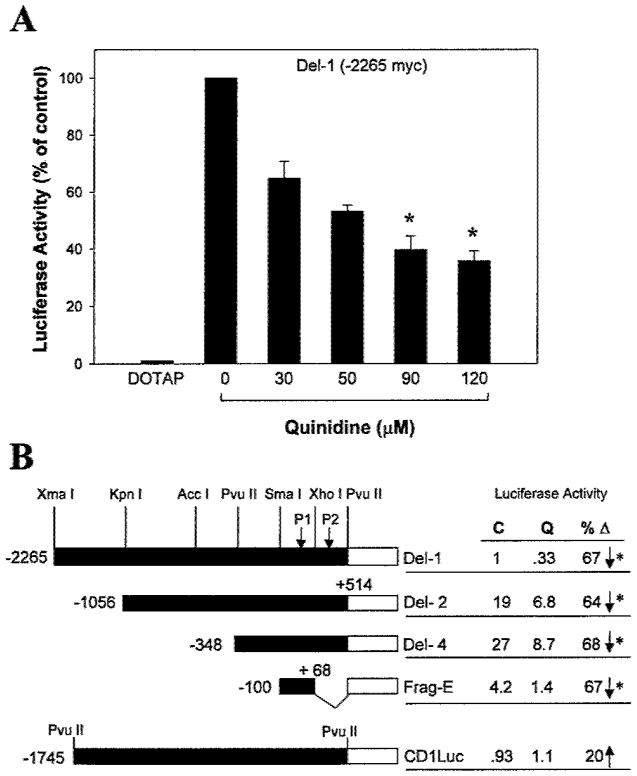

FIGURE 7 – Suppression of *c-myc* promoter activity by quinidine. (*a*) MCF-7 cells were transfected with 5 μg/dish of Del-1 (-2265 myc) *C-myc*-luciferase reporter plasmid or with the transfection mix alone (DOTAP). At the end of transfection cells were incubated for 24 hr in DMEM/5% FBS + the indicated concentrations of quinidine before preparing cell extracts for luciferase assay. Data shown are the mean luciferase activity ± SD of $n = 3$ experiments (90 and 120 μM quinidine) and $n = 2$ experiments (30 and 50 μM quinidine). The data are expressed as a percent of luciferase activity in control cells (100%). Luciferase activity in mock-transfected cells (DOTAP) was <0.01% that of control cells. Luciferase cpm in MCF-7 cell extracts in these experiments were: background (≤30), del-1 (200–500) and del-4 (2,800–6,000). *Significantly different from control (0 quinidine) cells ($p < 0.05$). (*b*) Structures of the reporter plasmids. *C-myc* and *cyclin D1* promoter regions are solid and the luciferase coding region is indicated in white. P1 and P2 are the sites of the transcription initiation from the respective *c-myc* promoters. The nucleotide locations of 5′ and 3′-ends of the myc-Luc constructs are given with respect to the P1. The effect of quinidine on *c-myc* promoter activity in 5′-deletion mutants is shown to the right of each promoter structure. Cells were transfected with 5 μg/dish of *c-myc*-Luc (Del-1, Del-2, Del-4, Frag-E) or *cyclin D1*-Luc (CD1) reporter plasmids. At the end of transfection cells were incubated for 24 hr in DMEM/5% FBS ± 90 uM quinidine before preparing cell extracts for luciferase assay. Luciferase activity driven by Del-1 in the absence of quinidine was set equal to one, and the activity of all the other promoters ± 90 μM quinidine was compared to 1. The percent change in luciferase activity by quinidine for each promoter is indicated. *Significantly different from control values ($p < 0.05$). Luciferase activity in cells transfected with promoterless construct was <2% of the activity in control cells transfected with Del-1. Data are the mean ± SD of at least $n = 3$ experiments.

To better define the region of the *c-myc* promoter responsive to quinidine, a series of 5′-deletion mutants of Del-1 was tested (Fig. 7*b*). The *cyclin D1*-luciferase (CD1) and promoterless luciferase (Luc) plasmids were used as controls. Relative luciferase activity driven by the various plasmids was compared to Del-1. Quinidine suppressed the activity of all the *myc* 5′-deletion mutants by 60–70%, but had a minimal effect on luciferase expression driven by the *cyclin D1* promoter, suggesting that the effect of quinidine is promoter specific and not related to more general effects associated with cell cycle arrest in G1. Quinidine did not inhibit the enzymatic activity of the purified luciferase protein (data not shown). We conclude that quinidine suppresses the activity of the *c-myc* promoter and that a 168 bp region of human c-myc promoter from −100 to +68 with respect to the P1 promoter is sufficient to confer responsiveness to quinidine.

Although quinidine does not appear to act by restoring TGFβ1 pathways that suppress Myc production, the TCE, a TGF-β1 control element, −86 bp to −63 bp with respect to P1, that was first identified in keratinocytes, is present in the quinidine responsive region of the c-*myc* promoter.[39] This element controls repression of the c-*myc* promoter by Rb and this might be important to the quinidine response.

The actions of quinidine on the c-*myc* Del-4 promoter and the cyclin D1 (CD1) promoter were compared in MCF-10A and MCF-7 cells. The cyclin D1 promoter was active in MCF-10A cells (877 cpm ± 23, mean ± range of duplicates in $n = 2$ experiments) and was not regulated by quinidine (90 μM, 24 hr) (894 cpm ± 23, $n = 2$). The c-*myc* Del-4 promoter, the most active of the c-*myc* promoter constructs in MCF-7 cells, was completely inactive in MCF-10A cells in 3 of 4 experiments. This was not an experimental artifact, because 2 of these experiments showed excellent activity of the cyclin D1 promoter in the MCF-10A cells and this same Del-4 construct was active in MCF-7 cells transfected in parallel with the MCF-10A cells. This result suggested that the cis-acting elements required for transcription of the *myc* gene differ in MCF-10A and MCF-7 cells.

Quinidine differentially regulates Rb/E2F1 in MCF-7 and MCF-10A cells

E2F transcription factors drive G1-S progression by activating the expression of genes required for entry into S-phase.[40,41] Two E2F consensus DNA binding sites are located between P1and P2 of the c-*myc* promoter and participate in the activation of c-*myc* transcription by E2F family members. These sites are present in Del-4 (−348 *myc)* and might contribute to its strong promoter activity in MCF-7 cells. E2F1 protein levels were reduced by 54% in MCF-7 cells exposed to 90 μM quinidine for 24 hr (Figs. 8,9) and total E2F transcriptional activity measured using an E2F-driven luciferase reporter gene decreased by 82 ± 2% (mean ± SE, $n = 3$). Quinidine did not affect protein levels of 2 other c-*myc* transcriptional activators, Sp1 and Sp3,[42] either at 4 hr or 24 hr (Fig. 8). The results suggest that decreased E2F activity contributed to the suppression of c-*myc* promoter activity as well as Myc protein levels observed in MCF-7 cells exposed to quinidine for 24 hr. There was, however, no decrease in E2F1 protein in MCF-7 cells after a 4 hr incubation with 90 μM quinidine (data not shown), implying that quinidine inhibition of early myc mRNA and protein induction (Figs. 2,5) occurred by a different mechanism. Nevertheless, Myc acts a positive regulator of E2F protein levels.[43] Therefore, suppression of early Myc expression by quinidine might contribute to the fall in E2F1 levels that occurred by 24 hr.

Hypophosphorylated Rb protein regulates E2F transcriptional activity by sequestering E2F in an inactive state in the Rb binding pocket. Using antibodies that recognize total Rb or only the phos-

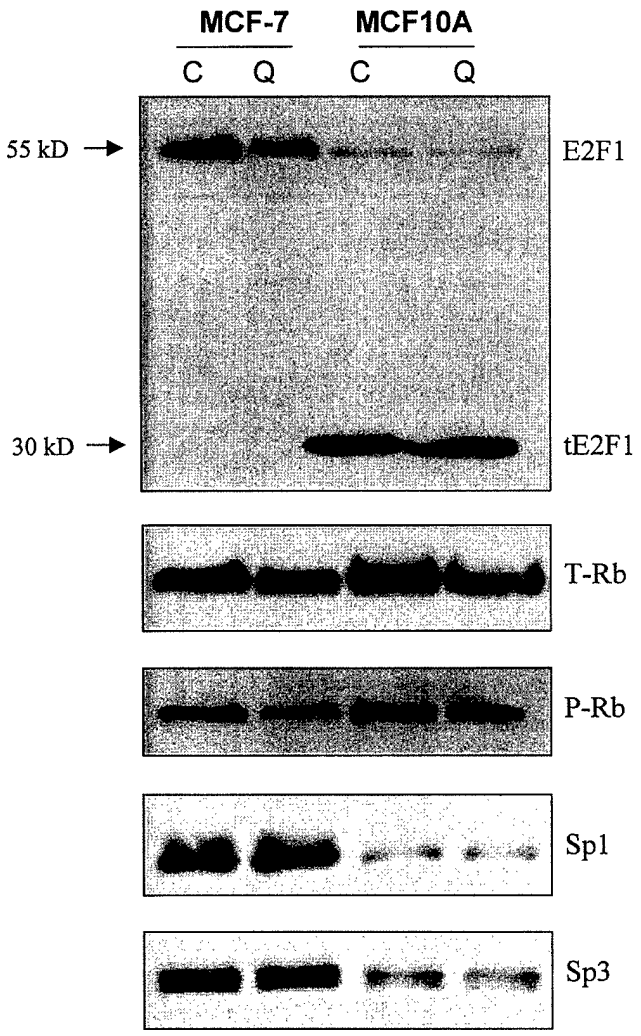

FIGURE 8 – Differential actions of quinidine on Rb and E2F1 in MCF-7 and MCF-10A cells. Cells from confluent flasks were subcultured in DMEM + 5% FBS ± 90 μM quinidine. Control (C) and quinidine-treated (Q) cells were harvested after 24 hr and levels of immunoreactive E2F1, total Rb (T-Rb), phospho ($Ser^{807/811}$)Rb (P-Rb), Sp1 and Sp3 were measured by Western blot. Total protein per lane was identical in MCF-7 and MCF-10A cells: E2F1 (60 μg/lane), T-Rb (80 μg/lane), P-Rb (60 μg/lane), Sp1 (10 μg/lane) and Sp3 (40 μg/lane). Data shown are representative of 2–4 independent experiments.

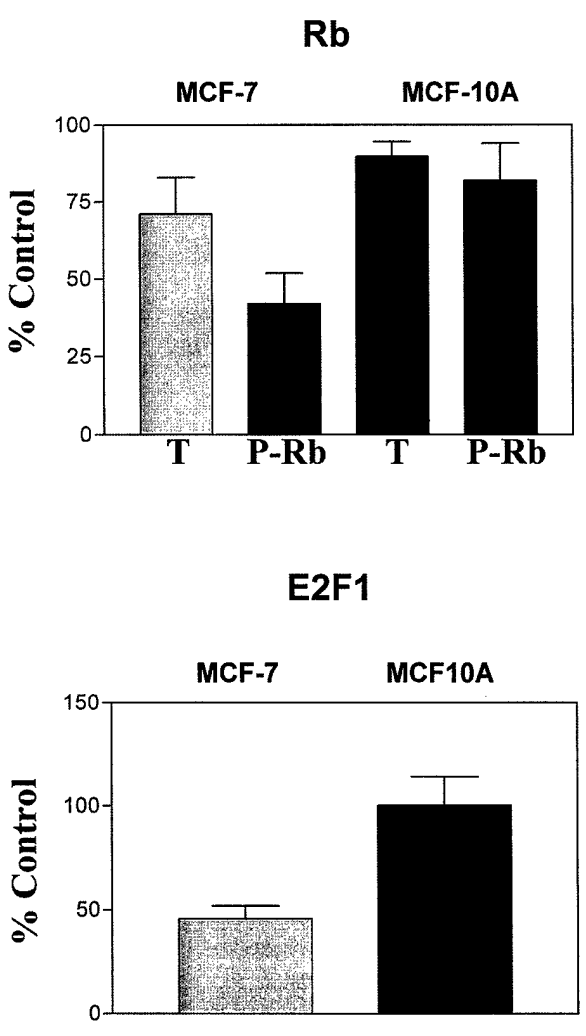

FIGURE 9 – Phospho($Ser^{807/811}$)Rb and E2F1 are decreased in quinidine-treated MCF-7 cells. Western blot immunoreactive signals corresponding to Total Rb, phosphoRb (p-Rb), and 55 kDa E2F1 protein levels obtained from extracts of cells exposed to 90 μM quinidine for 24 hr were quantified by densitometry. The value of the control signal for each protein was set to 100% in each experiment. Data shown are the signal in quinidine-treated cells expressed as a fraction of the control. Data shown are the mean ± SE of $n = 4$ experiments for MCF-7 cells and the mean and range of $n = 2$ experiments for E2F1 and Total Rb in MCF-10A cells, and the mean ± SE of $n = 3$ experiments for p-Rb in MCF-10A cells.

phorylated form of Rb ($Ser^{807/811}$) we showed that quinidine-treated MCF-7 cells were relatively depleted of phosphorylated Rb (Figs. 8,9). Immunoprecipitation of total Rb confirmed the presence of increased E2F1 bound to Rb after quinidine treatment compared to control MCF-7 cells (data not shown). Thus, quinidine acts via at least 2 mechanisms to reduce levels of free E2F1 protein resulting in suppression of E2F-mediated gene activation.

E2F1, Sp1 and Sp3 protein levels were lower in MCF-10A cells than in MCF-7 cells and did not change with quinidine (90 μM, 24 hr) treatment (Figs. 8,9). Rb protein phosphorylation levels were nearly identical in control and in quinidine treated MCF-10A cells. These observations support the hypothesis that quinidine regulation of E2F1 in MCF-7 cells is critical to its actions on growth and Myc expression. In addition, MCF-10A cells expressed a unique E2F1 immunoreactive protein, which we refer to as truncated, or tE2F1 (Fig. 8). This 30 kDa protein bound E2F1 antibodies from 2 commercial sources highly specifically. The monoclonal antibodies that were used recognize 2 regions within the E2F1 Rb binding domain and we conclude that MCF-10A cells express a truncated, E2F1-like protein that retains the Rb binding domain. This protein appears to be transcriptionally inactive. We could not detect luciferase activity in MCF-10A cells transfected with the E2F driven-luciferase reporter gene (data not shown) using as a positive control for the transfection assays, the cyclin D1-driven luciferase reporter gene. Collectively, our results suggest that the 55 kDa E2F-1 plays a minor role in driving proliferation in MCF-10A cells. This idea merits more rigorous examination, however the observed quinidine resistance of MCF-10A cells fits well the model that quinidine inhibition of E2F-1 transcriptional activity is important for its antiproliferative action and suppression of Myc expression.

DISCUSSION

In the present study, we demonstrated that pharmacological inhibition of mammary epithelial tumor cell proliferation by quin-

idine was closely associated with reduced Myc protein expression. Quinidine reduced Myc expression by 50–70% at all levels of investigation including protein, mRNA and c-*myc* promoter activity in MCF-7 cells. Given the importance of Myc to cell survival and growth and the redundancy built into signaling pathways that control these processes, quinidine is a remarkably effective Myc expression inhibitor. Quinidine interfered with estrogen-inducible *myc* expression, *ras*-MAPK pathways stimulating *myc* and mechanisms invoked by the release of cells from confluency into fresh serum leading to myc activation all of which are likely to engage components of growth factor signaling pathways.

The cdk/Rb/E2F pathway plays a critical role in G1 cell cycle progression and cellular differentiation.[40,41] Rb regulates levels of free E2F transcription factors. Unphosphorylated Rb acts as a tumor suppressor protein and sequesters E2F proteins in a transcriptionally inactive state by binding them in the Rb binding pocket. Phosphorylation of Rb or the binding of certain oncogenic viral proteins to this binding pocket, causes the release of E2F1, 2 and 3 and triggers G1-S cell cycle progression. Our results showed that after 24 hr in quinidine MCF-7 cells exhibit an overall suppression in the activity of the cdk/Rb/E2F pathway. Eighty percent of MCF-7 cells were arrested in G1/G0 phase of the cell cycle.[3,4] Protein levels of cdk4 and cyclin D1 were reduced and levels of the cyclin-dependent kinase inhibitor, p21/WAF1, were increased favoring the retention of retinoblastoma protein in its hypophosphorylated, tumor suppressor state.[2] Myc expression and that of a Myc target protein, E2F1, were suppressed, but levels of the transcription factors, Sp1 and Sp3, were unaffected by quinidine treatment. E2F activated transcription was decreased by 82% in MCF-7 cells incubated with quinidine for 24 hr. We conclude that suppression of E2F transcriptional activity is an important mechanism of quinidine action.

We also propose the idea that hypophosphorylated retinoblastoma is an important mediator of the response to quinidine. Hypophosphorylated Rb is a transcriptional repressor of myc. The activity of the human c-myc promoter was inhibited by quinidine in transiently transfected MCF-7 cells and the quinidine responsive region, −100 bp to +68 bp, contains the Rb responsive region. Quinidine did not promote the differentiation of MDA-MB-468 human breast tumor cells that lack Rb protein (Strobl, unpublished) and the reintroduction of Rb into Rb −/− SAOS cells, elicited a large cytoplasm phenotype remarkably similar to that seen in quinidine-treated MCF-7 cells.[44]

The acute rise in Myc that occurred 90 min after exposure to estradiol or subculturing in fresh serum, was suppressed by quinidine independently of its actions upon E2F1 or Rb. E2F1, Sp1 and Sp3 proteins levels did not change during a 4 hr incubation of MCF-7 cells with quinidine and the appearance of hypophosphorylated Rb in quinidine-treated MCF-7 cells occurred between 12 and 24 hr.[2] Ionic changes elicited by quinidine might attenuate the rapid induction of c-*myc* in MCF-7 cells.

In lymphocytes, a rapid induction of c-*myc* gene expression was initiated in response to stimuli that raised intracellular Ca^{+2} and pharmacological inhibition of potassium channels prevented the rise in intracellular Ca^{+2} in many cell systems.[45,46] Quinidine blocked potassium channels in MCF-7 cells at concentrations that antagonize c-*myc* induction in MCF-7 cells, causing membrane depolarization within 3 min.[3,4] Membrane depolarization can alter intracellular Ca^{+2} by reducing the driving force for calcium entry through non-selective cation channels.[46] In addition, quinidine has been reported to inhibit inositol 1,4,5-trisphosphate binding to its receptor thereby blocking Ca^{+2} release from intracellular stores.[47]

MCF-10A cells continued to proliferate in the presence of quinidine and Myc protein levels were not significantly reduced. In comparison with MCF-7 cells, MCF-10A cells maintained high levels of phosphorylated Rb expression in the presence of quinidine. MCF-10A cells also failed to differentiate in response to treatment with either quinidine or c-*myc* antisense oligonucleotides and these results are consistent with the hypothesis that both hypophosphorylated Rb and reduced Myc expression are required for the Oil Red O differentiation response in mammary epithelial cells.

MCF-10A cells exhibited evidence of a highly expressed 30 kDa immunoreactive E2F1-like protein. MCF-10A cells expressed extremely low levels of 55 kDa E2F1 protein. We could not demonstrate transcriptional activation of an E2F-driven luciferase reporter gene in MCF-10A cells and in gel mobility shift assays using extracts of MCF-10A cells, Botos *et al.*,[48] could find no evidence for the presence of E2F1 binding to the DNA consensus sequence for E2F. We conclude that MCF-10A cells over express a 30 kDa protein that retains a Rb binding domain, but lacks E2F DNA binding and transcriptional activity. The binding of a truncated E2F1-like protein to hypophosphorylated Rb could competitively inhibit the binding of other Rb pocket protein binding partners or interfere with the ability of hypophosphorylated Rb to promote differentiation. The altered E2F-1/Rb pathway in MCF-10A cells is a likely explanation for their resistance to quinidine actions on Myc and cell differentiation.

ACKNOWLEDGEMENTS

The authors are grateful to Dr. B. Vogelstein, Johns Hopkins University and Dr. R. Pestell, Albert Einstein College of Medicine for providing myc-luciferase and cyclin D1-luciferase constructs, respectively.

REFERENCES

1. Hondeghem LM, Roden DM. Agents used in cardiac arrhythmias. In: Katzung BG, ed. Basic and clinical pharmacology, 8th ed. New York: Lange Medical Publications, 2001, 219–244.
2. Zhou Q, Melkoumian ZK, Lucktong A, Moniwa M, Davie JR, Strobl JS. Rapid induction of histone hyperacetylation and cellular differentiation in human breast tumor cell lines following degradation of histone deacetylase-1. J Biol Chem 2000;275:35256–3.
3. Woodfork K, Wonderlin W, Peterson V, Strobl J. Inhibition of ATP-sensitive potassium channels causes reversible cell-cycle arrest of human breast cancer cells in tissue culture. J Cell Physiol 1995;162: 163–71.
4. Wang S, Melkoumian Z, Woodfork K, Cather C, Davidson A, Wonderlin W, Strobl J. Evidence for an early G1 ionic event necessary for cell cycle progression and survival in the MCF-7 human breast carcinoma cell line. J Cell Physiol 1998;176:456–64.
5. Wonderlin WF, Woodfork K, Strobl J. Changes in membrane potential during the progression of MCF-7 human mammary tumor cells through the cell cycle. J Cell Physiol 1995;165:177–85.
6. Amati B, Land H. Myc-Max-Mad: a transcription factor network controlling cell cycle progression, differentiation and death. Curr Opin Genet Dev 1994;4:102–8.
7. Henriksson M, Luscher B. Proteins of the Myc network: essential regulators of cell growth and differentiation. Adv Cancer Res 1996; 68:109–82.
8. Deming SL, Nass SJ, Dickson RB, Trock BJ. C-myc amplification in breast cancer: a meta-analysis of its occurrence and prognostic relevance. Br J Cancer 2000;83:1688–95.
9. Nass SJ, Dickson RB. Defining a role for c-Myc in breast tumorigenesis. Breast Cancer Res Treat 1997;44:1–22.
10. Dubik D, Shiu RP. Transcriptional regulation of c-myc oncogene expression by estrogen in hormone-responsive human breast cancer cells. J Biol Chem 1988;263:12705–8.
11. Dang CV. C-Myc target genes involved in cell growth, apoptosis and metabolism. Mol Cell Biol 1999;18:1–11.
12. Staller P, Peukert K, Kiermaier A, Seoane J, Lukas J, Karsunky H, Moroy T, Bartek J, Massague J, Hanel F, Eiler, M. Repression of p15INK4b expression by Myc through association with Miz-1. Nat Cell Biol 2001;3:392–9.
13. D'Cruz CM, Gunther EJ, Boxer RB, Hartman JL, Sintasath L, Moody SE, Cox JD, Ha SI, Belka GK, Golant A, Cardiff RD, Chodosh LA. c-MYC induces mammary tumorigenesis by means of a preferred pathway involving spontaneous Kras2 mutations. Nat. Med 2001;7: 235–9.
14. Ebinuma H, Saito H, Saito Y, Wakabayashi K, Nakamura M, Kurose

I, Ishii H. Antisense oligodeoxynucleotide against c-myc mRNA induces differentiation of human hepatocellular carcinoma cells. Int J Oncol 1999;15:991–9.
15. Canelles M, Delgado MD, Hyland KM, Lerga A, Richard C, Dang CV, Leon J. Max and inhibitory c-Myc mutants induce erythroid differentiation and resistance to apoptosis in human myeloid leukemia cells. Oncogene 1997;14:1315–27.
16. Griep AE, Wesphal H. Antisense Myc sequences induce differentiation of F9 cells. Proc Natl Acad Sci USA 1988;85:6806–10.
17. Holt JT, Redner RL, Neinhuis AW. An oligomer complimentary to c-myc mRNA inhibits proliferation of HL-60 promyelocytic cells and induces differentiation. Mol Cell Biol 1988;8:963–73.
18. Prochownik EV, Kukowska J, Rodgers C. c-Myc antisense transcripts accelerate differentiation and inhibit G1 progression in murine erythroleukemia cells. Mol Cell Biol 1988;8:3683–95.
19. Kasid A, Lippman M, Papageorge A, Lowy D, Gelmann E. Transfection of v-ras^H DNA into MCF-7 human breast cancer cells bypasses dependence on estrogen for tumorigenesis. Science 1985;228: 745–28.
20. Strobl JS, Kirkwood KL, Lantz TK, Lewine MA, Peterson VA, Worley JF. Inhibition of human breast cancer cell proliferation in tissue culture by the neuroleptic agents pimozide and thioridazine. Cancer Res 1990;50:5399–405.
21. Strobl JS, Lippman ME. Prolonged retention of estradiol by human breast cancer cells in tissue culture. Cancer Res 1979;39:3319–27.
22. Alitalo K, Schwab M, Lin C, Varmus H E, Bishop JM. Homogeneously staining chromosomal regions contain amplified copies of an abundantly expressed cellular oncogene (c-myc) in malignant neuroendocrine cells from a human colon carcinoma. PNAS 1983;89: 1707–11.
23. He TC, Sparks AB, Rago C, Hermeking H, Zawel L, da Costa LT, Morin PJ, Vogelstein B, Kinzler KW. Identification of c-MYC as a target of the APC pathway. Science 1998;281:1509–12.
24. Albanese C, Johnson J, Watanabe G, Eklund N, Vu D, Arnold A, Pestell RG. Transforming p21ras mutants and c-Ets-2 activate the cyclin D1 promoter through distinguishable regions. J Biol Chem 1995;270:23589–97.
25. Vindelov L, Christensen I. Detergent and proteolytic enzyme-based techniques for nuclear isolation and DNA content analysis. Methods Cell Biol 1994;41:219–29.
26. Chomczynski P, Sacchi N. Single-step method of RNA isolation by acid guanidium thiocyanate-phenol-chloroform extraction. Anal Biochem 1987;162:156–9.
27. Jing Y, Zhang J, Waxman S, Mira-y-Lopez R. Upregulation of cytokeratins 8 and 18 in human breast cancer T47D cells is retinoid-specific and retinoic acid receptor-dependent. Differentiation 1996; 60:109–17.
28. Bacus SS, Kiguchi K, Chin D, King CR, Huberman E. Differentiation of cultured human breast cancer cells (AU-565 and MCF-7) associated with loss of cell surface HER-2/neu antigen. Mol Carcinogen 1990;3:350–62.
29. Mehta RR, Bratescu L, Graves JM, Green A, Mehta RG. Differentiation of human breast carcinoma cells by a novel vitamin D analog: 1α-hydroxyvitamin D5. Int J Oncol 2000;16:65–73.
30. Douglas AM, Grant SL, Goss GA, Clouston DR, Sutherland RL, Begley CG. Oncostatin M induces the differentiation of breast cancer cells. Int J Cancer 1998;75:64–73.
31. Giunciuglio D, Culty M, Fassina G, Masiello L, Melchiori A, Paglialunga G, Arand G, Ciardiello F, Basolo F, Thompson EW, Albini A. Invasive phenotype of MCF10A cells overexpressing c-Ha-ras and c-erbB-2 oncogenes. Int J Cancer 1995;63:815–22.
32. Gross-Mesilaty S, Reinstein E, Bercovich B, Tobias KE, Schwartz AL, Kahana C, Ciechanover A. Basal and human papillomavirus E6 oncoprotein-induced degradation of Myc proteins by the ubiquitin pathway. Proc Natl Acad Sci USA 1998;95:8058–63.
33. Alexandrow M, Kawabata M, Aakre M, Moses H. Overexpression of the c-Myc oncoprotein blocks the growth-inhibitory response but is required for the mitogenic effects of transforming growth factor beta 1. Proc Natl Acad Sci USA 1995;92:3239–43.
34. Derynck R, Feng X. TGF-β receptor signaling. Biochem Biophys Acta 1997;1333:F105–50.
35. Chen C, Knag Y, Massague J. Defective repression of c-myc in breast cancer cells: a loss at the core of the transforming growth factor β growth program. Proc Natl Acad Sci USA 2001;98:992-999.
36. Sun L, Chen C. Expression of transforming growth factor β type III receptor suppresses tumorigenicity of human breast cancer MDA-MB-231 cells. J Biol Chem 1997;272:25367–72.
37. Chen C, Wang X, Sun L. Expression of transforming growth factor β (TGFβ) type III receptor restores autocrine TGFβ1 activity in human breast cancer MCF-7 cells. J Biol Chem 1997;272:12862–7.
38. Prall OW, Rogan EM, Musgrove EA, Watts CK, Sutherland RL. c-Myc or cyclin D1 mimics estrogen effects of cyclinE-cdk2 activation and cell cycle reentry. Mol Cell Biol 1998;18:4499–508.
39. Pietenpol J, Munger K, Howley P, Stein R, Moses HL. Factor-binding element in the human c-myc promoter involved in transcriptional regulation by transforming growth factor β1 and by the retinoblastoma gene product. Proc Natl Acad Sci USA 1991;88:10227–31.
40. Sears RC, Nevins JR. Signaling networks that link cell proliferation and cell fate. J Biol Chem 2002;277:11617–20.
41. Trimarchi JM, Lees JA. Sibling rivalry in the E2F family. Nat Rev Mol Cell Biol 2002;3:11–20.
42. Majello B, De Luca P, Suske G, Lania L. Differential transcriptional regulation of c-myc promoter through the same DNA binding sites targeted by Sp1-like proteins. Oncogene1995;10:1841–8.
43. Oster SK, Ho CSW, Soucie EL, Penn LZ. The *myc* oncogene: marvelously complex. Adv Cancer Res 2002;84:82–154.
44. Huang H-J, Yee J-K, Shew J-Y, Chen P-L, Bookstein R, Friedmann T. Suppression of the neoplastic phenotype by replacement of the RB gene in human cancer cells. Science 1988;242:1563–6.
45. Liburdy RP, Callahan DE, Harland J, Dunham E, Sloma TR, Yaswen P. Experimental evidence for 60 Hz magnetic fields operating through the signal transduction cascade. Effects on calcium influx and c-MYC mRNA induction. FEBS Lett 1993;334:301–8.
46. Wonderlin WF, Strobl JS. Potassium channels, proliferation and G1 progression. J Membr Biol 1996; 154: 91-107.
47. Mesra UK, Gawdi G, Pizzo SV. Chloroquine, quinine and quinidine inhibit calcium release from macrophage intracellular stores by blocking inositol 1,4,5-triphosphate binding to its receptor. J Cell Biochem 1997;64:225–32.
48. Botos J, Smith R III, Kochevar DT. Retinoblastoma function is a better indicator of cellular phenotype in cultured breast adenocarcinoma cells than retinoblastoma expression. Exp Biol Med 2002;227: 354–62.

Available online at www.sciencedirect.com
SCIENCE DIRECT®
ELSEVIER
Biochemical Pharmacology xxx (2004) xxx–xxx
Biochemical Pharmacology
www.elsevier.com/locate/biochempharm

Differentiation-inducing quinolines as experimental breast cancer agents in the MCF-7 human breast cancer cell model

Anna R. Martirosyan[a,1], Rayhana Rahim-Bata[a,1], Andrew B. Freeman[a], Charles D. Clarke[a], Rachael L. Howard[a], Jeannine S. Strobl[a,b,*]

[a]*Department of Biochemistry & Molecular Pharmacology, West Virginia University, Morgantown, WV 26506, USA*
[b]*Mary Babb Randolph Cancer Center, West Virginia University, Morgantown, WV 26506, USA*

Received 19 January 2004; accepted 3 May 2004

Abstract

The purpose of this work is to develop agents for cancer differentiation therapy. We showed that five antiproliferative quinoline compounds in the National Cancer Institute database stimulated cell differentiation at growth inhibitory concentrations (3–14 μM) in MCF-7 human breast tumor cells in vitro. The differentiation-inducing quinolines caused lipid droplet accumulation, a phenotypic marker of differentiation, loss of Ki67 antigen expression, a cell cycle marker indicative of exit into G_0, and reduced protein levels of the $G_1 - S$ transcription factor, E2F1. The antimalarial quinolines, chloroquine, hydroxychloroquine and quinidine had similar effects in MCF-7 cells, but were 3–10 times less potent than the NSC compounds. NSC3852 and NSC86371 inhibited histone deacetylase (HDAC) activity in vitro and caused DNA damage and apoptosis in MCF-7 cells, consistent with their differentiation and antiproliferative activities. However, the HDAC assay results showed that for other compounds, direct HDAC enzyme inhibition was not required for differentiation activity. E2F1 protein was suppressed by all differentiation quinolines, but not by non-differentiating analogs, quinoline and primaquine. At equivalent antiproliferative concentrations, NSC69603 caused the greatest decrease in E2F1 protein (90%) followed by antimalarials quinidine and hydroxychloroquine. NSC69603 did not cause DNA damage. The other NSC compounds caused DNA damage and apoptosis and reduced E2F1 levels. The physicochemical properties of NSC3852, NSC69603, NSC86371, and NSC305819 predicted they are drug candidates suitable for development as experimental breast tumor cell differentiation agents. We conclude DNA damage and reductions in E2F1 protein are mechanistically important to the differentiation and antiproliferative activities of these quinoline drug candidates.

Keywords: Breast cancer; Differentiation therapy; E2F; MCF-7; Novel antitumor agents; Quinolines

Abbreviations: HDAC, histone deacetylase; MTS, 3-(4,5-dimethylthiazol-2-yl)-5-(3-carboxylmethoxyphenyl)-2-(4-sulfophenyl)-2H-tetrazolium; PAMPA, parallel artificial membrane permeation assay; Rb, retinoblastoma protein; Amodiaquin, 4-[(7-chloro-4-quinolinyl)amino]-2-[diethylamino)methyl]phenol; Chloroquine, N4-(7-chloro-4-quinolinyl)-*N1*,*N1*-diethyl-1,4-pentanediamine; Halofantrine, 1,3-dichloro-α-[2-(dibutylamino)ethyl]-6-(trifluoromethyl)-9-phenanthrenemethanol; Hydroxychloroquine , 2-[[4-[(7-chloro-4-quinolinyl)amino]pentyl]ethylamino]ethanol; Mefloquine, piperidinyl-2,8-bis(trifluoromethyl)-4-quinolinemethanol); Quinidine , (9*S*)-6′-methoxycinchonan-9-ol; Quinine, (8-α,9*R*)-6′-methoxycinchonan-9-ol; Primaquine, *N*4-(6-methoxy-8-quinolinyl)-1,4-pentanediamine; NSC10010, *N*,*N*-bis(2-methyl-6-methoxy-4-quinaldyl)-1,9-diamine-nonane dihydrochloride hydrate; NSC3852, 5-nitroso-8-quinolinol; NSC69603, 4-(2-(2,5-dimethoxyphenyl)vinyl)quinoline; NSC86371, 2-[2-(8-hydroxy-5-methyl-7-quinolyl)vinyl]-1,6-dimethyl iodide; NSC305819, 1-(2,8-bis(trifluoromethyl)-4-quinolinyl)-3-(tertbutylamino)-1-propanol

* Corresponding author. Tel.: +1 304 293 7151; fax: +1 304 293 6846.
E-mail address: jstrobl@hsc.wvu.edu (J.S. Strobl).
[1] The first two authors contributed equally to this work.

Differentiation therapy involves the use of drugs that modulate gene expression to control tumor growth. Interest in cancer differentiation agents as an alternative or supplement to traditional cancer chemotherapeutic drugs has increased in recent years. Histone deacetylases (HDACs) are the target of a number of tumor differentiation agents [1–3]. Catalytic HDAC inhibitors elicit a common profile of responses in tumor cells including histone hyperacetylation, elevated expression of the cyclin-dependent kinase inhibitor, p21/WAF-1, cell cycle arrest and apoptosis. Of note, many HDAC enzyme inhibitors that cause differentiation and apoptosis in human tumor cells were first identified as antifungal or antiprotozoal agents [4–6].

We observed growth arrest and differentiation in human breast tumor cells after treatment with the natural cinchona tree bark antimalarial, quinidine [7]. Quinidine-treated MCF-7 cells displayed an enlarged cytoplasm filled with

0006-2952/$ – see front matter © 2004 Published by Elsevier Inc.
doi:10.1016/j.bcp.2004.05.003

lipid-droplets. Cells were morphologically indistinguishable from cells treated with the histone deacetylase inhibitor trichostatin A, and comparable changes in the G_1 cell cycle protein profile including induction of p21/WAF, hypophosphorylation of retinoblastoma protein (pRb) and histone H4 hyperacetylation were observed. However, quinidine did not inhibit histone deacetylase catalytic activity suggesting that differentiation agents can engage alternative biochemical pathways. On this basis, we screened a panel of antimalarials and breast tumor cell antiproliferative quinolines from the NCI database for in vitro breast tumor differentiation activity to identify new experimental differentiation agents. Five differentiation quinolines are described which differ in their effects on histone deacetylase, DNA and apoptosis.

1. Materials and methods

1.1. Chemicals

Quinidine, chloroquine, primaquine, amodiaquin, quinine, quinoline, quinolinic acid and trichostatin A (TSA) were purchased from Sigma Chemical Company . Hydroxychloroquine and the NSC investigational compounds were gifts. Water soluble compounds were prepared as 1000× stocks and diluted directly into the assays. An equal volume of water was used as the solvent control. All other compounds were prepared as 1000–10,000× stock solutions in dimethyl sulfoxide and were diluted in tissue culture medium or assay buffer as appropriate; the final concentration of the solvent was $\leq$0.1% in all experiments, and an equal concentration of dimethyl sulfoxide was added to control groups. All other reagents were purchased from Sigma or Fisher Scientific.

1.2. Antibodies

Ki67 antibodies were purchased from Dako Corporation; E2F-1 and β-catenin antibodies were obtained from Santa Cruz Biotechnology, Inc. Peroxidase-conjugated secondary antibodies were used at dilutions recommended by the suppliers and reactions were visualized using Super Signal Pierce.

1.3. Cell culture

The MCF-7 human breast cancer cell line (passages 43–60) was grown in Dulbecco's modified Eagle's medium supplemented with 10% heat-inactivated fetal bovine serum, 2 mM glutamine, and 40 μg/ml gentamicin at 37 °C in a humidified atmosphere of 6% CO_2/94% air. Cells were passaged weekly. Experiments were conducted with cell populations sub-cultured from confluent flasks into medium containing 5% serum. MCF10A (ATCC) were grown in Mammary epithelial growth medium.

1.4. MTS assay

3-(4,5-Dimethylthiazol-2-yl)-5-(3-carboxymethoxyphenyl)-2-(4-sulfophenyl)-2H-tetrazolium (MTS) (Promega) is metabolized by mitochondria in living cells to a colored formazan product. MCF-7 cells were plated in 96-well plates and incubated for 24 h without drugs. Serial dilutions of each compound or the solvent alone were added to the wells in triplicate and cells were incubated for 48 h before addition of the MTS substrate. Absorbance (490 nm) was determined after a 2 h incubation at 37 °C with MTS. Concentration–response data were fit by nonlinear regression using PrismGraphPad software to obtain the MTS IC_{50} values.

1.5. Cell differentiation end-points

Oil Red O: Cells were plated onto sterile glass coverslips placed into 35 mm^2 tissue culture dishes, and MTS IC_{50} levels of compounds were added for 48 h. To measure cytoplasmic lipid droplet accumulation cells were fixed, stained with Oil Red O and counterstained with Mayer's hematoxylin [8]. The threshold used to define a positive Oil Red O response was $\geq$10% of cells containing at least 1–10 lipid droplets/cell. For most compounds, 1 μM was the lowest concentration tested. Trichostatin A was used as the positive control for these assays, and 10 nM TSA caused a positive Oil Red O response in MCF-7 cells.

Ki67 index: Immunocytochemical detection of the cell cycle marker, nuclear Ki67, was performed as described previously [9]. The Ki67 index was calculated using the formula:

$$\frac{\%\ \text{Ki67 negative cells in treated cells}}{\%\ \text{Ki67 negative cells in control cells}}.$$

E2F-1 protein: E2F-1 protein levels in whole cell extracts were measured by Western blot analysis 48 h following addition of solvent or experimental compound (MTS IC_{50} levels) to the cell culture medium. E2F-1 chemiluminescent signals were captured using autoradiography and densitometric spot analysis with automatic background subtraction of the signals was performed using a FluorChem instrument (Alpha Innotech, San Leandro, CA). The E2F1 signals were normalized to the β-catenin signal [8] because previous studies showed that quinolines did not alter the levels of β-catenin).

1.6. HDAC assay

Compounds were screened for direct HDAC inhibition using HeLa cell extracts and a commercial assay kit (HDAC Fluorescence Activity Assay, BIOMOL Research Laboratories, Inc., Plymouth Meeting, PA). MTS IC_{50} levels of each compound were added to cell extracts diluted in reaction buffer. Reactions were initiated by the addition of substrate (40 μM final concentration), and were con-

ducted for 10 min at 37 °C in triplicate wells of a 96-well plate. Product was quantified using 360 nm excitation and 460 nm emission (Cytofluor4000, PerSeptive Biosystems, Inc., Framingham, MA). Trichostatin A was used as the positive control in these assays; concentration–response experiments showed that HDAC activity in HeLa cell extracts was inhibited by trichostatin A with an IC_{50} value of 8.5 nM. Compounds active as HDAC inhibitors in HeLa cell extracts were retested in MCF-7 nuclear extracts prepared using the method of Dignam et al. [10].

1.7. Apoptosis determinations

The release of nucleosomal fragments into the cytoplasm of apoptotic cells was quantified using the Cell Death Detection ELISA^{PLUS} kit (Roche Applied Science). The nucleosome-enrichment fraction was calculated as the ratio of the absorbance (405 nm) of treated cultures/solvent exposed cultures. The positive control, 30 μM etoposide, showed a nucleosome-enrichment fraction of 2.7.

1.8. Comet assay

MCF-7 cells were exposed to MTS IC_{50} levels of compounds or solvent alone for 24 h, then harvested and resuspended in ice-cold PBS (1.5×10^5 cells/ml). Fifty microliters of the cell suspension and 500 μl of 42 °C low melting point agarose were mixed, and 75 μl of the cell suspension spread over a Comet slide (Trevigen). Slides were processed in alkali solution as per the instructions of the manufacturer (Trevigen) and electrophoresed at 4 °C. DNA Comets were visualized after staining with SYBR green using a Nikon Eclipse TS100 microscope and FITC-cube at 640×. In cells with DNA damage, DNA fragments move from the cell nucleus (Comet head) into a tail-like structure. The Comet images were analyzed using the LAI Automated Comet Assay Analysis System (Loats Associates, Inc.). DNA damage was quantified by the tail moment = %DNA × distance traveled.

1.9. Parallel artificial membrane permeation assay (PAMPA)

Artificial membranes were prepared by treating Multi-Screen-IP PAMPA filter plates (Millipore Corp.) with a 1% (w/v) solution of lecithin in dodecane (5 μl/96-well filter). Acceptor and donor wells separated by the lipid membrane contained 5% DMSO in PBS, pH 7.4. As a measure of the ability of the test compounds to undergo intestinal absorption, each compound was added to the donor wells in duplicate at a final concentration of 500 μM. Incubations were performed at room temperature for 24 or 48 h, and then the contents of the acceptor and donor wells were transferred to UV transparent half-volume Corning 96-well plates (Fisher Scientific). The concentration of the test compounds in the donor well and acceptor wells was quantified by UV spectrophotometry using a SpectraMax 250 (Molecular Devices Corporation) and molar extinction coefficients of each compound.

1.10. Statistical analysis

Data were analyzed for statistical significance using a one-way ANOVA followed by Dunnett's *t*-test to compare treated groups to the appropriate solvent control group. The level of statistical significance used was $P < 0.05$.

2. Results

2.1. Cell differentiation activity

All of the compounds examined in the differentiation assays were antiproliferative in MCF-7 cells. Two antiproliferative measures, sulforhodamine blue (SRB) staining (GI_{50}) a growth arrest index reported by the NCI (http://dtp.nci.nih.gov or http://cactus.nci.nih.gov/ncidb2/), and inhibition of MTS metabolism (IC_{50}), independently determined under our experimental conditions are presented in Table 1. Our aim was to identify antiproliferatives capable of inducing cell differentiation. Differentiation activity was measured by accumulation of cytoplasmic lipid droplets and elevations in Ki67 index (Table 1). Lipid droplet accumulation was used as an end-point for differentiation activity because it occurs in MCF-7 cells induced to differentiate by treatment with Vitamin D analogs or histone deacetylase inhibitors [11,12]. Table 1 lists the lowest concentration (μM) of compound that induced the appearance of lipid droplets in MCF-7 cells during a 48 h incubation. Compounds that did not yield a positive Oil Red O response were not considered further. However, because the Oil Red O response lacked a mechanistic basis, we used a cell cycle marker, the Ki67 index as the more definitive indicator of differentiation activity. Ki67 is a nuclear protein in all actively cycling cells that is lost when cells exit the cell cycle and enter G_0 [13]. A Ki67 index = 1 reflects no change from control cells. The larger the Ki67 index, the greater the proportion of G_0 cells in the population. To compare differentiation activity among all the quinolines at equally antiproliferative concentrations, Ki67 assays were performed at a single concentration, the MTS IC_{50}.

Compounds **1–8** are antimalarials (Table 1 and Fig. 1). Among the antimalarials, quinolines with a 4-substitution were most active in these differentiation assays. Chloroquine (**1**), hydroxychloroquine (**2**), amodiaquin (**3**), quinidine (**4**) and quinine (**5**) were positive for lipid droplet accumulation and had Ki67 indeces >1 (Table 1). Mefloquine (**6**) was the only 4-substituted quinoline antimalarial that did not promote differentiation. The unsubstituted quinoline ring (**9**) was completely inactive. Halofantrine (**7**), an antimalarial phenanthrene, and primaquine (**8**), an

Table 1
Differentiation activity

#	NSC #	Name	Oil Red O (μM)	MTS IC50 (μM)	SRB GI50 (μM)	Ki67 index	HDAC activity (% control)
1	14050	Chloroquine	1	33	19	6.6*	91 ± 6
2	4375	Hydroxychloroquine	5	57	nd	3.6	94 ± 1
3	13453	Amodiaquin	10	7	nd	2.4	86 ± 4
4	10004	Quinidine	10	113	nd	5	100 ± 13
5	5362	Quinine	30	40	60	4.1	102 ± 14
6	157387	Mefloquine	Negative	3	nd	0.3	90 ± 2
7	305789	Halofantrine	5	11	10	1.4	81 ± 13
8	149765	Primaquine	2.5	3	16	1.1	95 ± 14
9		Quinoline	Negative	62	nd	0.4	96 ± 7
10	2039		15	8	2	1.6	95 ± 4
11	3852		10	10	2	7.2*	69 ± 6*
12		Quinolinic acid	Negative	28	nd	0.4	99 ± 6
13	69603		1	14	0.9	6*	111 ± 7
14	305819		1	7	13	5.8*	90 ± 17
15	124637		1	13	14	3.4	127 ± 14
16	4239		1.3	0.7	2	1.9	96 ± 4
17	10010		3.5	4	5.4	8.3*	94 ± 8
18	86371		1	6	nd	6*	65 ± 5*
19	86373		1	13	nd	4.7	97 ± 2
20	86372		2	0.2	0.1	0.8	91 ± 7
21	85700		1	7	7	4.1	97 ± 1
22	85701		0.5	4	4	2.7	90 ± 7
23	4238		0.7	0.4	2	1.9	109 ± 13

Numbers in the first column correspond to compound structures **1–23** (Figs. 1 and 2). For each compound, the lowest concentration that produced an Oil Red O response is shown. Antiproliferative activity is reported as the IC_{50} level for inhibition of mitochondrial metabolism of MTS following a 48h exposure to each compound. Data are the average IC_{50} of $n = 3$ experiments performed with 10 concentrations of each compound in triplicate. For comparison, the GI_{50} for sulforhodamine blue (SRB) staining reported on the NCI website is presented (nd: not determined). The Ki67 index is a measure of the fraction of G_0 cells in a population where a Ki67 index >1 indicates more G_0 cells in the population. Data shown are the average of at least $n = 3$ experiments in cells exposed for 48 h to the MTS IC_{50} level of each compound. Inhibition of histone deacetylase (HDAC) activity in vitro by IC_{50} levels of each compound is expressed as a percent of HDAC activity in solvent control groups. Data are the mean ± S.E.M. of at least $n = 3$ experiments/compound assayed in duplicate. Statistically significant differences in Ki67 index and HDAC activity ($P < 0.05$) are indicated by (*).

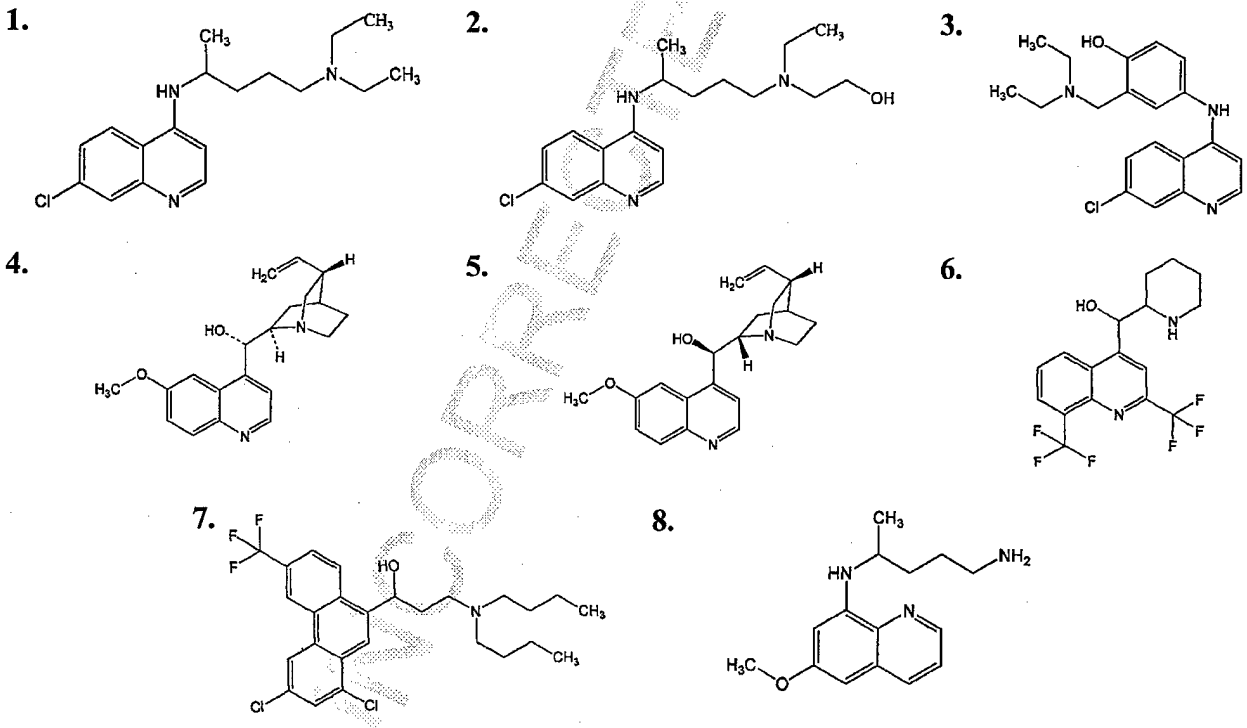

Fig. 1. Antimalarials. Chemical structures are presented and labeled numerically. Numeric labels correspond to NSC # and common names presented in Table 1.

Simple Quinoline Rings

9.

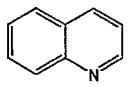

10.

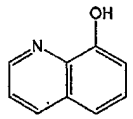

11.

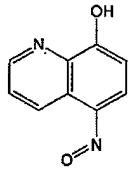

12.

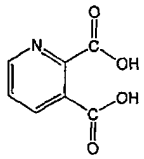

4-Substituted Quinolines

13.

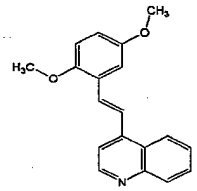

14.

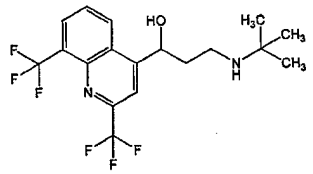

15.

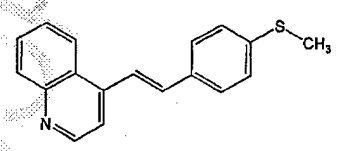

16.

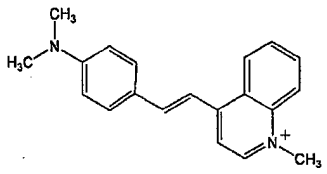

17.

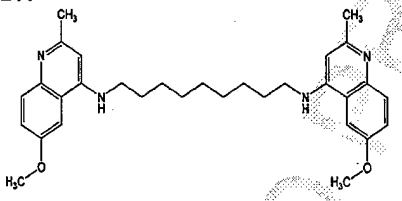

7-Substituted Quinolines

18.

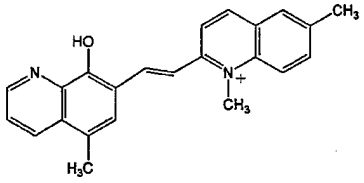

19.

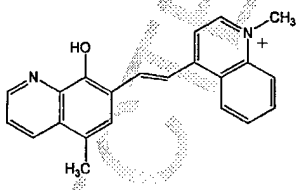

20.

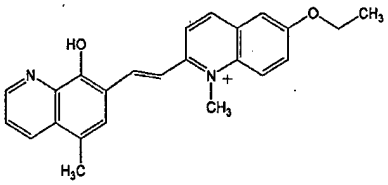

5-Substituted Quinolines

21.

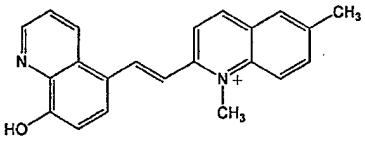

22.

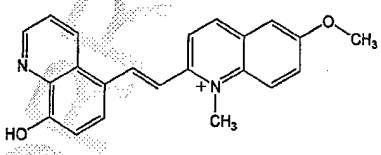

2-Substituted Quinoline

23.

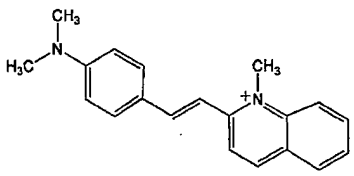

Fig. 2. NSC compounds. Chemical structures are presented and labeled numerically. Numeric labels correspond to NSC# presented in Table 1.

8-aminoalkyl substituted quinoline antimalarial gave mixed differentiation responses. Both compounds caused lipid droplet accumulation without effect upon the cell cycle marker, Ki67. We concluded antimalarial activity per se was not predictive of differentiation activity in this data set.

The antiproliferative quinoline NSC compounds shown in Fig. 2 were tested for differentiation activity in the same assays. Two minimally substituted quinolines (**10**, NSC2039 and **11**, NSC3852) and quinolinic acid (**12**) were included. Five 4-substituted quinolines, **13–17**, were tested: NSC69603 (**13**), NSC305819 (**14**), NSC124637

(15), NSC4239 (16) and NSC10010 (17). Three of these 4-substituted quinolines, similar to the antimalarial amodiaquin, contained phenyl substituents (13 (NSC69603), 15 (NSC124637), 16 (NSC4239)) and one was a bisquinoline (17 (NSC10010)). Compounds 13 (NSC69603), 17 (NSC10010), 21 (NSC86372), 22 (NSC85701) bore methoxy substituents as did the differentiating antimalarials, quinidine (4) and quinine (5). Quinidine and quinine differ in structure only as stereoisomers. Five NSC compounds and chloroquine (1) showed greater differentiation activity than quinidine (4) based upon the magnitude of the Ki67 index. The Ki67 index in MCF-7 cells after treatment with compounds 11 (NSC3852), 13 (NSC69603), 14 (NSC305819), 17 (NSC10010), 18 (NSC86371), and 1 (chloroquine) was statistically significantly greater than that of control cells. This group of compounds is referred to as the differentiation-inducing quinolines.

2.2. HDAC activity

All compounds were screened in HeLa cell nuclear extracts for the ability to directly inhibit human histone deacetylase activity (Table 1). Only compounds 11 (NSC3852) and 18 (NSC86371) significantly inhibited HDAC activity in HeLa cell extracts. Both compounds also statistically significantly inhibited HDAC in MCF-7 cell nuclear extracts, but in comparison with TSA, are weak HDAC inhibitors.The data show that HDAC inhibition might contribute to MCF-7 cell differentiation in response to compound 11 (NSC3852) and compound 18 (NSC86371). In contrast, direct inhibition of HDAC is unlikely to contribute to the differentiation response in MCF-7 cells by the other differentiation quinolines.

2.3. E2F-1 protein

The transcription factor E2F-1 is critical to the G1–S phase transition [14]. MCF-7 cells exposed to all of the differentiation quinolines for 48 h showed suppressed E2F-1 protein levels (Fig. 3). However, E2F-1 protein was unchanged in MCF-7 cells treated with compounds 8 (primaquine) and 9 (quinoline) that failed to induce differentiation. The data are consistent with the hypothesis that down-regulation of E2F-1 protein is characteristic of in vitro activity by differentiation quinolines, and facilitates the induction of differentiation.

2.4. Growth arrest and cell death

MCF-7 cell growth in the presence of the antimalarial compounds 1 (chloroquine), 2 (hydroxychloroquine), and 4 (quinidine), (Fig. 4A) and the differentiation-inducing

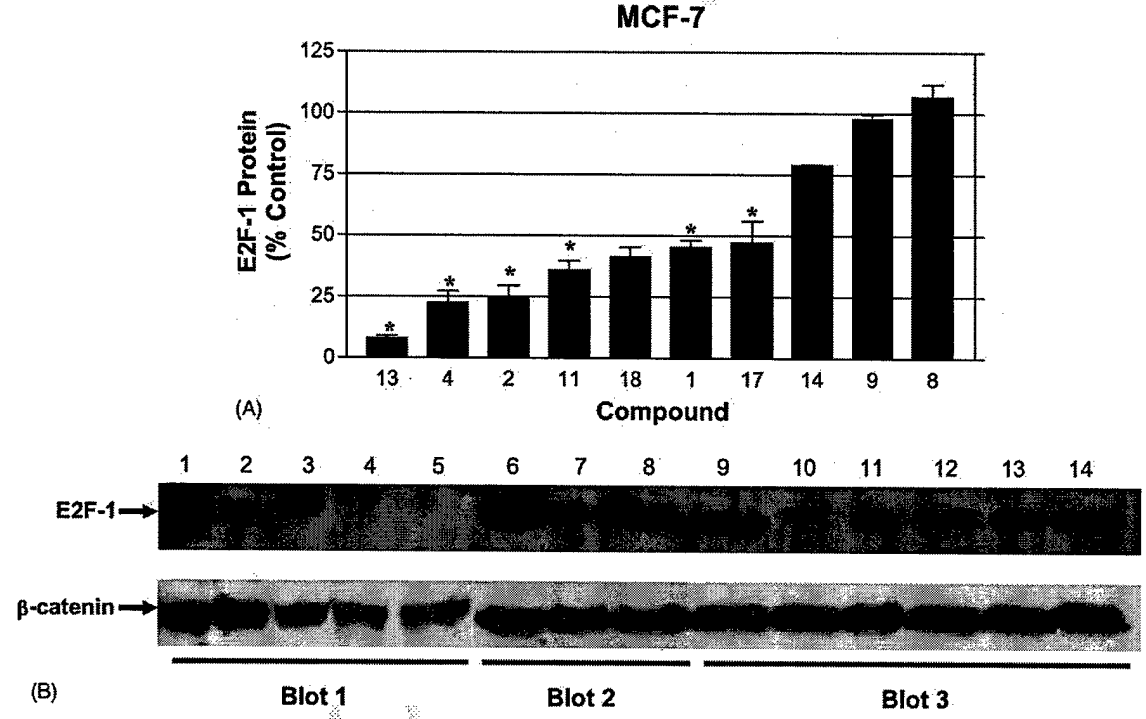

Fig. 3. Western blot analysis of E2F-1. MCF-7 cells were exposed to IC_{50} levels of compounds for 48 h. E2F-1 and β-catenin levels were detected using chemiluminescent autoradiography and quantified densitometrically using a FluorChem image analysis system. After normalization for the β-catenin levels in each lane, the E2F-1 protein levels were expressed as a percentage of the appropriate solvent control. Panel A is a summary of $n = 3$ or $n = 2$ experiments. Panel B is a composite of three Western blots showing the E2F-1 and β-catenin signals in control and treated cell extracts. Panel B, lanes 1–7 ($n = 3$) and lanes 8–14 ($n = 2$). Panel B: lane 1, 0.1% DMSO control; lane 2, 4 (quinidine); lane 3, 1 (chloroquine); lane 4, 2 (hydroxychloroquine); lane 5, 13 (NSC69603); lane 6, 0.1% DMSO control; lane 7, 11 (NSC3852); lane 8, 17 (NSC10010); lane 9, 0.1% DMSO control; lane 10, 18 (NSC86371); lane 11, 14 (NSC305819); lane 12, 8 (primaquine) (in water); lane 13, 9 (quinoline) (in water); lane 14, water control.

quinolines (Fig. 4B and C) were compared to confirm that MTS activity was a valid antiproliferative indicator. DNA damage was assessed on an individual cell basis using the Comet assay. The greater the DNA damage, the longer the Comet tail as quantified by the tail-moment (Fig. 5A). After 24 h, DNA damage by compounds **11** (NSC3852), **14** (NSC305819), **17** (NSC10010) and **18** (NSC86371) in MCF-7 cells was apparent. No damage to DNA by compound **1** (chloroquine) or **13** (NSC69603) was detectable. Similar results for all compounds were obtained after 48 h (data not shown). In MCF10A cells, very little DNA damage occurred except in response to compound **18** (NSC86371) (Fig. 5B). Short-term (48 h) growth experiments were conducted with MCF10A to assess the toxicity of the differentiation quinolines on non-transformed mammary epithelial cells (Fig. 6). MCF10A cell numbers were significantly reduced by all the differentiating quinolines. In comparison with the solvent treatment alone, compound **14** (NSC305819) was growth suppressive and less toxic than chloroquine to the normal cells. Compound **17** (NSC10010) was clearly toxic, and compounds **11** (NSC3852) and **18** (NSC86371) had intermediate effects on MCF10A cell numbers.

MCF-7 cells undergo a slow apoptotic response that can be quantified using the nucleosome release ELISA. After 72 h, apoptosis was detected in response to all of the differentiation-inducing quinolines except compound **13** (NSC69603) (Fig. 7). In summary, all differentiation-inducing quinolines caused growth suppression in MCF-7 and MCF10A cells, but exhibited variable capacities to induce DNA damage and apoptosis. Compound **13** (NSC69603) was unique in its ability to cause equivalent growth suppression in the absence of DNA damage or apoptosis.

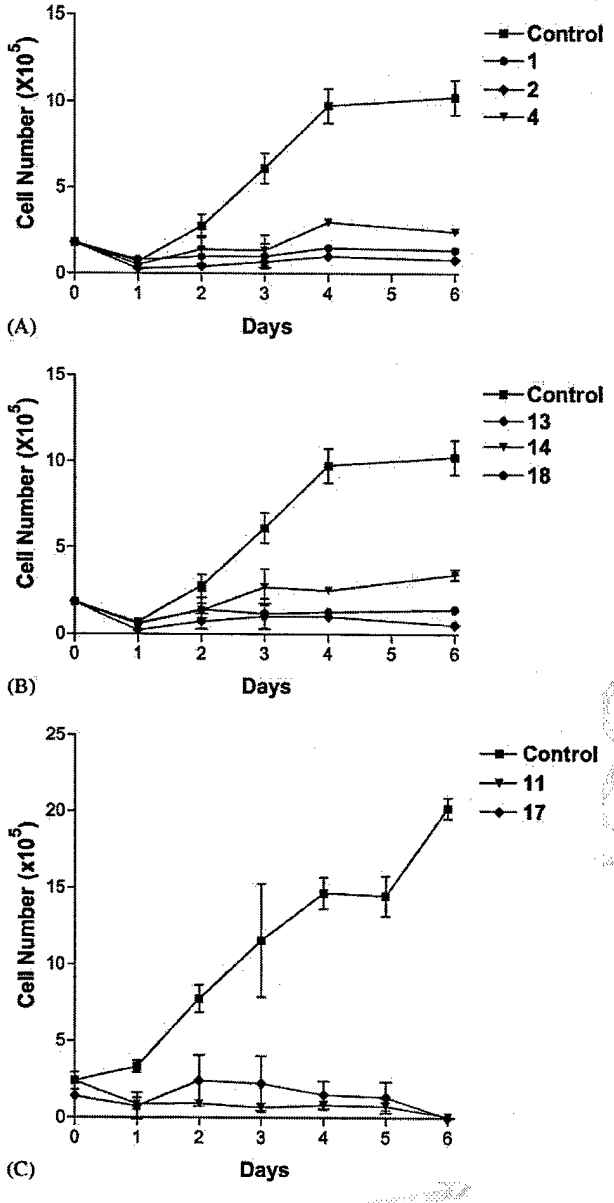

Fig. 4. MCF-7 growth inhibition. MCF-7 cells were grown in the presence of MTS IC_{50} levels of the quinoline differentiation compounds for 6 days. Data are the mean and range of duplicate determinations in two independent experiments.

2.5. Pre-drug development screens

Drugs frequently exhibit a common set of physicochemical properties summarized by Lipinski et al. [15]. To facilitate drug development, these properties have been reported for the NSC compounds (http://cactus/nci.nih.gov/ncidb2/). As summarized in Table 2, compounds **11** (NSC3852), **13** (NSC69603), **14** (NSC305819) and **18** (NSC86371) meet the Lipinski rule of fives: a molecular weight ≤500, <5 hydrogen-bond donors, <10 hydrogen-bond acceptors, and a oil–water partition (log *P*) between −1 and +5 [15]. Compound **17** (NSC10010) had a log $P > 5$, but otherwise met the specifications defined by Lipinski et al. Compound **18** (NSC86371), a quarternary amine,

Table 2
Predicted oral absorption of quinoline compounds

Compounds	Molecular weight (g/mol)	HIA >15%	PAMPA 24 h (μM)	PAMPA 48 h (μM)
1 (chloroquine)	319.9	1	25.8 ± 4.0*	51.1 ± 0.2*
11 (3852)	174.2	2	3.2 ± 1.8	7.1 ± 4.0
13 (69603)	291.3	1	10.2 ± 6.5	0
14 (305819)	394.4	1	59.1 ± 16*	64.8 ± 5.7*
17 (10010)	500.7	1	0	1.2 ± 1.2
18 (86371)	341.4	0	Nd	Nd

Chloroquine is the reference compound for a drug with very good oral absorption. HIA: human intestinal absorption predicted in silico using ADME/Tox Screen (Pharma Algorithms, North America, Toronto, Canada) where 0 = poor absorption predicted, 1 = non-restricted passive diffusion, and 2 = paracellular transport of small molecule or passive diffusion. PAMPA: parallel artificial membrane permeation assay. Concentrations of compounds in the acceptor wells (mean ± S.E.M. of $n = 3$ experiments performed in duplicate) after 24 or 48 h are shown. Statistically significant transfer of compounds across the membrane ($P < 0.05$) is indicated by (*). Nd: not determined.

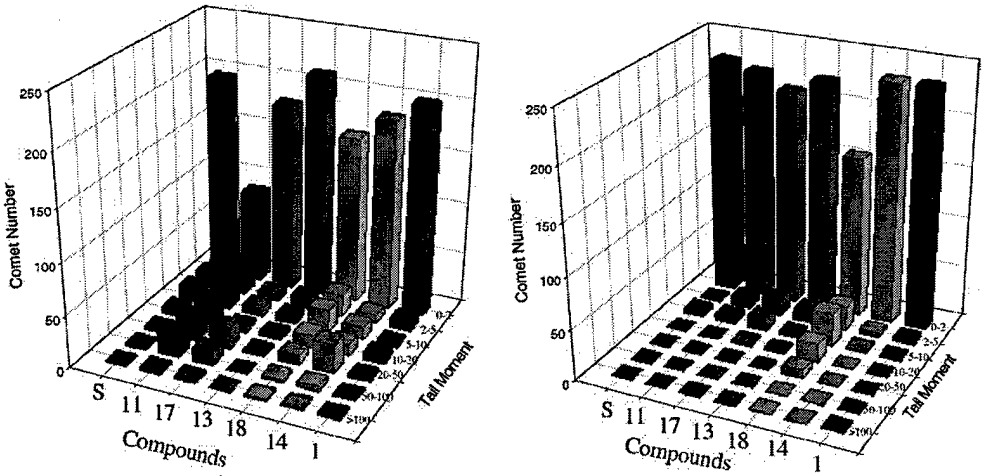

Fig. 5. Comet assay of DNA damage. (A) MCF-7 cells or (B) MCF10A cells were exposed to MTS IC_{50} levels of the quinoline differentiation compounds or chloroquine for 24 h. Damaged DNA released from the nuclear "head" and the Comet tail length was analyzed as a measure of the total DNA damage in individual cells. Eighty cells were analyzed/experimental condition. Low (0–2) Comet tail moments in control cells are indicative of minimal DNA breakage. Data shown are pooled results of three independent experiments in each cell line.

has a fixed positive charge, indicative of poor oral absorption.

A rapid in vitro assay for transcellular permeation of drugs through artificial lipid membranes (PAMPA) is an experimental approach to predicting gastrointestinal drug absorption [16]. Gastrointestinal drug absorption properties predicted by PAMPA were Compound **14** (NSC305819) >> Compound **1** (chloroquine) > Compound **13** (NSC69603) >> Compound **11** (NSC3852) (Table 2). Compound **17** (NSC10010) showed poor permeability in our studies indicating that oral administration of this bisquinoline differentiation agent, as well as of Compound **18** (NSC86371) could mask antitumor activity in whole animal studies. In contrast, Compounds **11** (NSC3852), **13** (NSC69603), and **14** (NSC305819) are predicted to be active after oral administration.

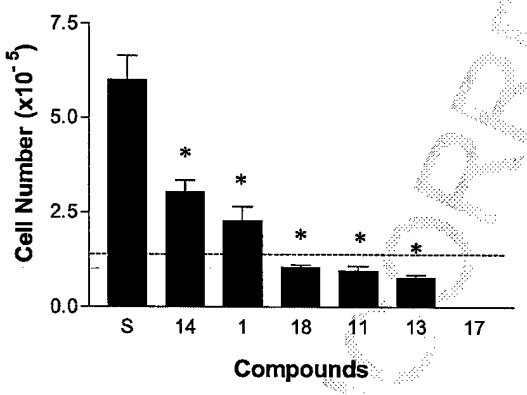

Fig. 6. MCF10A cell growth. MCF10A cells were incubated for 48 h in the presence of MCF-7 IC_{50} levels of differentiation quinolines, then harvested and viable cells counted. Data represent the mean ± range of three experiments. The dashed line indicates the number of cells plated at 0 time.

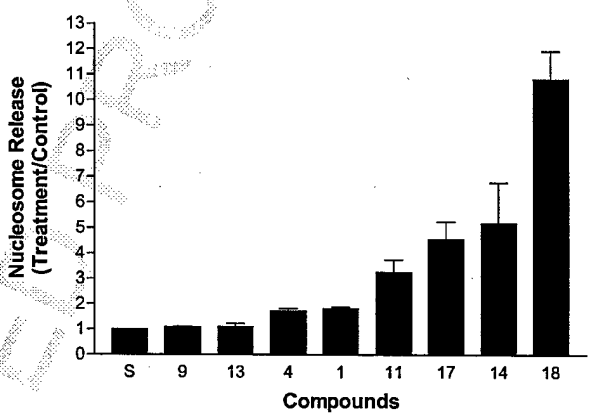

Fig. 7. Nucleosome ELISA for apoptosis. MCF-7 cells were treated with MTS IC_{50} levels of the quinoline differentiation compounds for 72 h. DNA–histone nucleosome complexes in the cell cytosol were quantified immunochemically. Apoptosis measured as nucleosome release is reported here as the ratio of treated/control values obtained in a single experiment performed in triplicate except for quinidine and chloroquine where the data represent $n = 3$ independent experiments performed in triplicate.

3. Discussion

Using the Ki67 index as a primary functional screen for agents that promote differentiation in MCF-7 cells, we identified six compounds for which differentiation contributed significantly to their antiproliferative activities. These compounds lacked a discernable common chemical structure other than the quinoline ring, however they shared an important functional capacity to suppress E2F1 protein levels. E2F1 is widely recognized as a cell cycle regulatory protein that fosters cell proliferation by stimulating the G1–S cell cycle transition. Moreover, E2F1

plays a modulatory role in cell differentiation. Down-regulation of E2F1 is a necessary pre-condition for cells to undergo differentiation, and E2F1 overexpression can act to suppress the differentiation response. Finally, under certain conditions, E2F1 is a pro-apoptotic protein. Because of its involvement in three critical cell decisions: growth, differentiation, and death, E2F1 is an attractive molecular target for drug discovery [17–19].

As a working model to explain the mechanism of action of the differentiation-inducing quinolines, we propose that strong suppression of E2F1 alone inhibits growth by preventing cell cycle progression and fosters differentiation by creating a permissive environment for cell differentiation. Moderate suppression of E2F1, in conjunction with induction of DNA damage, promotes differentiation through the activation of the p53–Rb pathway as well. Compound **13** (NSC69603) is an example of a quinoline differentiation compound that might act primarily through the suppression of E2F1. Compound **13** decreased total cell E2F1 levels by 90% but lacked DNA damage or apoptotic activity. Additional experiments are needed to test the hypothesis that E2F1 is the principal target of Compound **13**. Compounds **11** (NSC3852), **17** (NSC10010) and **18** (NSC86371) are examples of quinoline differentiation compounds that caused DNA damage and decreased E2F1 levels albeit more modestly (~50%). We know from previous work in MCF-7 cells that DNA damage causes Rb hypophosphorylation via increased p53 and the induction of the cyclin-dependent kinase inhibitor, p21/WAF-1 [9,20]. We propose that DNA damage and E2F1 suppression are important to the mechanism of action of Compounds **11, 17 and 18.** E2F1 complexes with hypophosphorylated Rb causing growth arrest through E2F1 sequestration. Cell differentiation is fostered by recruitment of co-repressor complexes to the promoter regions of E2F1 target genes by the E2F1–Rb complex [21,22].

Compounds **11** (NSC3852) and **18** (NSC86371) were identified as in vitro HDAC inhibitory quinolines at concentrations that induced differentiation in MCF-7 cells, 10 and 6 μM, respectively. Compound **11** (NSC3852) caused a similar decrement in E2F1 protein levels (60–70%) and also DNA damage. Hence, for these agents, three mechanisms potentially contributed to cell growth inhibition and differentiation: E2F1 suppression, DNA damage and HDAC inhibition. Although there is yet no direct evidence that gene specific changes in histone acetylation are required for the differentiation response in MCF-7 cells, comparison of the activity of a pair of compounds, Compound **11** (NSC3852) and Compound **10** (NSC2039, 8-quinolinol) provided indirect evidence for the involvement of HDAC. Compounds **10** and **11** differ only with respect to the presence of the nitroso substitution in Compound **11** (NSC3852). In the presence of the nitroso substitution, HDAC activity was inhibited ($P < 0.05$) and the Ki67 index was elevated ($P < 0.05$) while the 8-quinolinol analog, compound **10** (NSC2039), had no statistically significant effect on either HDAC activity or the Ki67 index. This pair of compounds will enable us to probe the mechanism of action of Compound **11** (NSC3852) in intact cells.

Compounds **11** (NSC3852), **13** (NSC69603) and **14** (NSC305819) exhibit drug-like chemical properties consistent with oral activity. Data available on the National Cancer Institute web site indicate that Compounds **11** and **13** sufficiently potent to exert antitumor activity in vivo. Compound **13** (NSC69603) demonstrated modest in vivo activity in two mouse mammary tumor models and the P388 leukemia model in mice. Compound **11** (NSC3852) showed activity against P388 leukemia growth in mice in NCI screening trials. There are no reported tests of in vivo antitumor activity of Compound **14** (NSC305819). The mechanism of action of Compound **14** in MCF-7 cells is the least clear as it caused a modest 25% decrease in E2F1 protein, minimal DNA damage, and no HDAC inhibition. However, Compound **14** (NSC305819) was the least toxic of all the differentiation-inducing quinolines in MCF10A cells and might have tumor selective activity. In conclusion, the differentiation-inducing quinolines comprise a new category of experimental breast cancer differentiation agents. Their use as lead compounds will complement ongoing efforts to develop differentiation therapies for breast cancer.

Acknowledgments

Hydroxychloroquine sulfate was the kind gift of Mylan Pharmaceuticals, Inc. Dr. Robert Schultz (Drug Synthesis & Chemistry Branch, Developmental Therapeutics Program, Division of Cancer Treatment and Diagnosis, National Cancer Institute, Bethesda, MD) provided the investigational compounds (National Service Center, NSC), including the antimalarials, mefloquine (NSC157387) and halofantrine methylsulfate (NSC305789). This work was supported by DAMD 17-00-1-500, DAMD 17-02-1-0622, WVU School of Medicine and the Spurlock Cancer Research Fund.

References

[1] Marks PA, Rifkind RA, Richon VM, Breslow R. Inhibitors of histone deacetylase are potentially effective anticancer agents. Clin Cancer Res 2001;7:759–60.

[2] Vigushin DM, Coombes RC. Histone deacetylase inhibitors in cancer treatment. Anti-cancer Drugs 2002;13:1–13.

[3] Weidle UH, Grossmann A. Inhibtion of histone deacetylases: a new strategy to target epigenetic modifications for anticancer treatment. Anticancer Res 2000;20:1471–86.

[4] Marks PA, Richon VM, Rifkind RA. Histone deacetylase inhibitors: inducers of differentiation or apoptosis of transformed cells. J Natl Cancer Inst 2000;92:1210–6.

[5] Darkin-Rattray SJ, Gurnett AM, Myers RM, Dulski PM, Crumley TM, Allocco JJ, et al. Apicidin: a novel antiprotozoal agent that inhibits

parasite histone deacetylase. Proc Natl Acad Sci (USA) 1996;93: 13143–7.

[6] Furumai R, Matsuyama A, Kobashi N, Lee K-H, Nishiyama M, Nakajima H, et al. FK228 (Depsipeptide) as a natural prodrug that inhibits class I histone deacetylases. Cancer Res 2002;62:4916–21.

[7] Zhou Q, Melkoumian ZK, Lucktong A, Moniwa M, Davie JR, Strobl JS. Rapid induction of histone hyperacetylation and cellular differentiation in human breast tumor cell lines following degradation of histone deacetylase-1. J Biol Chem 2000;275:35256–63.

[8] Melkoumian ZK, Martirosyan AR, Strobl JS. Myc protein is differentially sensitive to quinidine in tumor versus immortalized breast epithelial cell lines. Int J Cancer 2002;102:60–9.

[9] Zhou Q, McCracken MA, Strobl JS. Control of mammary tumor cell growth in vitro by novel cell differentiation and apoptosis agents. Breast Cancer Res Treat 2001;75:107–17.

[10] Dignam JD, Lebovitz RM, Roeder RG. Accurate transcription initiation by RNA polymerase II in a soluble extract from isolated mammalian nuclei. Nucl Acid Res 1983;11:1475–89.

[11] Mehta RR, Bratescu L, Graves JM, Green A, Mehta RG. Differentiation of cultured human breast carcinoma cells by a novel Vitamin D analog: 1-alpha-hydroxyVitamin D5. Int J Oncol 2000;16:65–73.

[12] Munster PN, Troso-Sandoval T, Rosen N, Rifkind R, Marks PA, Richon VM. The histone deacetylase inhibitor suberoylanilide hydroxamic acid induces differentiation of human breast cancer cells. Cancer Res 2001;61:8492–7.

[13] Van Dierendonck JH, Keijzer R, Van de Velde CJ, Cornelisse CJ. Nuclear distribution of the Ki-67 antigen during the cell cycle: comparison with growth fraction in human breast cancer cells. Cancer Res 1989;49:2999–3006.

[14] Trimarchi JM, Lees JA. Sibling rivalry in the E2F family. Nat Rev Mol Cell Biol 2002;3:11–20.

[15] Lipinski CA, Lombardo F, Dominy BW, Feeney PJ. Experimental and computational approaches to estimate solubility and permeability in drug discovery and development settings. Adv Drug Deliv Res 1997; 23:3–25.

[16] Hidalgo IJ. Assessing the absorption of new pharmaceuticals. Curr Top Med Chem 2001;1:385–401.

[17] Dick FA, Dyson N. pRB contains an E2F1-specific binding domain that allows E2F1-induced apoptosis to be regulated separately from other E2F activities. Mol Cell 2003;12:639–49.

[18] Wong CF, Barnes LM, Dahler AL, Smith L, Serewko-Auret MM, Popa C, et al. E2F modulates keratinocyte squamous differentiation: implications for E2F inhibition in squamous cell carcinoma. J Biol Chem 2003;278:28516–22.

[19] D'Alo F, Johansen LM, Nelson EA, Radomska HS, Evans EK, Zhang P, et al. The amino terminal and E2F interaction domains are critical for C/EBP alpha-mediated induction of granulopoietic development of hematopoietic cells. Blood 2003;102:3163–71.

[20] Orr MS, Watson NC, Sundaram S, Randolph JK, Jain PT, Gewirtz DA. Ionizing radiation and teniposide increase p21/waf1/cip1 and promote Rb dephosphorylation but fail to suppress E2F activity in MCF-7 breast tumor cells. Mol Pharmacol 1997;52:373–9.

[21] Brehm A, Miska EA, McCance DJ, Reid JL, Bannister AJ, Kouzarides T. Retinoblastoma protein recruits histone deacetylase to repress transcription. Nature 1998;391:597–601.

[22] Morrison AJ, Sardet C, Herrera RE. Retinoblastoma protein transcriptional repression through histone deacetylation of a single nucleosome. Mol Cell Biol 2002;22:856–65.

Breast Cancer Research and Treatment **75:** 107–117, 2002.

Report

Control of mammary tumor cell growth *in vitro* by novel cell differentiation and apoptosis agents

Qun Zhou[1], Meredith A. McCracken[2], and Jeannine S. Strobl[1,2]
[1]*Department of Biochemistry and Molecular Pharmacology,* [2]*Genetics and Developmental Biology Program, West Virginia University, Morgantown, WV, USA*

Key words: apoptosis, breast cancer, cell differentiation agents, chloroquine, MCF-7, quinidine, quinine

Summary

The use of breast tumor differentiating agents to complement existing therapies has the potential to improve breast cancer treatment. Previously we showed quinidine caused MCF-7 cells to synchronously arrest in G1 phase of the cell cycle, transition into G0 and undergo progressive differentiation. After 72–96 h cells became visibly apoptotic. Using several analogs of quinidine we determined that MCF-7 cell cycle exit and differentiation are typical of quinoline antimalarial drugs bearing a tertiary amine side chain (chloroquine, quinine, quinidine). Differentiated cells accumulated lipid droplets and mammary fat globule membrane protein. Apoptosis was assayed by a nucleosome release ELISA. Quinidine and chloroquine triggered apoptosis, but not quinine, a quinidine stereoisomer that displayed weak DNA binding. The apoptotic response to quinidine and chloroquine was p53-dependent. A 4–15-fold induction of p21(WAF1) protein was observed in cells treated with quinidine or chloroquine prior to apoptosis, but p21(WAF1) was not increased in cells that differentiated in response to quinine. Chloroquine was most active in stimulating MCF-7 apoptosis, and quinine was most active in promoting MCF-7 cell differentiation. We conclude, distinct mechanisms are responsible for breast tumor cell differentiation and activation of apoptosis by quinoline antimalarials. Alkylamino-substituted quinoline ring compounds represented by quinidine, quinine, and chloroquine will be useful model compounds in the search for more active breast tumor differentiating agents.

Introduction

Our laboratory is investigating the use of quinoline antimalarials as inexpensive drugs with low toxicity for adjuvant breast cancer treatment. Quinidine is a natural alkaloid that is derived from the bark of the cinchona tree. Quinidine is used therapeutically to treat cardiac arrhythmia and malaria. Quinine is present in cinchona tree bark in even higher concentrations than quinidine. Quinine has antimalarial activity equivalent to that of quinidine but is not used as an antiarrhythmic agent [1]. Interestingly, quinidine and quinine are stereoisomers (Figure 1). In quinidine, the secondary alcohol of the side-chain in the 4-position of the quinoline ring is the dextrorotary conformation while in quinine the 4-hydroxyl group exists in the levorotatory conformation. The synthetic alkaloid, chloroquine is a more potent antimalarial than either quinidine or quinine. Chloroquine is a 4-alkylamino substituted quinoline that also possesses a chlorine substitution at the 7-position of the ring. Despite chloroquine's structural similarities with quinine and quinidine, chloroquine has a different mechanism of antimalarial activity, and chloroquine-resistant malaria responds to quinine treatment. The quinoline ring by itself lacks antimalarial or antiarrhythmic activity indicating that therapeutic properties are conferred by the side chain substituents. This group of pharmacologically active compounds might have anticancer properties.

We reported previously that quinidine causes moderate growth arrest and morphologic differentiation of human breast cancer cells *in vitro* [2–4]. In an experiment which compared MCF-7 cell numbers after 5

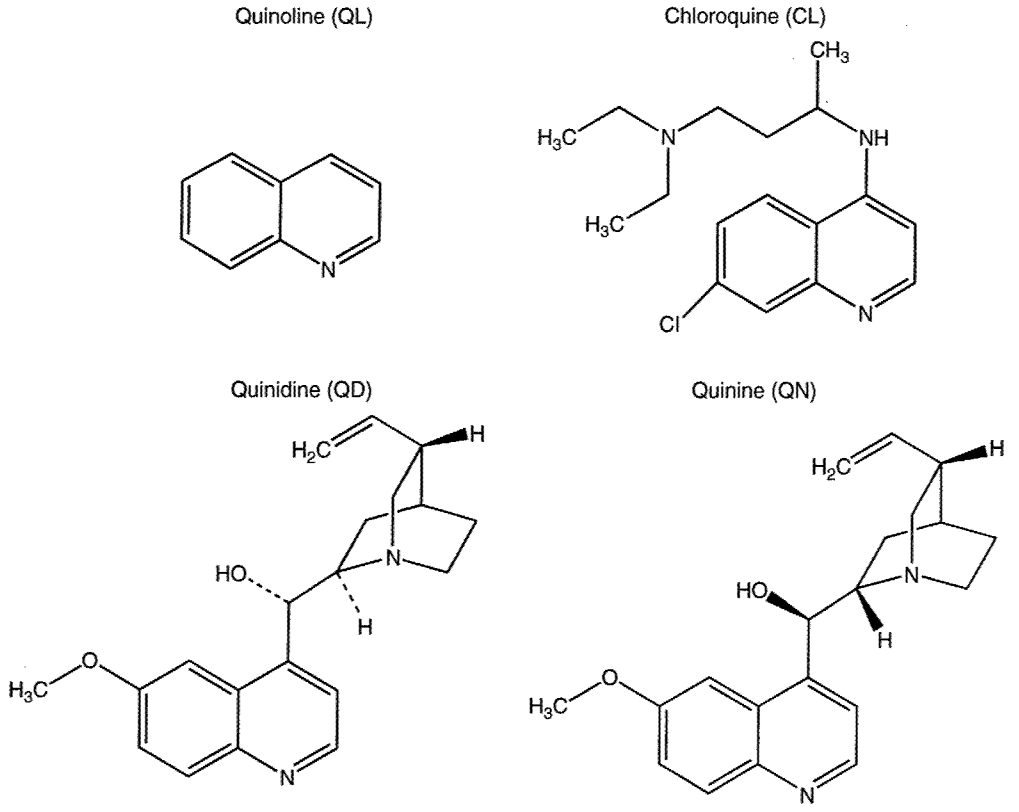

Figure 1. Structures of antimalarials.

days growth in the presence and absence of quinidine, 25 μM quinidine was found to reduce the increase in cell numbers by 50% [2]. Quinidine promoted cell cycle arrest in G1, exit into G0 marked by a loss of expression of Ki67 antigen, and lipid droplet accumulation and cytoplasmic enlargement, morphological evidence of cellular differentiation [3, 4]. Accumulation of MCF-7 cells in the G1/G0 phase of the cell cycle was maximal between 24 and 48 h with 90 μM quinidine. The potassium channel blocking activity of quinidine is implicated in the G1 arrest of MCF-7 cells, although the signaling pathway has not yet been elucidated [3]. The mechanism of quinidine action on growth in MCF-7 cells involves a number of changes in cell cycle proteins that regulate progression through G1 phase [4, 5]. Quinidine (90 μM) treatment caused increased p21(WAF1), p53, and p27 protein levels, and decreased cyclin D1, phosphorylated pRb, and Myc. Quinidine also raised levels of acetylated histone H4, a response that has been correlated with cellular differentiation in breast tumor cells [4, 6]. The differentiation response to quinidine in MCF-7 cells was well developed by 48–72 h. In cells continously exposed to quinidine for 72–96 h, apoptotic nuclei stained with Hoechst dye were apparent [3], suggesting that quinidine causes both growth arrest, via cell cycle arrest and differentiation, and cell death.

The present report describes the results of a comparative study of the effects of quinidine, quinoline and two additional quinoline antimalarials, quinine and chloroquine on MCF-7 cell apoptosis and differentiation. Our data show that quinoline antimalarials inhibit growth of human breast cancer cells *in vitro* and support the hypothesis that quinoline antimalarials cause cellular differentiation and apoptosis via distinct pathways.

Materials and methods

Chemicals

Chloroquine (CL), Oil Red O (ORO), quinidine (QD), quinine (QN), quinoline (QL) and trichostatin A (TSA) were purchased from Sigma Chemical Company (St. Louis, MO).

Tissue culture

Permanent cell lines derived from patients with breast carcinoma were used in these studies. MCF-7 cells between passage numbers 30–50, MCF-7*ras*, T47D and MDA-MB-231 cells were maintained in Dulbecco's Modified Eagle's medium (DMEM) (BioWhittaker, Walkersville, MD) supplemented with 10% heat-inactivated fetal bovine serum (FBS) (Hyclone Laboratories, Inc., Logan, Utah), and 40 ug/ml gentamicin. Experiments were performed in DMEM/5%FBS. The cells were cultured at 37°C in a humidified atmosphere of 93% air/7% CO_2.

MTS (3-(4,5-dimethylthiazol-2-yl)-5-(3-carboxymethoxyphenyl)-2-(4-sulfophenyl)-2H-tetrazolium) assay

MCF-7 cells were plated at 4.0×10^3 cells/well in 96-well plates in 225 µl of DMEM/5% FBS. Twelve hours after plating, the test agents were added and the cells were incubated for an additional 48 h. Cell growth was measured using a MTS assay kit (CellTiter 96 AQueous one solution assay, Promega, Madison, WI) according to the manufacturer's instructions. Assays were repeated at least three times. The concentration of each agent that inhibited cell growth by 50% (IC50) was determined using nonlinear regression analysis to fit the inhibition data (Prism 3.0, GraphPad Software, Inc., San Diego, CA).

Ki67 immunohistochemical assay

An immunohistochemical assay for Ki67 antigen was performed according to the protocol described by Wang et al. [3]. MCF-7 cells (2×10^5/dish) were plated on ethanol-washed glass coverslips in 35 mm^2 dishes. Twelve hours after plating, test compounds were added to the medium using the IC50 determined in the MTS assay. Forty-eight hours later, the cells were fixed in acetone:ethanol (50:50) on ice for 10 min, and washed with PBS-0.15% bovine serum albumin (BSA, fraction V, Sigma) (PBS-BSA). Cells were incubated for 10 min with 0.3% hydrogen peroxide in methanol, rinsed with PBS-BSA, and incubated for 30 min with 10% horse serum in PBS-BSA. Cells were incubated for 60 min with the primary antibody Ki67 (MIB-1, Dako Corporation, Glostrup, Denmark) diluted in PBS-BSA (1:77). After rinsing with PBS-BSA, the secondary antibody, biotinylated horse anti-mouse IgG (Vector Laboratories, Burlingame, CA) diluted in PBS-BSA (1:250) was added for 30 min. The cells were rinsed with PBS-BSA and incubated for 30 min with the avidin-biotin-peroxidase reagent (Vector Laboratories). After rinsing with PBS, the antigen-antibody complexes were visualized using diaminobenzidine (Stable DAB, Research Genetics, Huntsville, AL). The cells were counterstained with Mayer's hematoxylin (Fisher Scientific, Pittsburgh, PA), and the coverslips mounted using Permount (Fisher). Ki67 negative cells were visualized by light microscopy (400 × objective, Ortholux microscope, Ernst Leitz, Wetzlar, Germany). The percentage of Ki67 negative cells in a population of at least 500 cells per experimental condition was determined.

Oil red O assay

Lipid droplet accumulation in the cytoplasm was measured using Oil Red O (ORO) staining [7]. MCF-7 cells (1×10^5 per dish) were plated on ethanol-washed glass coverslips in 35 mm^2 dishes. Cells were treated with drug or vehicle for 48–72 h, fixed in 10% formaldehyde-0.2% calcium acetate in PBS for 3 min and stained for 10 min using the ORO stock solution (0.5% ORO in 98% isopropanol) diluted 6:4 in distilled water. The coverslips were rinsed in tap water, counterstained with Mayer's Hematoxylin solution, and mounted using 50:50 (v/v) glycerol/water. Lipid droplet accumulation was visualized by light microscopy (400 ×). Positive ORO cells had at least 10 lipid droplets per cell. The percentage of positive ORO cells was determined by counting at least 300 cells per experimental condition.

Western blotting

Cells were harvested from confluent T-75 flasks and subcultured (1×10^6) in 100 mm^2 dishes. Cell lysates were prepared by scraping cells into ice-cold harvesting buffer (1% SDS-10 mM Tris–HCl, pH 7.4). The lysates were boiled for 5 min, and protease inhibitors added (Protease Inhibitor Mixture, Roche Applied Sciences, Indianapolis, IN). The supernatants were collected after centrifugation in an Eppendorf microcentrifuge (14,000 rpm, 5 min) at 4°C. The protein concentration of the supernatant was determined using a BCA protein assay (Pierce, Rockford, IL) and BSA as a standard. Equal amounts of protein were loaded onto 12% SDS-polyacrylamide mini-gels. Colored

molecular weight protein markers (Amersham Pharmacia Biotech Inc., Piscataway, NJ) were used to estimate the molecular weight of the immunoreactive proteins. Proteins were transferred to polyvinylidene difluoride membranes (PVDF, Invitrogen, Carlsbad, CA) and blocked overnight at 4°C using 3% non-fat milk blocking buffer (3 g non-fat dry milk per 100 ml of TBS (20 mM Tris–HCl, pH 7.5, 0.5 M NaCl) and 0.05% (v/v) Tween 20. Membranes were incubated for 3 h at room temperature with the following primary antibodies: mouse monoclonal anti-p21 (WAF1) (Ap-1), mouse monoclonal anti-p53 (Ap-5) (Oncogene, Cambridge, MA) or mouse anti-human milk fat globule membrane (MFGM) protein (MAB-4043, Chemicon International, Temecula, CA). The primary antibodies were diluted 1 : 500 in Western washing solution (0.1% non-fat dry milk, 0.1% albumin (chicken egg), 1% (v/v) FBS, 10% (v/v) of 10 × PBS, pH 7.3, 0.2% (v/v) Tween-20). After washing three times with Western washing solution and one time with TBS, the antigen-antibody complexes were incubated 1 h at room temperature with HRP (horseradish peroxidase)-conjugated secondary antibody (anti-mouse IgG-HRP, Santa Cruz Biotechnology) diluted 1 : 3000 in Western washing solution. After washing three times with TBS, antibody binding was visualized using enhanced chemiluminescence (SuperSignal West Pico, Pierce) and autoradiography.

Densitometric analysis

Autoradiograms of the Western immunoblots were scanned using ChemiImager software (Alpha Innotech Corporation, San Leandro, CA). The blots were adjusted for brightness and contrast, and the mean density for each band was analyzed using ChemiImager analysis program. The background value was subtracted from each individual object.

Cell death ELISA (enzyme-linked immunosorbent assay)

Apoptotic cells were measured using the cell death ELISA kit (Roche Applied Science). Cells (4.0×10^3) were plated in each well of 96-well plates and treated in triplicate with either drug or vehicle (control cells) for 48 or 72 h. Cell cytoplasmic fractions were prepared and 20 µl aliquots were transferred into streptavidin-coated microtiter plates (MTP) for analysis as per the instructions of the supplier. Apoptosis, measured as nucleosome release into the cytoplasmic fraction, was quantified spectrophotometrically (A_{405} nm, EL340 Biokinetics Reader, Bio-Tek Instruments, Winooski, Vermont) using ABTS (2,2-Azino-di-3-ethylbenzthiazolin-sulfonat) as the substrate.

P21(WAF1) ELISA

Cells were plated (1×10^6 cells/100 mm^2 dish); 12 h later MTS IC50 of each test agent were added to the medium and incubated for 24 h. Fifty micrograms protein aliquots of the cell lysates were assayed for p21(WAF1) using a colorimetric ELISA (Oncogene, Boston, MA) according to the manufacturer's instructions.

DNA binding assay

Chloroquine, quinidine, and quinine emit an intense blue fluorescence when excited by ultraviolet light [8]. Intercalation into DNA quenches the chloroquine fluorescence [9], and this principle is the basis of the fluorescence assay we used to assess DNA binding by quinidine and quinine. Stock solutions of chloroquine, quinidine, and quinine in water were diluted 1 : 1 in 10 mM Tris, 1 mM EDTA, pH 8 (TE) or TE containing 1 µg of lambda DNA (Invitrogen, Carlsbad, CA) to a final concentration of 100 µg drug/ml. The final reaction volume was 20 µl. Drugs or drugs plus DNA were incubated for 15 min at room temperature in the dark in a 96-well plate (Nunc Immunoplate, Nunc Nalge International). Fluorescence was then measured using a CytoFluor4000 (PerSeptive Biosystems) instrument using an excitation wavelength of 360 nm and an emission wavelength of 460 nm. Background fluorescence from TE alone or TE plus DNA samples was subtracted from each measurement as appropriate. Data were expressed as the fluorescence quench ratio defined as the average fluorescence of drug alone (Em1) divided by that of drug in the presence of DNA (Em2).

Statistical analysis

Data are expressed as the mean ± SE for n number of replicates as indicated in the figure legends. One-way ANOVA (analysis of variance) followed by Bonferroni's t-tests were used to assess statistically significant differences between control- and drug-treated groups (GraphPad Instat, Intuitive Software for Science, San Diego, CA).

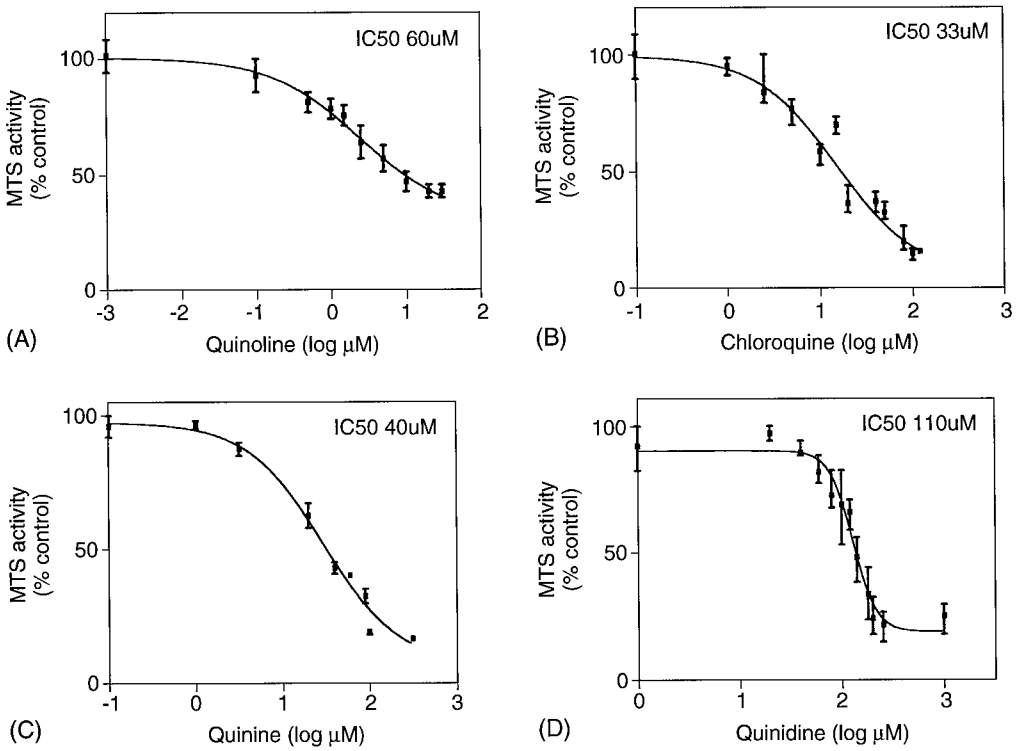

Figure 2. Antimalarials inhibited MTS metabolism in MCF-7 cells. MCF-7 cells (4000 cells/well) were grown in 96 well plates in the presence of increasing concentrations of each antimalarial for 48 h. Cell growth was estimated using the MTS assay. The IC50 value for each agent was determined using nonlinear regression analysis to fit inhibition data. Data are the mean ± SE of three independent experiments performed in quadruplicate. MTS activity of untreated cells was set 100%. The IC50 value for each antimalarial is shown in each panel.

Results

Antimalarials inhibit growth and promote MCF-7 cell differentiation

Quinidine inhibits MCF-7 cell proliferation, and to test whether this is a general response to structurally related chemicals, the effects of quinidine, quinine, chloroquine, and quinoline on MCF-7 cell growth were compared. The MTS assay directly measures mitochondrial metabolic activity; none of the test agents directly inhibited mitochondrial metabolism of MTS after a 2 h or a 6 h exposure (data not shown). Therefore, MTS activity measured after 48 h incubation with these compounds is a valid measure of the number of surviving cells (Figure 2). The IC50 was estimated for each drug in the MTS assay, and the order of potency of the compounds was chloroquine (IC50, 33 μM) > quinine (IC50, 40 μM) > quinoline (IC50, 62 μM) > quinidine (IC50, 110 μM). The effects of chloroquine, quinine, quinoline, and quinidine on cell numbers were investigated using the IC50 values determined in the MTS assay. Chloroquine (IC50, 33 μM) caused a ~60% decrease in cell numbers after a 60 h incubation as compared with control, growing MCF-7 cells suggesting that chloroquine caused cell death. In parallel cell cultures incubated with MTS IC50 of quinoline, quinidine, and quinine, the cell numbers after 60 h did not differ from the plating density. These compounds may primarily arrest cell growth, or alternatively permit a limited amount of proliferation balanced by cell loss (Figure 3).

Earlier studies showed quinidine caused G1 arrest and exit from the cell cycle [3]. Ki67 is a nuclear protein that is expressed throughout the cell cycle. The absence of Ki67 protein is a marker for non-proliferating cells that have entered G0 phase, and, therefore, provides a means of monitoring whether cell cycle exit might contribute to growth arrest [10]. By measuring Ki67 expression immunohistochemically, chloroquine (33 μM), quinidine (110 μM), and quinine (40 μM) were shown to promote exit from the cell cycle by 48 h. Under normal culture conditions, 95% of MCF-7 cells are engaged in the cell cycle, and express Ki67 antigen; 5% of the cells in the control population were negative for immunore-

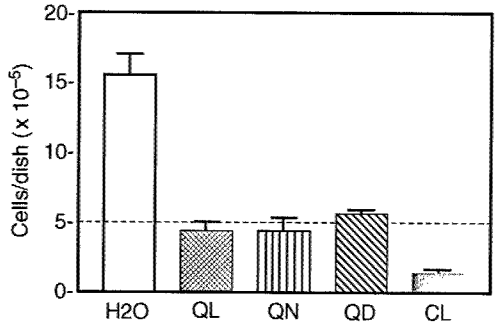

Figure 3. Effects of antimalarials on cell growth. MCF-7 cells (5×10^5) growing in 60 mm^2 dishes in DMEM/5%FBS were treated with concentrations of antimalarials corresponding to 50% inhibition of MTS activity as measured at 48 h. After 60 h incubation with antimalarials or solvent alone, viable cells that excluded trypan blue were counted using hemacytometer. Data are the mean of $n = 3 \pm$ SE independent experiments.

active Ki67 (Figure 4(A)). The percentage of Ki67 negative MCF-7 cells after 48 h growth in the presence of chloroquine, quinidine or quinine increased 6–7-fold to 30–40% compared to control cells ($p < 0.01$) (Figure 4(A)). Thus, growth inhibition by chloroquine, quinine, and quinidine can be explained in part by exit of cells from the cell cycle. Quinoline (62 μM), however, caused cell numbers to stabilize without shifting cells into G0.

Quinine, chloroquine, and quinidine also were similar in their ability to promote a more differentiated phenotype in MCF-7 cells, the accumulation of ORO positive lipid droplets in the cytoplasm [11] (Figure 4(B)). Quinoline was inactive in this assay as well. The data suggest that the stereoisomers, quinidine, and quinine act similarly, but with different potency, causing growth arrest, exit from the cell cycle and differentiation. Chloroquine was more potent and more toxic than quinidine and quinine. Chloroquine caused cell cycle exit; examination of the cells after ORO staining revealed morphologic evidence of differentiation (lipid droplets) as well as apoptotic cell death (condensed cells with heavy nuclear staining with hematoxylin). Quinoline caused arrest of cell growth without promoting cell cycle exit or any evidence of differentiation. Quinoline-treated cells showed no evidence of cytotoxicity, and the mechanism for the growth arrest is unclear.

In breast cells, the human milk fat protein is another cell differentiation marker [12]. The monoclonal antibody MFGM identifies antigens found on the milk fat globule membrane, which surrounds milk fat [13]. The expression of MFGM protein was measured by western blot analysis in MCF-7 cells exposed to antimalarials for 48 h. The densitometric signals in arbitrary units derived from scanning the immunoblots

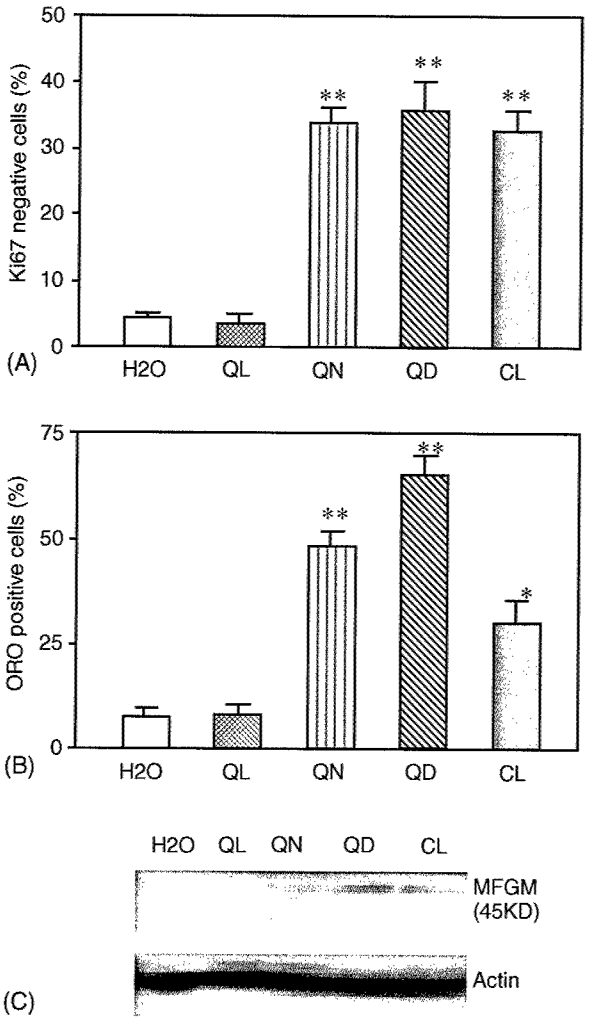

Figure 4. Cell differentiation by antimalarials. Ki67 expression, lipid droplet accumulation and human MFGM levels were measured in MCF-7 cells. MCF-7 cells were grown in 35 mm^2 dishes on sterile glass coverslips in DMEM/5%FBS. Cells were treated with solvent (distilled H_20) or the MTS IC50 of each antimalarial for 48 h (A) Ki67 immunoreactivity was performed as previously described by Wang et al. [3]. The data represent the mean percentage of Ki67 negative cells in each treatment group ($n = 3 \pm$ SE); 500 cells per experiment were counted. (B) Lipid droplet accumulation was measured using ORO staining in MCF-7 cells treated with antimalarials. The data represent the percentage ORO positive cells in each treatment group ($n = 3 \pm$ SE); 300 cells per treatment were counted. (C) Protein aliquots (25 ug) from the cell lysates were separated by 12% SDS-polyacrylamide gel electrophoresis and analyzed by western blotting using an antibody specific for MFGM. Actin protein was used as a loading control. Data are representive of two independent experiments. Statistically significant differences between control and treatment groups are indicated (*, $p < 0.05$; **, $p < 0.01$).

is provided in parantheses following each treatment. Quinidine (8872), quinine (7548), and chloroquine (8205) increased MFGM protein compared with control (5241) MCF-7 cells (Figure 4(C)). In contrast, MFGM protein levels were not changed by quinoline (5312) treatment. Changes of MFGM in MCF-7 cells by quinidine, quinine, and chloroquine are consistent with induction of lipid droplets. The coinduction of MFGM, and lipid droplets support our conclusion that quinidine, quinine, and chloroquine caused differentiation in MCF-7 cells.

Effect of antimalarials on apoptosis in MCF-7 cells

Morphological evidence that quinidine activated apoptosis in MCF-7 cells [3] prompted examination of apoptosis in cells exposed to antimalarials using the nucleosome release assay. Levels of apoptosis after 48 and 72 h were measured over a range of concentrations that spanned the respective MTS IC50 values for each compound. Etoposide (30 uM), a topoisomerase II inhibitor, elicits nucleosomal laddering in MCF-7 cells and was used as a positive control for this assay [14]. The enrichment of apoptotic response, defined as the ratio of the apotosis signal in the presence and absence of MTS IC50 concentrations of antimalarials, calculated after 48 and 72 h is summarized in Table 1. The concentration-response curve measured for each compound at 72 h is shown in Figure 5.

Quinidine and chloroquine stimulated nucleosome release in MCF-7 cells in a concentration-dependent fashion ($p < 0.05$). Chloroquine was more potent than quinidine and apoptosis was more extensive in cells exposed to chloroquine than quinidine. In contrast, quinoline, and quinine treatments did not change nucleosome release as compared with controls ($p > 0.05$). Quinoline displayed incomplete inhibition of MTS activity, no differentiating activity, and was not expected to activate apoptosis. However quinine inhibited MTS metabolism nearly as potently as chloroquine, and stimulated cellular differentiation. The experiments provide evidence that apoptosis, measured by nucleosome release, is differentially stimulated by the stereoisomers, quinidine, and quinine, while exit from the cell cycle, differentiation, and antimalarial activity are all stereo non-selective responses.

Table 1. The apoptosis enrichment factor was calculated using data obtained from ELISA, and is the ratio: units of absorbance drug treatment group/units of absorbance control group

Compounds	Apoptosis enrichment factor (mean ± SE, $N = 3$)	
	48 h	72 h
Quinoline (62 uM)	1.00 ± 0.06	1.09 ± 0.03
Quinine (40 uM)	1.13 ± 0.09	1.19 ± 0.07
Quinidine (110 uM)	1.50 ± 0.10*	1.73 ± 0.09*
Chloroquine (33 uM)	1.75 ± 0.14*	1.82 ± 0.07*
Etoposide (30 uM)	2.74 ± 0.13*	1.23 ± 0.20
Trichostatin A (35 nM)	0.96 ± 0.06	0.91 ± 0.05

Results of treatment times of 48 h and 72 h are compared.
Data shown are the mean ± SE of three experiments performed in triplicate.
*, $p < 0.05$ for drug treatment versus control.

To investigate the stereoselectivity of the apoptotic response further, levels of p53 and a downstream target of p53, p21(WAF1), were measured in MCF-7 cells exposed for 24 h to quinidine, quinine, chloroquine or quinoline. At their MTS IC50 levels, quinidine and chloroquine elevated p53 protein in MCF-7 cells, but in cells exposed to quinine and quinoline, p53 was undetectable (Figure 6(A)). Protein p21(WAF1) was increased in chloroquine and quinidine treated cells, but not in quinine or quinoline treated cells (Figure 6(B)). An ELISA was performed on MCF-7 whole cell extracts to quantify the changes in p21(WAF1) protein in response to the antimalarials (Figure 7(A)). Trichostatin acid (TSA) was used as a positive control for these experiments. Transcription of p21(WAF1) and p21(WAF1) protein levels have been shown to be increased by TSA [15, 16]. Chloroquine caused a 10–15-fold elevation in p21(WAF1) levels in MCF-7 cells at 24 h (Figure 7(B)). The p21(WAF1) response to chloroquine exceeded that of the potent histone deacetylase inhibitor, TSA. Quinidine elevated p21(WAF1) levels 4–5-fold, approximately the same as TSA, but neither quinine nor quinoline raised p21(WAF1) protein.

Moreover, p21(WAF1) protein expression in response to quinidine (90 uM) was different in wild type p53 and mutant p53 human breast cancer cells. Quinidine treatment increased p21(WAF1) protein in MCF-7 and MCF-7*ras* cells (wild type p53) (Figure 8), but p21(WAF1) protein was not detectable in malignant MDA-MB-231 and T47D cells (mutant p53) using western blot analysis. We previously reported that quinidine (90 uM) induced cellular differentiation in all of these lines of breast cancer cells [4].

DNA binding by antimalarials

Chloroquine intercalates into DNA [9, 17, 18], but DNA intercalation is not required for antimalarial

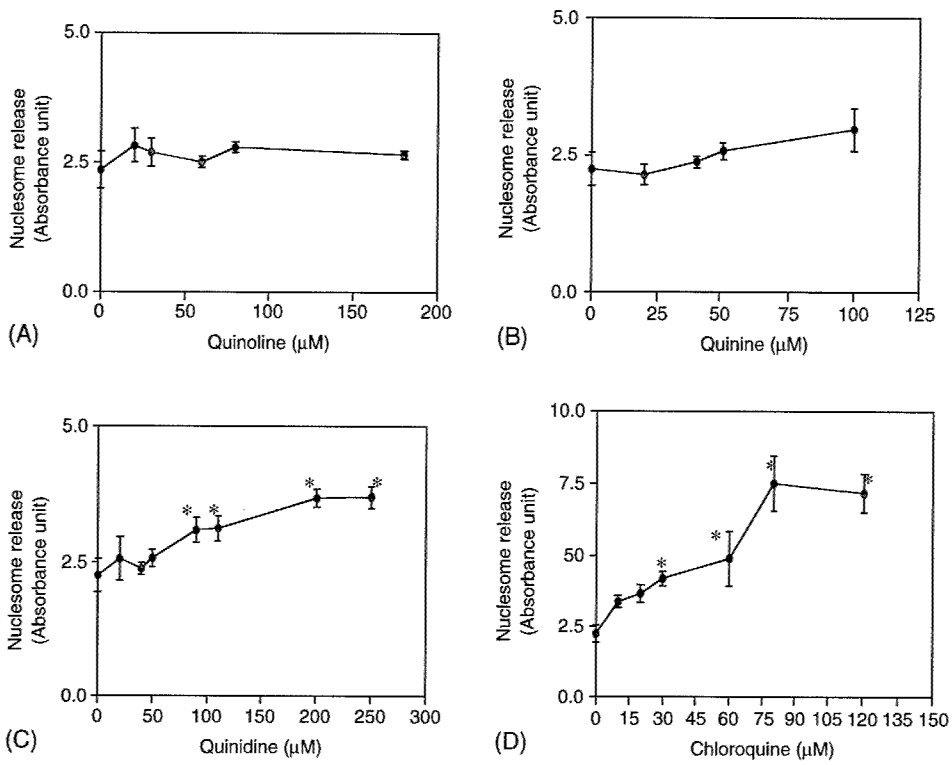

Figure 5. Nucleosome release apoptosis assay. MCF-7 cells (4000 cells/well) were grown in 96 well plates in the presence of increasing concentrations of antimalarials for 72 h. Nuclesome release was measured using the histone-DNA cell death detection kit as described in 'Materials and methods.' The level of nucleosomes released in each sample is indicated by the absorbance at 405 nm. Data are the mean ± SE of three independent experiments performed in triplicate. Statistically significant differences between control and drug treatment groups at specific drug concentrations are indicated (*, $p < 0.05$). Note the change in scale of the x-axis in Panel D.

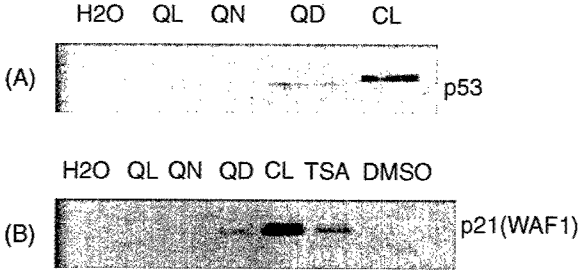

Figure 6. Western blot analysis of p21(WAF1) and p53 protein expression in human breast cancer cells. MCF-7 cells (1×10^6) were grown in 100 mm^2 dishes and treated with MTS IC50 of antimalarials for 24 h. Protein aliquots (50 μg) from the cell lysates were separated by 12% SDS-polyacrylamide gel electrophoresis and analyzed by western blotting using (A) mouse monoclonal antibody for p53. Data shown represent three independent experiments that showed the same results (B) mouse monoclonal antibody for p21(WAF1) (single experiment).

activity. We hypothesize that DNA intercalation is responsible for chloroquine-induced apoptosis, and that p53 induction by chloroquine is a consequence of DNA damage arising from intercalation. Our hypothesis predicts that chloroquine and quinidine but not quinoline and quinine intercalate into DNA. The binding of chloroquine, quinidine, and quinine to DNA was measured in an *in vitro* cell-free assay. The fluorescence signal from 2 μg of free chloroquine, quinidine, and quinine dissolved in 10 mM Tris-1 mM EDTA, pH 8 was equivalent. The addition of lambda DNA to solutions of chloroquine and quinidine, but not quinine, caused a statistically significant fluorescence quenching (Figure 9). The average fluorescence quench ratio for chloroquine in four independent experiments was 2.9 while that for quinidine was 1.8. Quinine exhibited a fluorescence quench ratio of 1.1 which was not statistically significant. The results imply stereo-selective DNA binding by quinidine, and are consistent with the pattern of quinidine activation of nucleosome release, p53 and elevations in p21(WAF1) protein levels. This is the first report of quinidine binding to DNA. Using an assay that measured changes in plasmid superhelical density, quinine was reported to intercalate into DNA, however this binding is relatively weak compared to chloroquine [18].

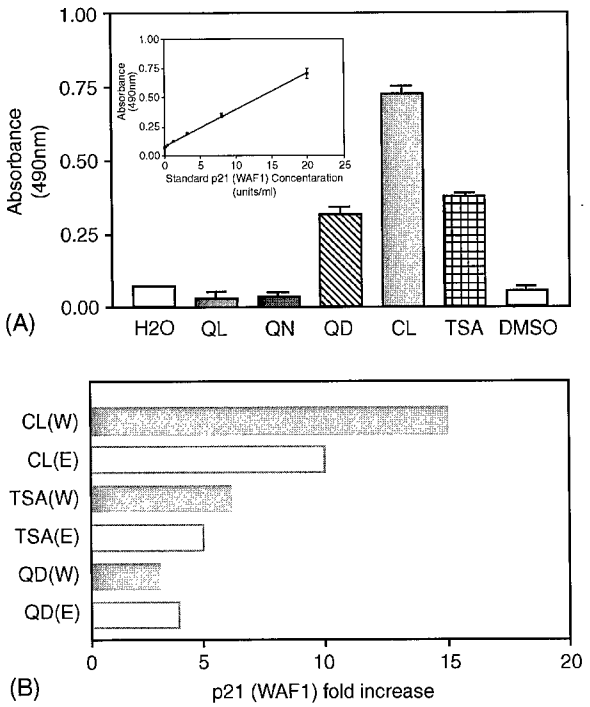

Figure 7. Effect of antimalarials on p21(WAF1) protein expression in MCF-7 human breast cancer cells. (A) p21(WAF1) ELISA. MCF-7 cells (1×10^6) were plated in 100 mm^2 dishes in DMEM/5% FBS, treated with solvent (distilled-H_2O or 0.01% DMSO) or MTS IC50 of each antimalarial for 24 h, and cell lysates prepared. TSA was dissolved in DMSO; antimalarials were dissolved in distilled H_2O. Proteins (50 μg) from the cell lysates were assayed using p21(WAF1) ELISA kit as detailed in 'Materials and methods' using a 20 min incubation time. Data are the mean ± SE of two independent experiments. (B) Comparison of p21(WAF1) protein changes detected in ELISA (E) and western blot analysis (W). W represents the fold increase in the signal density determined by densitometry; E represents the fold increase in absorbance in the ELISA. Fold increase is equal to drug treatment group divided by the control.

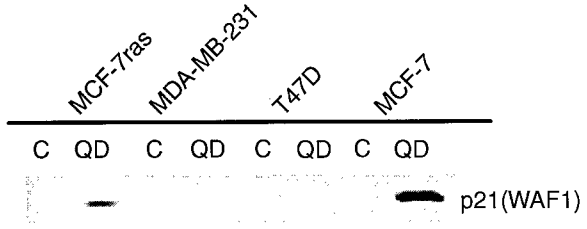

Figure 8. Effect of antimalarials on p21(WAF1) protein expression in human breast cancer cells. MCF-7, MDA-MB-231, T47D and MCF-7*ras* cells (1×10^6) were exposed to quinidine (90 μM) for 24 h. Protein aliquots (50 μg) from the cell lysates were separated by 12% SDS-polyacrylamide gel electrophoresis and analyzed by western blotting using mouse monoclonal antibody for p21(WAF1) (single experiment).

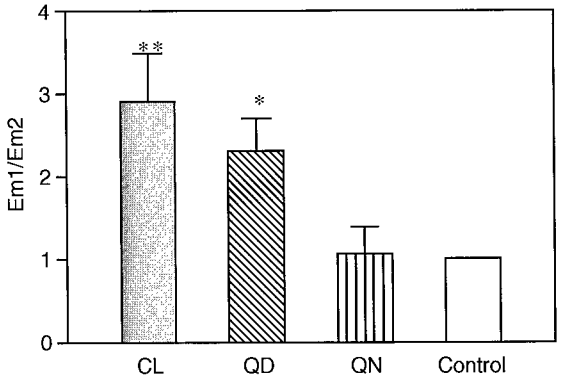

Figure 9. Fluorescence quench assay for DNA binding activity. Changes in antimalarial fluorescence upon DNA binding were measured using an excitation wavelength of 360 nm and an emission wavelength of 460 nm. Data were expressed as the fluorescence quench ratio defined as the average fluorescence of drug alone (Em1) divided by that of drug in the presence of DNA (Em2). Data represented the mean ± SE of three independent experiments. Statistically significant differences between control and treatment groups are indicated (*, $p < 0.01$; **, $p < 0.001$).

Discussion

In an effort to develop new anti-cancer therapeutic agents, we explored the anti-tumor potential of quinoline antimalarials using MCF-7 human breast cancer cells as our model system. The results of our experiments show antimalarial compounds inhibited cell growth *in vitro*, and two mechanisms for growth inhibition were identified: (1) promotion of cell cycle exit and cell differentiation and (2) activation of p53-dependent apoptosis.

Chloroquine was the most active apoptosis-inducing agent. DNA damage is a well-established apoptotic trigger that engages p53 protein as well as downstream targets of p53 including p21(WAF1) [19, 20]. Because chloroquine intercalates into DNA [21], and stimulates both p53 and p21 (WAF1) protein expression in MCF-7 cells we hypothesize that DNA damage is involved in the apoptotic response to chloroquine. The specific mechanism by which chloroquine might create DNA damage is unclear. Chloroquine is an unusual DNA intercalator because it has a two membered planar ring structure (Figure 1); in contrast, typical DNA intercalators have three or more fused planar rings [9, 21]. In addition, the tertiary aminoalkyl side-chain of chloroquine is modeled to occupy the minor groove of DNA, and this could have consequences for many DNA binding proteins and enzymes [21, 22]. Chloroquine has been reported to inhibit mammalian topoisomerase I and II [23, 24]. Inhibition of topoisomerase II activity is a clas-

sic response to DNA intercalating agents [25, 26] and topoisomerase inhibition is a potential mechanism of action of chloroquine in MCF-7 cells. Alternatively, the 10–15-fold increase in p21(WAF1) protein elicited in MCF-7 cells by chloroquine might be sufficient to activate apoptosis in the absence of DNA damage. Sheikh et al., showed that plasmid driven p21(WAF1) over expression in human breast tumor cell lines stimulated apoptosis [27]. In either this model or the DNA damage model, induction of p21(WAF1) protein emerges as a marker that can be used to screen compounds for apoptotic activity in human breast tumor cell lines.

Quinidine also increased p53 and p21 (WAF1) protein levels and stimulated apoptosis in MCF-7 cells, but was less active than chloroquine. An interesting feature of the apoptotic response of MCF-7 cells to quinidine, was the stereoselectivity. Quinine, a stereoisomer of quinidine, did not increase p53 or p21(WAF1) protein levels and did not trigger apoptotic cell death. Quinine was also less effective than either quinidine or chloroquine in binding DNA. The stereoisomers, quinine, and quinidine should prove very valuable in elucidating the mechanisms for apoptosis by quinoline drugs.

The MCF-7 response to quinine demonstrated that apoptotic cell death was not obligatory for cell growth arrest by antimalarial agents. Chloroquine, quinidine, and quinine all increased the percentage of G0 MCF-7 cells. Cell transition into the quiescent G0 phase is prerequisite for differentiation. Using lipid droplet accumulation measured by ORO staining and induction of the MFGM as markers of mammary cell differentiation, all three quinoline antimalarials were observed to induce differentiation in MCF-7 cells. Cell differentiation therapies such as FR901228, SAHA, and pyroxamide have recently entered into clinical trials and are an active area of cancer research [28, 29]. We propose on the basis of the data presented that quinoline antimalarial drugs be considered prototype compounds for the development of novel agents to stimulate breast tumor cell differentiation. Induction of differentiation by quinine was dissociated from both p21(WAF1) and apoptosis, and we conclude that differentiation is a distinct mechanism for inhibition of cell growth by antimalarials. Based on the differential response of MCF-7 cells to quinine and quinidine, we believe that a screening system based upon Ki67 expression is preferable to p21(WAF1) for identification of compounds that promote breast tumor cell differentiation.

Previous studies in our laboratory demonstrated that differentiation of MCF-7 cells by quinidine was associated with histone H4 hyperacetylation [4]. Elucidation of the regulation of histone acetylation state by antimalarials is expected to provide important insight into how quinoline antimalarials regulate breast tumor cell differentiation.

Acknowledgements

This work was supported by the Charleston Area Medical Center Foundation (8-2001), West Virginia University School of Medicine, and the US Army (DAMD 17-99-1-9449, DAMD 17-00-1-0500).

References

1. Webster Jr LT: Drugs used in the chemotherapy of protozoal infections: malaria. In: Goodman AG, Goodman LS, Rall TW, Murad F (eds) The Pharmacological Basis of Therapeutics. 7th edn MacMillan Publishing Company, NY, 1985, pp 1029–1048
2. Woodfork KA, Wonderlin WF, Peterson VA, Strobl JS: Inhibition of ATP-sensitive potassium channels causes reversible cell-cycle arrest of human breast cancer cells in tissue culture. J Cell Physiol 162: 163–171, 1995
3. Wang S, Melkoumian ZK, Woodfork KA, Cather C, Davidson AG, Wonderlin WF, Strobl JS: Evidence for an early G1 ionic event necessary for cell cycle progression and survival in the MCF-7 human breast carcinoma cell line. J Cell Physiol 176: 456–464, 1998
4. Zhou Q, Melkoumian ZK, Lucktong A, Moniwa M, Davie JR, Strobl JS: Rapid induction of histone hyperacetylation and cellular differentiation in human breast tumor cell lines following degradation of histone deacetylase-1. J Biol Chem 275: 35256–35263, 2000
5. Melkoumian ZK, Martirosyan AR, Strobl JS: Myc protein is differentially sensitive to quinidine in tumor versus immortalized breast epithelial cells. Int J Cancer (in revision)
6. Munster PN, Troso-Sandoval T, Rosen N, Rifkind R, Marks PA, Richon VM: The histone deacetylase inhibitor suberoylanilide hydroxamic acid induces differentiation of human breast cancer cells. Cancer Res 61: 8492–8497, 2001
7. Graham KA, Buick RN: Sodium butyrate induces differentiation in breast cancer cell lines expressing the estrogen receptor. J Cell Physiol 136(1): 63–71, 1988
8. Udenfriend S: Drugs and toxic agents. In: Fluorescence Assay in Biology and Medicine. Vol 1, Academic Press, NY, 1962, pp 400–443
9. Hahn FE: Chloroquine. In: Corcoran JW, Hahn FE, (eds) Antibiotics, Vol III, Mechanism of Action of Antimicrobial and Antitumor Agents. Springer-Verlag Press, NY, 1975, pp 58–78
10. Van Dierendonck JH, Keijzer R, Van De Velde CJ, Cornelisse CJ: Nuclear distribution of the Ki-67 antigen during the cell cycle: comparison with growth fraction in human breast cancer cells. Cancer Res 49(11): 2999–3006, 1989

11. Bancroft JD, Cook HC: Manual of Histological Techniques. Churchill Livingstone, Edinburgh 1984, pp 132–133
12. Munster PN, Srethapakdi M, Moasser MM, Rosen N: Inhibition of heat shock protein 90 function by ansamycins causes the morphological and functional differentiation of breast cancer cells. Cancer Res 61(7): 2945–2952, 2001
13. Turnbull JE, Baildam AD, Barnes DM, Howell A: Molecular expression of epitopes recognized by monoclonal antibodies HMFG and HMFG-2 in human breast cancers: diversity, variability and relationship to prognostic factors. Int J Cancer 38(1): 89–96, 1986
14. Giocanti N, Hennequin C, Balosso J, Mahler M, Favaudon V: DNA repair and cell cycle interactions in radiation sensitization by the topoisomerase II poison etoposide. Cancer Res 53(9): 2105–2111, 1993
15. Yoshida M, Horinouchi S: Trichostatin and leptomycin. Inhibtion of histone deacetylation and signal-dependent nuclear export. Ann NY Acad Sci 886: 23–36, 1999
16. Kim YB, Ki SW, Yoshida M, Horinouchi S: Mechanism of cell cycle arrest caused by histone deacetylase inhibitors in human carcinoma cells. J Antibiot (Tokyo) 53(10): 1191–1200, 2000
17. Davidson MW, Griggs BG, Boykin DW, Wilson WD: Molecular structural effects involved in the interaction of quinoline methanolamines with DNA. Implications for antimalarial action. J Med Chem 20: 1117–1122, 1977
18. Esposito F, Sinden RR: Supercoiling in prokaryotic and eukaryotic DNA: changes in response to topological perturbation of plasmids in *E. coli* and SV40 *in vitro*, in nuclei and in CV-1 cells. Nucl Acids Res 15: 5105–5124, 1987
19. Vogelstein B, Kinzler KW: Has the breast cancer gene been found? Cell 79(1): 1–3, 1994
20. El-Deiry WS, Tokino T, Waldman T, Oliner JD, Velculescu VE, Burrell M, Hill DE, Healy E, Rees JL, Hamilton SR: Topological control of p21WAF1/CIP1 expression in normal and neoplastic tissues. Cancer Res 55(13): 2910–2919, 1995
21. O' Brien RL, Allision JL, Hahn FE: Evidence for intercalation of chloroquine into DNA. Biochim Biophys Acta 129(3): 622–624, 1966
22. Michael RO, Williams GM: Chloroquine inhibition of repair of DNA damage induced in mammalian cells by methyl methanesulfonate. Mutat Res 25(3): 391–396, 1974
23. Sorensen M, Sehested M, Jensen PB: pH-dependent regulation of camptothecin-induced cytotoxicity and cleavable complex formation by the antimalarial agent chloroquine. Biochem Pharmacol 54(3): 373–380, 1997
24. Snyder RD: Use of catalytic topoisomerase II inhibitors to probe mechanisms of chemical-induced clastogenicity in Chinese hamster V79 cells. Environ Mol Mutagen 35(1): 13–21, 2000
25. Chen AY, Liu LF: DNA topoisomerases: essential enzymes and lethal targets. Annu Rev Pharmacol Toxicol 34: 191–218, 1994
26. Solary E, Bertrand R, Pommier Y: Apoptosis induced by DNA topoisomerase I and II inhibitors in human leukemic HL-60 cells. Leuk Lymphoma 15(1–2): 21–32, 1994
27. Sheikh MS, Rochefort H, Garcia M: Overexpression of p21WAF1/CIP1 induces growth arrest, giant cell formation and apoptosis in human breast carcinoma cell lines. Oncogene 11(9): 1899–1905, 1995
28. Yoshida M, Furumai R, Nishiyama M, Komatsu Y, Nishino N, Horinouchi S: Histone deacetylase as a new target for cancer chemotherapy. Cancer Chemother Pharmacol (suppl 1): S20–26, 2001
29. Marks PA, Richon VM, Rifkind RA. Histone deacetylase inhibitors: inducers of differentiation or apoptosis of transformed cells. J Natl Cancer Inst 92(15): 1210–1216, 2000

Address for offprints and correspondence: JS Strobl, Department of Biochemistry and Molecular Pharmacology, Robert C Byrd Health Sciences Center, West Virginia University, Morgantown, WV, 26506, USA; *Tel.*: 304-293-7151; *Fax*: 304-293-6854; *E-mail*: jstrobl@hsc.wvu.edu